EVALUATION OF A COLD THERMAL ENERGY STORAGE SYSTEM USING ALTERNATIVE REFRIGERANTS

by

Salah Ali Alshaibani

A Thesis Presented to the Faculty of the
American University of Sharjah
College of Engineering
in Partial Fulfillment
of the Requirements
for the Degree of

Master of Science in
Mechanical Engineering

Sharjah, United Arab Emirates

May 2016

Approval Signatures

We, the undersigned, approve the Master's Thesis of Salah Ali Alshaibani.

Thesis Title: Evaluation of a Cold Thermal Energy Storage System Using Alternative Refrigerants

Signature	**Date of Signature** (dd/mm/yyyy)
_____	_____
Dr. Saad A. Ahmed Professor, Department of Mechanical Engineering Thesis Advisor	
_____	_____
Dr. Mohamed A. Gadalla, Professor, Department of Mechanical Engineering Thesis Co-Advisor	
_____	_____
Dr. Essam M. Wahba, Associate Professor, Department of Mechanical Engineering Thesis Committee Member	
_____	_____
Dr. Zarook Shareefdeen, Associate Professor, Department of Chemical Engineering Thesis Committee Member	
_____	_____
Dr. Mamoun Abdel-Hafez Department Head, Department of Mechanical Engineering	
_____	_____
Dr. Mohamed El-Tarhuni, Associate Dean, College of Engineering	
_____	_____
Dr. Leland Blank Dean, College of Engineering	
_____	_____
Dr. Khaled Assaleh, Interim Vice Provost for Research and Graduate Studies	

Acknowledgements

All praises and thanks goes to Allah for giving me the strength and ability to finish this thesis. I take this opportunity to thank my parents for their endless support and encouragement to strive to pursue my dreams. My sincere appreciation and respect also goes to my wife Maryam, for her support in all aspects of my life

I would like to express my profound gratitude to Dr. Saad Ahmed and Dr. Mohamed Gadalla, for their time and effort to support my work throughout my Master's program. I thank them for giving me the opportunity to pursue my interest in experimental research. Special thanks goes to the thesis committee: Dr. Essam Wahba, and Dr. Zarook Shareefdeen, for their time and effort devoted in reviewing this thesis.

Dedication

In the name of Almighty Allah, the source and origin of all knowledge of present and otherwise, I dedicate this effort of mine to

My father and mother, whose kindness, is a constant source of strength

Abstract

This study provides a detailed comparison study between clathrate hydrate of R134a and R404a refrigerants in a direct contact thermal energy storage system. Numerous closed loop cycles using hydrate of each refrigerant have been evaluated to compare the clathrate characteristics formation and the overall performance of the direct contact thermal storage closed loop system. The input parameters for conducting the comparison include the compressor speed and the mass flow rate of the refrigerant used to form refrigerant clathrate. Results of this investigation show that using R134a is better than R404a in forming the cold storage refrigerant clathrate. For R134a, the overall system coefficient of performance based on the first law of thermodynamics is evaluated under different operating conditions and found to be varying between 4.10 and 5.77. The exergy analysis shows that the exergy recovered varies between 50% and 66%. For R134a clathrate, a high system coefficient of performance of 5.77 (COP) and a high exergy recovered of 66% are obtained at the lowest tested compressor speed of 2300 rpm and a high refrigerant mass flow rate of 0.96 kg/min. At the compressor speed of 2300 rpm with refrigerant R134a, the system exergy recovered are 62%, 64% and 66% of the exergy input for mass flow rates of 0.48, 0.72, and 0.96 kg/min, respectively. On the other hand, the overall system coefficient of performance for R404a clathrate shows lower values when compared to R134a formation. For R404a, the system coefficient of performance varies between 2.9 and 3.48 while the exergetic efficiency varies between 38% and 58%. At the operating compressor speed of 2300 rpm and refrigerant R404a, the system exergy recovery are about 52%, 55% and 58% for mass flow rates of 0.48, 0.72 and 0.96 kg/min, respectively. Current results show that the thermal system operates more efficiently with R134a refrigerant than with R404a refrigerant. It also shows that the best system performance is achieved at the lowest compressor speed while the effect of refrigerant mass flow rate is insignificant. These results are in agreement with an earlier study by Kiatsiriroat et al. using refrigerant R12 and R22 [1] and [2]. Finally, the current research results conclude to use of R134a refrigerant to form the clathrate hydrate in thermal storage systems.

Search Terms: Refrigerant clathrate hydrates, gas hydrates, clathrate formation, cold thermal energy storage, R134a and R404a calthrates, direct contact heat transfer, COP

Table of Contents

List of Figures

List of Tables

Nomenclature

C_p	Specific heat (kJ/kg)
$\dot{E}x_{rec}$	Rate of exergy recovered during the charging period (kW)
$\dot{E}x_{in}$	Rate of exergy flow-in during the charging period (kW)
Δh	Enthalpy change during the charging process (kJ/kg)
Δh_l	Latent heat of refrigerant hydrate (kJ/kg)
m_{ref}	Mass of refrigerant inside the direct storage tank (kg)
m_{water}	Mass of water inside the direct storage tank (kg)
m_{cl}	Mass of refrigerant clathrate hydrate inside the storage tank. (kg)
$\dot{m}$	Mass flow rate of refrigerant during the charging process. (kg/s)
N	Revolution per minute
Q_{evap}	Total load inside the direct thermal energy storage. (kJ)
$\dot{Q}_{evap}$	Rate of heat removal inside the storage tank. (kW)
$Q_{total-exp}$	Total energy stored (Experimental) .(kJ)
$Q_{total-mod}$	Total energy stored (Model) .(kJ)
Δt	Time change (s)
$Tavg$	Average charging Temperature (℃)
$T_{in-evap}$	Refrigerant temperature into evaporator. (℃)
T_0	Ambient temperature. (℃)
$\dot{W}_{comp}$	Rate of work of the compressor. (kW)

Greek Symbols

η_v	Volumetric efficiency of the compressor	-

Subscript

avg	Average
cl	Clathrate hydrate
cl,tank	Clathrate hydrate inside storage tank

$comp$	Compressor
$cycle$	Actual cycle
$evap$	Evaporator
exe	Exergy
exp	Experimental
h	Enthalpy values
i	Specific time
$Ideal$	Reversible (ideal) cycle
l	Latent heat
phc	Phase change
ref	Refrigerant
$ref, tank$	Quantity of refrigerant inside the tank
s	Sensible heat
sim	Simulation
$total$	Total charging time

Abbreviations

COP	Coefficient of performance
CTES	Cold thermal energy storage
HTF	Heat transfer fluid
HVAC	Heating ventilating and air conditioning
LHES	Latent heat energy storage
PCM	Phase change materials
TES	Thermal energy storage
VSD	Variable speed drive

Chapter 1: Introduction

1.1 Thermal Energy Storage

Thermal energy storage (TES) systems have been the main topic of research in the field of energy management for the last few decades due to their potential for storing thermal energy. They are considered to be the most promising and competitive solution for storing efficient thermal energy. Thermal energy storage systems are defined as temporary systems that hold thermal energy for later use [3,4]. This thermal energy can be in the form of cold thermal energy or hot thermal energy. The importance of TES systems lies in their capability to save cold thermal energy for later use which leads to savings in electrical power. One of the main advantages of TES is its capability of managing the mismatch of electricity between supply and demand. Furthermore, TES plays an important role in converting accessible electrical power to thermal energy and saving it for later use. This conversion of power can be employed to reduce energy consumption or transfer the energy load from peak periods to un-peak periods. Implementing thermal energy systems in buildings can help power producer (power stations) to manage the load and at the same time help power consumption (residents and factories) to improve the performance of conventional air-cooling systems. For example, storage of thermal energy would improve the performance of a power generation plant by load leveling, lead to higher efficiency and lower generation costs. Simultaneously, TES systems would help in shaving the peak electrical load consumed by commercial buildings and shifting it from daytime to nighttime. Usually, the electric load consumed during the day time is more than consumed at night time; Therefore, TES systems help in managing the electric load and balancing any mismatch between demand and supply of the electric load.

In general, TES systems are an important element of energy saving management for a variety of sectors such as the residential, commercial, industrial, and transportation sectors. The primary objective of TES systems is to alter energy patterns to promote a cleaner environment and financial savings. A cleaner environment and financial savings can occur by achieving the following points; Firstly, the use of surplus energy where the consumption of purchased energy can be reduced by storing surplus thermal energy such as heat collected from solar panels instead of water heater.

Secondly, shave of peak demand by production of thermal energy during of off peak hours and utilize it during high demand period. Thirdly, defer of conventional equipment by replacing or integrating new saving technologies with conventional equipment. Mainly, TES systems are integrated with conventional HVAC systems for cooling/heating applications. The influence of TES with HVAC systems has inspired many researchers to study such systems more deeply. Integrating TES with HVAC systems has helped greatly in reducing electric bills for buildings.

Thermal energy storage is mainly used to store thermal energy during periods of low electric tariffs. Then, during periods of high electric tariffs, the stored energy is used to cool a space, based on the stored temperature. One prospective technique of storing thermal energy is by using phase change materials (PCMs). Thermal energy systems use PCMs as the storage materials or media for storage purposes. It is reported by Zalba [5] that over 150 materials are used in research as PCMs for TES systems, while only 45 materials are commercially utilized.

In general, TES and PCM are of great importance in the field of storing thermal energy. There are two fundamental areas for studying thermal energy storage systems. The first area is related to the study of PCMs used in thermal storage and the second area is studying the heat exchangers for TES systems. Figure 1 shows the most important fundamentals in the study of thermal energy storage.

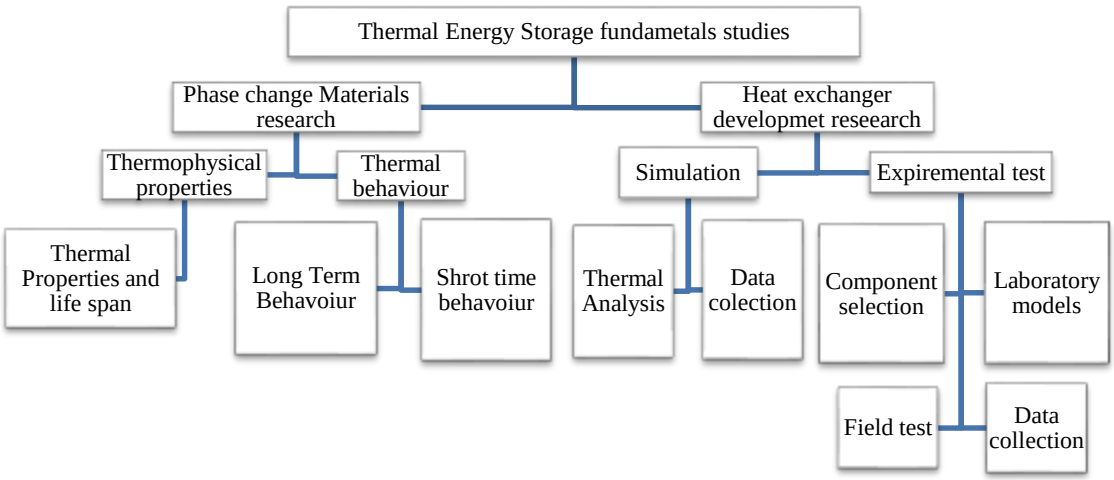

Figure 1: Fundamental areas for studies of thermal energy storage systems and properties. [5,6]

There are two main types of TES systems, latent heat thermal energy storage (LHTES) systems and sensible heat thermal energy storage (SHTES). PCMs, used in TES, can store internal energy in a sensible form or in a latent form. This is related to the internal energy of the PCM used in TES system. An overview of major storage forms is shown in Figure 2.

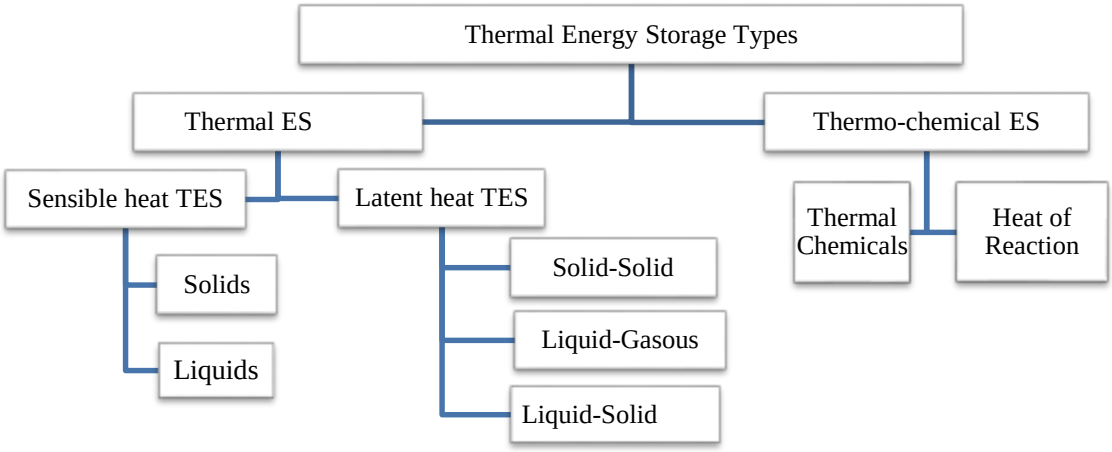

Figure 2: Types of thermal energy storage based on heat classification [6]

1.2 Significance of the Research

Heating, Ventilating and Air Conditioning (HVAC) systems are among the largest systems that consume electricity in buildings. This fact has forced researchers and engineers to focus on issues of energy management to manage the high load demand in buildings through different integrated systems [7]. A closer look at electricity consumption by HVAC systems shows noticeable findings; for example, HVAC systems consumes over 50% of the electricity in United States [8]. In Europe for example, electricity consumed by HAVC systems is around 40 % in commercial and residential buildings [9]. In Australia, 70 % of electricity is used for HVAC systems [10]. In the Middle East, more than 70 % of building electricity consumption is for cooling systems [11]. In general, it was estimated that the world electricity consumption increased by 58 % between the years 2001 and 2005 [10], in which more than 60 % is due to the HVAC system high electricity consumption. The growing reliance on HVAC systems in residential and commercial buildings has resulted in a huge increase in electricity demand. Therefore, developing methods to manage the high load demand of

HVAC systems will result in huge savings in electrical power consumed by HVAC systems.

Some methods are implemented to reduce the high load demand of HVAC system in buildings. One of these methods is to use thermal energy storage systems [12-14]. Thermal energy storage systems are capable of managing the high load demanded by HVAC systems by shifting the load demand of HVAC systems from on-peak to off-peak periods to level the cooling load in buildings.

Thermal energy storage systems are widely used in different building applications that are occupied during the day working hours, such as office buildings [15], hospitals and schools , churches and mosques [16,17] . In cold thermal energy storage systems, the energy is stored at low temperatures, usually below 10℃. Therefore, thermal energy can be classified according to the thermal medium stored [18]. For example, thermal storage can occur by sensible or latent storage. For sensible thermal storage, the chilled water technique is the most used technique in thermal storage in buildings. For the latent thermal storage, ice, ice slurry, and phase change materials are among the most used thermal storage techniques. Clathrates hydrates of refrigerants are considered among the phase change materials which are capable of storing thermal energy. In this research, clathrate hydrates of refrigerants are investigated as a storage medium for thermal storage systems. Thermal energy storage systems with refrigerant clathrate hydrates as a storage medium plays an important role in load management when integrated with buildings HVAC systems to manage the cooling load.

The cooling load can be managed by using a full load thermal storage or a partial load thermal storage. In the full load thermal storage, the compressors in the HVAC chillers are stopped to operate in on-peak hours and the building cooling demand is supplied from the thermal storage system. In the partial thermal storage, the load is shared between the chillers and the thermal storage system. Compared to conventional HVAC systems, HVAC using the thermal storage technique offers various advantages such as electricity managements, cost savings, system operation improvements, system capacity extension and equipment size reduction. Therefore, this study focuses on developing a thermal system that is capable of storing energy using clathrate hydrates of refrigerants. The system is built and designed to investigate the effect of different tested parameters with alternative refrigerants.

1.3 Literature Review

Direct cold thermal energy storage with refrigerant clathrate hydrates as a storage medium is the main topic of this thesis. Cold thermal storage systems are of great importance in the field of cooling and air conditioning. One of the main objectives of this thesis is to study different refrigerants clathrate hydrate which can be used in cold thermal energy storage systems. The importance of studying refrigerants for clathrate hydrate lies in their ability to save thermal energy. For example, most commercial buildings in tropical parts of the word use a tremendous amount of energy for HVAC systems. As a result, the electricity demand increases during the day time. Implementing direct cold thermal energy storage system with conventional air conditioning systems helps in shifting the electricity load from day time, peak time, to night time. This shifting is done by storing cold energy during the night and then utilizing it when needed or during the daytime.

Clathrate hydrates are group of non-stoichiometric, ice-like crystalline compounds formed through a combination of water molecule and CFCs molecules. It has been proven by many researchers that many chlorofluorocarbons (CFCs), hydroflourocarbon (HFCs) and hydro-chlorofluorocarbons (HCFCs) can combine with water molecules to form clathrate hydrate [19-25]. During clathrate hydrate formation, water molecules behave like a host substance while CFCs or HCFCs behave as a guest molecule.

The common gas hydrate crystalline structures are classified into three structures: structure s-I, structure s-II, and structure s-H, where each structure is composed of a certain number of cavities formed by water molecules. Refrigerant clathrate hydrate can form due to the interaction between refrigerants (i.e R134a, R22, R11, R404a, R407c…etc) and water under a hydrate formable temperature condition (5–12 °C). Refrigerants such as R12, R11, R21, R31, R141b, R22, R142b, R134a, R152a, and R125 can be utilized to form refrigerant clathrate hydrate, serving as guest molecules when contacting with water in a proper thermodynamic state.

Refrigerant clathrate hydrates are used in many applications in engineering science. The most particular use of refrigerant clathrate hydrate is in application of refrigeration, and air conditioning [26,27] . However, applications with CFCs are restricted due to environmental issues.

The advantage of using clathrate hydrates in application such as air conditioning and refrigeration is their ability to freeze at a temperature higher than water freezing temperature. Furthermore, refrigerant clathrate hydrates are used in the water desalination and treatment application. These applications use clathrate hydrate because only water can form clathrate hydrate at ambient temperature and atmospheric pressure [28]. Cold thermal energy storage system with refrigerant clathrate hydrates is integrated with buildings air conditioning systems (or what is known as buildings' chiller) to use the night surplus electric power to store thermal energy for daytime use [29].

Thermal storage systems using ice as a storage medium are integrated with HVAC systems which show a remarkable progress in load management due to their latent heat of fusion [30-33]. However, the ice manufacturing process for thermal storage requires a unique unit to achieve temperature below the freezing of ice. Therefore, storing thermal energy with temperature higher than the ice freezing point is a promising technology for managing the on-peak and off-peak cooling load demand of HVAC systems. Clathrate hydrates with thermal energy storage system have been demonstrated to be the most promising candidates for managing cooling load in HVAC systems [34,35]. Clathrate hydrate, or refrigerant hydrate, with a latent heat of fusion similar to that of ice, could be used as a storage medium for thermal energy systems.

Studying the behavior of refrigerant clathrate hydrates of HFCs and HCFCs is important to predict models and to generate comprehensive experimental data for these clathrate hydrates. Some research [24,36-38] are used to propose different model to predict the formation conditions of refrigerant clathrate hydrate. A thermodynamics model using the van der Waals and Platteeuw soild solution theory was used by Eslamimanesh et al. [28] to model the phase equilibrium of clathrate hydrates of refrigerant. They use a thermodynamic model (van der Waals-Platteeuw soild solution theory) for modeling phase equilibrium conditions of refrigerants R134a, R152a, R32, and R141b. The results of their model are compared to experimental data. By using the proposed method of dissociation pressure and temperature, they obtained to the results summarized in Table 1.

Table 1: Absolute average deviations of the hydrate dissociation pressure using van der Waals-Platteeuw soild solution theory

Refrigerant	Temperature Range (C)	HydrateDissociation Pressure (psig)
R-134a	(-7.84) - (10.34)	(6.87) - (60.48)
R-141b	(-4.74) - (8.34)	(1.131) - (5.83)
R-152b	(-8.43) - (15)	(11.19) - (64.35)
R-32	(0.85) - (20.94)	(25.16) - (215.96)

A general model using the cubic plus association equation of state (CPA Eos) for modeling the liquid phase and van der Waals-Platteeuw statical model for the hydrate phase was used by Nikbakht et al. [39] for estimating the hydration dissociation of refrigerant 1,1,1,2-tetrafluoroethane or R134a, 1,1-dichloro-1-fluoroethane or R141b and 1,1-difluoroethane or R 152. Another research by Karamoddin and Varaminiam [40] uses different models to estimate the hydration dissociation conditions of chloro-difluoro-methane, 1,1,1,2-tetrafluoroethane and 1,1-difluoroethane refrigerants using cubic simple equation of state (SRK and VPT) and the cubic plus association equation of state (CPA) to model the vapor and liquid phase, while the van der Waals-Platteeuw model was used for the solid hydrate phase.

In recent years, investigations of refrigerant clathrate hydrate with thermal systems are being studied to integrate such technology with air conditioning system to shift the cooling load from peak hours to off-peak hours. For example, electric power demand for air conditioning units has been increasing during the past few decades. This high consumption of electric power by air conditioning units can be managed by using refrigerant clathrate hydrate with thermal storage system. These kinds of cold management are called “load leveling” or “load shaving”.

A study conducted by Wu and Wang [46], shows different refrigerants that can form refrigerant clathrate hydrate and be utilized to store thermal energy. They show that cold clathrate hydrate and storage systems are used to store cold gas hydrate during the summer night, and then discharge the cold energy during the daytime.

They further investigate cold clathrate hydrate of refrigerant R134a with some additives. They concludes that the magnitude of the heat formation of refrigerants R134a and R141b clathrate hydrate are estimated to have a little difference from the heat formation of refrigerant R12 and R11 clathrate hydrate. They show that the degree of sub-cooling decreases when adding additives. They further show that the formation rate of clathrate hydrate is greatly accelerated by adding reasonable proportions of the additives. The results summarized by Jianghong et al. show that adding additives with the storage medium helps the dissolution rate of clathrate hydrate to accelerate, causing an increased release rate of the cold energy stored. The influence of different additives such as calcium hypochlorite or benzenesulfonic acid on the dissolution process of clathrate hydrate is studied more by Bi et al. [41].

Another study was conducted by Mori and Mori [42] to reveal the physical process of clathrate hydrate formation in the storage tank built-in vapor compression refrigeration cycle. Mori et al use refrigerant R12 as a working fluid that flows into a storage tank (heat exchanger) where refrigerant R12 and water are filled in a liquid state. Their experiment results in a cooling of the stored fluids (R12 and water) in the heat exchanger and then formation of R12 refrigerant clathrate hydrate as a cooled storage medium. They conclude their experiments by observing that clathrate hydrate appears in two different forms, making separate layers in the heat exchanger. The two separate layers are: one in the form of slurry particles appears at the bottom of the heat exchanger, and one as floating foam on the free surface of the water phase inside the heat exchanger.

Studies such as Bi et al. [41] and McCormack [43] conducted detailed comparison direct contact thermal energy storage and indirect contact thermal energy storage. The results of their research are summarized in Table 2. Another study by Abdullah A. K. et al. [44] studies the growth rate of gas hydrate for refrigerant R22. Their test is made in a direct contact heat transfer crystallizer. They aim to investigate the three phases (vapor, liquid, and soild) of hydrate R22 in the direct heat transfer crystiliser. Abdullah's et al paper shows a numerical and experimental formation rate of gas hydrate in the crystallizer. The experimental parameters used are different initial temperature,different initial column height,different initial R22 drop diameter, and different R12 flow rates.

Table 2: Comparison between charging process of direct contact and indirect contact thermal energy storage systems

System mode	Advantage	Disadvantage
Charging process for direct contact TES	-High heat transfer performance between the PCM and refrigerant used -High temperature returning to the compressor -Indirect evaporator (heat exchanger) is not needed. -Low energy consumed by compressor	-Oil separator is needed -Filters are needed to dry any pass of water vapor to compressor
Charging process for indirect contact TES	-Filters are not needed since the water in evaporator is separated from the refrigerant -Oil separator is not needed - Regular refrigeration cycle -Regular compressor needed	-Evaporator heat exchanger is needed. - Relatively poor heat transfer between the water and refrigerant.

The results of their research shows an increase of clathrate hydrate with time and with the varation of the following parameters: First, by decrease in the initial temperature difference between the continous phase and R22 refrigerant drops. Second, by deacrease in the initial water level in the column. Third, by increase in the flow rate of refrigerant R22 drops. They further, concludes that adding additives such as active sodium chloride into the water has a storage inhibitting effect on the gas hydrate formation rate.

A study by Thonwik et al. [45] observe clathrate hydrates during ice formation between carbon dioxide and water in direct contact with a heat tank. The experiment is divided into two parts; For the first part, the carbon dioxide is mixed with water at a temperature of -15 to -60 ℃, and water temperature of 28℃ to exchange heat directly. The flow rate of carbon dioxide varies between 0.18 and 1 kg/min, while the volume of water is between 1 and 3 L.

While conducting the experiment, it is found that the effectiveness of the direct contact heat transfer between the carbon dioxide and the water is close to 100%. For

the second part, they studied the thermal behavior of the direct contact heat transfer technique between carbon dioxide and water. From his research, the following is concluded: 1) A decrease of water temperature is directly proportional to the mass flow rate of carbon dioxide and inversely proportional to the volume of water and the inlet temperature of carbon dioxide. 2) The effectiveness of a direct contact heat transfer between carbon dioxide and water is close to 100%. 3) The mass flow rate of carbon dioxide and temperature difference between the inlet and outlet of the storage tank are directly proportional.

Wu and Wang [46] studied the development of refrigerant R134a hydrate's potential in a cool storage tank with alcohol additives. The system they used was used to test the performance of both cool storage and release process and their industrial application. Their results show that adding n-butanol additives in a certain percentage (1.34%) accelerates the cool storage rate. They show that the lumped hydrate density increases apparently compared to pure R134a hydrate running. They conclude by adding additives to eliminate the hydrate floating during the hydration process, will leads to smooth and stable cool storage operation of the clathrate hydrate formation.

In summary, a review of the open literature sources shows different studies of refrigerant clathrate hydrate in terms of formation process, thermal storage capacity, and its potential in air conditioning applications. An overview of previous studies related to clathrate hydrate of different refrigerants is summarized in Table 3. In this research, the cold thermal storage of two refrigerants are investigated. The effect of variable a speed compressor and variation of mass flow rate are the main contribution to the previous work conducted to study clathrate hydrate. Furthermore, this research contribute to literature the best operating condition to form refrigerant clathrate hydrate and the time needed for charging process. This research mainly provides a comparison between refrigerant R134a and R404a in terms of system performance and in term of different working fluids to form refrigerant clathrate hydrate.

Table 3: Overview of previous studies related to cold storage system with different refrigerants

Author	Ref	Method used	Technique	Report Results
Eslamimanesh et al. [28]	R134a, R152a, R32, R141b	Theoretical Modeling	Van der Waals-Platteeuw Soild Solution theory	Results shows that the thermodynamic model well predict the experimental data in [24]
Bi et al. [41]	R141b	Experimental Research with Additives	Cold storage system	Research shows that the dissolution rate of gas hydrate accelerated, and cold energy released rate of cool storage system increase with additives
Kendoush et al. [44]	R12	Experimental Research	Direct transfer heat exchanger	Results shows that the clathrate hydrate of R12 will increase with time during the charging process and with variation of flow rate of R12
Wu and Wang [46]	R134a	Experimental Research with Additives	Cold storage System	Results shows that the degree of sub-cool decrease when adding additives. Adding additives helps dissolution rate of cold storage to accelerate
Xie et al. [47]	R141b	Experimental Research	Cold storage Apparatus	Research shows that decreasing of the coolant temperature and increasing the coolant flow rate increase the cold energy

1.4 Research Methodology

Different types of refrigerants used to form clathrate hydrate for cold thermal energy storage systems are discussed within this investigation. Experimental and theoretical studies are conducted to evaluate the performance of the direct storage system with different refrigerants at different parameters. A literature survey on direct thermal energy storage system is first collected. Different available resources related to clathrate hydrate are studied to understand the energy stored in direct thermal energy storage system with alternative refrigerants. The energy stored with different refrigerants is then modeled thermodynamically. The theoretical analysis mainly focuses on the first and second law of thermodynamics. Once the theoretical analysis is conducted, experimental tests are conducted to verify the theoretical results obtained using refrigerant properties. The main tools to evaluate the thermal energy system with different refrigerants hydrate are the energy and the exergy analysis. Both energy and exergy analyses are used to study the effect of different parameters on the overall performance of the system. Variable parameters such as compressor speed and refrigerant mass flow rate are used to study the effect of each on the overall performance of the storage process.

1.5 Objective and Scope

Recent research shows that phase change materials (PCMs) are considered to be a good candidate for storing thermal energy. Water in particular is considered to be the most effective thermal carrier due to its high latent heat of fusion. Therefore, this thesis mainly studies a comparison between refrigerant R134a and R404a in direct cold thermal energy storage (CTES) to form refrigerant clathrate hydrate as a storage medium. Within the research, a thermal energy storage apparatus is designed and built to investigate different clathrate hydrates of refrigerants for direct thermal storage. Thermodynamic assessments are conducted to study different refrigerants with storage systems. The apparatus used for direct cold storage was designed to work under different speeds by using a variable speed drive. It was also designed to work with different refrigerants. Furthermore, the apparatus is capable of operating in single stage and multi stage direct storage. It consists of a direct contact storage tank, variable speed compressor, manual expansion valve, and water-cooled condenser.

This research mainly focuses on using a single stage direct storage system with different refrigerants. Furthermore, this research compares between clathrate formation of refrigerant R134a and refrigerant R404a.

Thermodynamics assessment for different refrigerants are studied and analyzed in order to find the best control/operating strategy in terms of heat transfer fluid inlet temperature, refrigerant mass flow rate, and energy / exergy efficiencies to achieve high storage performance.

Various experimental and theoretical parametric studies are carried out for different refrigerants and the results are discussed. The goals of these experiments are 1) to verify the mathematical equations used to model the thermal storage system experientially, 2) to determine the conditions under which clathrate hydrate formed for the tested refrigerants, 3) to study the characteristics of the system while forming different clathrate hydrates, and 4) to study the time at which clathrate formed.

Parametric studies are carried out for the storage system to investigate the effect of the selected parameters on the behavior of the storage system. The studied parameters used are the mass of water, mass flow rate of refrigerant, compressor speed and type of refrigerant. The working principles of the charging process of the thermal energy storage system are also studied under different operating parameters.

The outcome of this investigation includes a detailed analysis of the amount of cold energy stored, the mass of clathrate hydrate forms of different refrigerants, the overall temperature distribution inside the storage tanks during the cold storage process, the effect of compressor speed on the performance of the system, the characteristics of refrigerant R134a as a working fluid and refrigerant R404a as a working fluid.

The scope of this research involves studying different refrigerants at different operating conditions. The first and second laws of thermodynamics analysis are used as a tool to investigate the performance of each refrigerant within the thermal storage system. Different parametric studies are conducted and the best operating condition is chosen for high performance and low exergy destruction.

1.6 Problem Statement

Managing the electricity consumption of a building's HVAC systems is becoming increasingly important due to the increase in demand of heating and cooling and due to the environmental impacts caused by conventional fuels. Therefore, finding novel systems to manage cooling load in buildings without affecting indoor air quality is an ongoing research topic. One way of achieving load management in HVAC systems is to design thermal energy storage systems that can be integrated with an existing HVAC system. Every thermal storage system has specific design requirements and each presents opportunities for load management. Load management in HVAC systems can be achieved by designing thermal storage systems that are capable of integrating with HVAC systems to make more use of load leveling. Recent research has demonstrated that a combination of thermal storage technologies can offer effective solutions for load management and thermal comfort. Therefore, the topic of this research aims to develop a design of a cold thermal energy storage system using clathrate hydrates of refrigerants as a storage medium. Developing a thermal system with clathrate hydrates of refrigerants as a cooling medium for thermal energy storage systems is the main topic of this research. The design of the direct system discussed within this research can help in reducing the high consumption of HVAC systems and level the load at on-peak hours.

1.7 Thesis Organization

This thesis is divided into six chapters through which they evaluate the performance of the thermal energy storage system used to conduct the tests for different refrigerant hydrates. The first chapter provides a general background about thermal storage systems and the importance of such technologies. Survey of previous work related to thermal storage system and clathrate hydrates of refrigerants are discussed in first chapter. Furthermore, the objective and methodology of the research is presented in this chapter. Chapter 2 provides a classification of thermal energy storage systems. Some sections in Chapter 2 discuss indirect contact thermal storage system (Ice TES systems) and compare them to direct contact thermal energy storage system (Clathrate hydrate TES system). More related information such as phase change materials descriptions and applications are discussed in this chapter.

Chapter 3 shows the mathematical model of the direct thermal energy storage system built to conduct the experiments. The modeling of the components mainly focuses on the direct storage tank and the compressor of the thermal system. Chapter 4 provides a brief discussion of the experimental test components used in conducting the experimental results. All the components used in the testing lab to conduct the experiments are described in details in this chapter. The main results and analysis for thermal energy storage system with clathrate hydrate are summarized in chapter 5. All the obtained results for the system with the tested parameters of R134a and R 404a are represented and compared in Chapter 5. The last chapter in this thesis, Chapter 6, presents the conclusion and the recommendations of the research.

Chapter 2: Thesis Background

2.1 Classification of TES

Energy storage in thermal energy systems are classified into three types or methods: sensible, latent, and chemical methods of storing heat. In sensible heat storage, the heat capacity is determined by the specific heat of the medium (c_p) and the temperature change of the stored medium (ΔT). The temperature change in sensible heat storage depends on the application of heat storage. The use of latent heat in energy storage increases the energy capacity as previously explained. By considering the change of temperature in the sensible part and the phase change in the latent part, more capacity of energy can be stored in thermal systems. The following sections briefly explain the energy in sensible and the latent in thermal storage systems.

2.1.1 Sensible heat TES

In a sensible heat TES, energy or heat is stored by heating or cooling a storage medium through a heat transfer process between the storage medium and the heat transfer fluid (HTF). The sensible heat of the storage medium of a TES can be calculated by Equation 2.1 where the amount of heat stored depends on the specific heat of the medium, the temperature range, density, and the amount of storage material

$$Q_{sensible} = \int_{T\_initial}^{T\_Final} m\, C_p dT \qquad (2.1)$$

For example, water has a specific heat of 4190 J/kg, a temperature range of 0-100 ℃, and a density of 1000 kg/m^3. The temperature range mentioned 0-100 ℃ is excluding the phase change. The sensible heat capacity of some selected solid–liquid materials is shown in Table 4. The amount of heat stored depends on the specific heat of the material, temperature change, and the amount stored. Some materials like water, oil, specific kinds of rock bricks, concrete, and sand are good examples of materials used as energy storage mediums.

2.1.2 Latent heat TES

In latent heat TES, heat is absorbed or released when a storage material undergoes a phase change from solid to liquid or liquid to gas or vice versa. The constant heat released or heat gained during storage is then utilized, and this corresponds to the phase transition temperature of the phase change material.

Table 4: List of selected solid-liquid materials for sensible heat storage [48]

Medium	Fluid type	Temperature range (°C)	Density (kg/m3)	Specific heat (J/kg. K)
Rock		20	2560	879
Brick		20	1600	840
Concrete		20	1900-2300	880
Water		0-100	1000	4190
Caloriea HT43	Oil	12-260	867	2200
Engine oil	Oil	Up to 160	888	1880
Ethanol	Organic liquid	Up to 78	790	2400
Proponal	Organic liquid	Up to 97	800	2500
Butanol	Organic liquid	Up to 118	809	2400
Isotunaol	Organic liquid	Up to 100	808	3000
Isopentanol	Organic liquid	Up to 148	831	2200
Octane	Organic liquid	Up to 126	704	2400

The storage capacity of the latent heat with phase change materials is shown by the following equation [48]:

$$Q_{Latent} = \int_{T\_initail}^{T_{phC}} mC_p dT + m\Delta h_{latent} + \int_{T_{phc}}^{T\_final} mC_p dT \qquad (2.2)$$

The latent heat energy is much higher than the sensible heat energy for a given medium. For example, when water in its liquid phase changes to ice (solid ice), the latent heat at atmospheric pressure is around 334 kJ/kg. Among all the thermal heat storage techniques, latent heat energy storage (LHES) is the most attractive technique

used in storing thermal energy due to its ability to provide high energy and storage density, and in its ability to store thermal heat at a constant temperature due to its material characteristics.

In this research, the concept of latent heat TES is focused on. Within this thesis, several experiments were conducted to study the latent energy in a direct thermal storage system. Two heat transfer fluids such as refrigerant R134a and refrigerant R404a were used to conduct the experiments with water to form a new compound named clathrate hydrates.

2.2 Phase Change Materials for TES Applications

In thermal storage systems, phase change materials are used to store the thermal energy. The substance or material used as the phase change material can be organic or inorganic. Organics phase change materials are paraffin and fatty acids and inorganic phase change materials are aqueous salts solutions. Organic and inorganic phase change materials show a single melting point when they are pure, and show a range of melting points when they are mixed. The application of phase change material in energy storage is mentioned in some literature such as [49-51] for cooling buildings. For peak load shifting, some literature [52-54] provide information for peak shifting and seasonal storage. Phase change materials can be used to offer a thermal protection against hot or cold environments. This protection is due to the high thermal inertia. For instance, these materials are used to protect solid food, beverages, pharmaceutical products, biomedical products, and some chemical products. The following properties of phase change materials for thermal storage can be summarized from the literature [52,55]. Cold energy storage technologies that are suitable for air conditioning applications can be classified based on the type of a storage medium and the form in which the storage medium is used. Many researchers have provided reasonable analyses for most of the common storage media and phase change materials used in thermal storage systems.

Table 5: Characteristic of phase change material used for thermal storage

Thermo-physical Property	Characteristic of PCM
Thermo-physical	-Melting temperature in the desired operating temperature range. -High latent heat of fusion per unit volume. -High specific heat to provide additional significant sensible heat storage. -High thermal conductivity of both solid and liquid phases. -Small volume change on phase transformation and small vapor pressure at operating temperature. -Congruent melting of the phase change material for a constant storage capacity of the material with each freezing/ melting cycle.
Nucleation and crystal growth.	-High nucleation rate to avoid sub-cooling of the liquid phase during solidification, and to assure that melting and solidification process occurs at the same temperature. -High rate of crystal growth, so that the system can meet the demand for heat recovery from the storage system.
Chemical properties.	-Complete reversible freeze/melt cycle. -No degradation after a large number of freeze/melt cycles. -No corrosiveness to the construction/encapsulation materials. -Non-toxic, non-flammable and non-explosive.
Economics.	-Abundant. -Available. -Cost effective. -Easy recycling and treatment. -Good environmental performance based on live cycle -Assessment (LCA).

2.3 Direct Contact TES Systems

Storing thermal energy using clathrate hydrates as a storage medium has shown great promise in cooling efficient facilities. Clathrate hydrate (or refrigerant gas hydrate) are ice-like crystalline compounds in which small molecules are entrapped in a cage of water molecules under high pressure and low temperature [39]. Latent heat thermal storage with clathrate hydrates has proven the efficiency and effectiveness of storing cold energy in direct energy storage systems. Clathrate hydrates of refrigerants are also known as inclusion compounds formed by the inclusion of molecules of one kind of guest substance in the cavities of the crystal lattice of another host substance [56]. Clathrate hydrates are characterized to have a high heat of formation which makes them ideal materials for cold storage. The density of clathrate hydrates is extremely high; therefore it is possible for thermal systems using clathrate hydrates as a storage medium to provide a high cooling capacity equivalent, or one that is much larger than the conventional storage such as water/ice or chilled water storage. High density can be considered as one of the advantages of clathrate hydrates. For clathrate hydrates of refrigerants to be capable of thermally stored, they must be formed at an atmospheric pressure and temperature range between 5℃ to 13℃. Clathrate hydrates are formed by directly mixing water and refrigerants at a certain pressure and temperature. One disadvantage of this energy technology is that the quantity of refrigerant used as a working fluid for the refrigeration unit might decrease with the formation process of clathrate hydrate.

The system used in this research consists of a direct thermal energy storage system and a fan coil unit (FCU). The purpose of the FCU connected with the direct thermal storage system is to utilize the cold energy stored. The FCU is used as a heat exchanger with internal coils connected inside the storage tank. The internal coils are used to discharge or melt the clathrate hydrate, cold stored material, formed. Therefore, when the cold energy is needed, warm fluid is directed through internal discharge coils which melt the clathrate hydrate that previously formed. As the cold storage material melts, a boundary layer of water forms between the discharge coils and the remaining clathrate hydrate. This separation layer causes the heat transfer between the cold medium and the discharge coils to be through natural convection rather than conduction.

For the direct thermal energy system used in this research, water is kept at a certain quantity inside the tank where it will mix with refrigerant. Usually, the refrigeration unit is used to charge the thermal storage system. The quantity inside the tank represents the quantity of energy stored. Different refrigerants have different storage quantities based on the latent heat of fusion of the refrigerant used. Table 6 shows the latent heat of fusion, formed pressure and temperature of some selected refrigerants which are used for clathrate hydration.

Table 6: Thermal properties of guest material for refrigerants hydrates [57]

Guest Material of Refrigerant Gas Hydrate	Type	Hydrate Melting Point Temperature (℃)	Pressure (atm)	Hydrate Fusion Heat (kJ/ kg)
Chlorofluorocarbon				
CFC 12	R12	11.8	4.39	316
CFC-11	R11	8.5	0.54	334
Hydro-chlorofluorocarbon				
HCFC-21	R21	8.7	1.00	337
HCFC-31	R31	17.8	2.82	427
HCFC-142b	R141b	8.4	0.42	344
HCFC-22	R22	16.3	8.15	380
HCFC-141b	R141b	8.4	0.42	344
Hydro-fluorocarbon				
HFC-134a	R134a	10.0	4.10	358
HFC-152a	R152a	15.0	4.34	383
HFC-125	R125	11.2	9.44	362

Direct thermal energy storage with clathrate hydrates (or refrigerant clathrate hydrates) has many advantages compared to the other thermal storage technique. This technique of thermal storage is given the name “direct contact thermal energy storage system” due to the direct interaction between the water and the heat transfer fluid, which is in this case R134a or R404a. There are three types of refrigerant hydrates: (S-I, S-II, and S-H) as shown in Figure 3.

Different types of hydrates can be formed under different conditions. For this study, refrigerant clatharte hydrates, which are mainly the type S-II gas hydrates formed under low pressure (below 1 MPa) with a suitable phase change temperature for a thermal storage system.

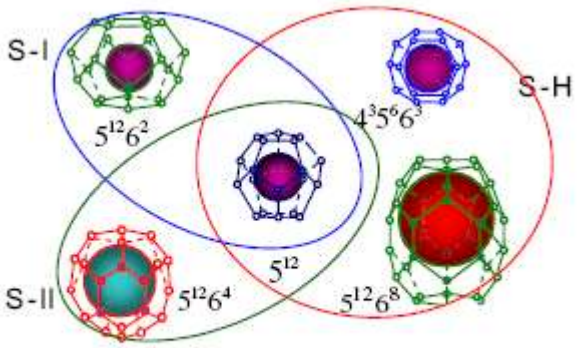

Figure 3: Types of hydrate structure and their cage arrangement [58]

Refrigerant clathrate hydrates have high heat of fusion ranges between 270-430 (kJ/kg) as shown in Table 6. Refrigerants gas hydrates have the ability to form during the charging period and to dissolve during the discharging period with a large latent heat of fusion. Based on the information in Table 6, it is obvious that refrigerants gas hydrates have a larger heat of fusion than other technique used for thermal storage such as eutectic salts, paraffin waxes, and fatty acids. Direct thermal energy storage systems with latent heat of fusion near to that of ice have shown the advantage of allowing the use of chilled water as a circulation medium rather than antifreeze coolant or brine, which are used in indirect thermal energy storage systems (ice storage systems). It can also be seen from Table 6 that the melting temperature of some refrigerant hydrates is a little higher. This melting temperature can be reduced through additional additives such as $NaCl$, $Cacl_2$ and ethylene glycol to make hydrates more suitable for air conditioning applications [57].

2.4 Indirect Contact TES Systems

The most popular thermal storage system is the ice storage system. The forming of 1kg of ice requires a removal of 152 kJ of heat. Similarly, adding 152kJ of heat to ice will turn it to water. An ice thermal storage system operates in the fashion of adding

or removing heat from water. The processes of thermal energy storage will be explained below and ice thermal storage will be studied as an example of a thermal storage system.

In the past 20 years, much efforts has been spent researching topics of thermal energy storage and particularly latent heat thermal energy storage. Water as a storage medium is the most commonly used phase change material for cold storage latent heat. According to Dincer and Rosen [3], latent heat thermal energy storage has attracted an increasing interest due to its high volumetric capacity and low heat transfer losses. Today, there are more than 150 PCM suitable for latent energy storage, some of which some are commercialized, while the rest are in the literature. Despite some of the disadvantage of ice storage systems such as low melting temperature, ice storage is the most extended period phase change material and is used for long term cold storage. Ice storage has a; high latent heat capacity (335 kJ/kg), high specific heat, and high density.

Ice thermal storage system is usually integrated with HVAC systems for cooling applications. During the early hours of the day, buildings require a minor cooling capacity. During this time, the chiller of the building is used to charge the ice storage system or in other words to form ice in the storage ice tank. Producing ice during off-peak periods is economically an effective measure for shifting on-peak period power demand to the off-peak nighttime hours [58]. Since the electricity price during off-peak hours is lower than that of on-peak hours, implementing an ice storage system in the air conditioning system is a cost-effective measure, and its application is increasing [59-63].

Note that ice forms at a temperature of 0℃, thus a specific cooling unit are used to achieve this low temperature. This process of forming ice is called the *charging process* of the thermal system. After ice is formed, it stays for a certain period in the storing tanks. This process is called the *storing process.* At noon time, when chillers are usually run at full load, the role of the ice storage system begins. Now in buildings where the ice storage system is integrated with HVAC systems, the full load of the chiller is reduced and the cooling needed by the building is covered by both the HVAC and the ice storage system systems. The process of utilizing coolness from ice storage systems is called *discharge process.*

Chapter 3: System Modeling and Analysis

3.1 Introduction

In this section, the mathematical modeling of the main components of direct thermal storage system is presented. The direct thermal storage system host two main processes: charging and discharging. The charging process occur during the production of cold energy, while the discharging process is the utilization of the stored cold energy. To formulate the mathematical model of the system, the mass flow rate of refrigerant is varied between 0.48 kg/min and 0.96 kg/min. The compressor is regulated by a variable speed control varying from 2000 rpm to 3000 rpm. The mass of water in the tank is fixed at 11kg for all experiments. The refrigerants used within this experiment are R134a refrigerant and R404a refrigerant. The system starts by evacuating all the air inside then inject water and liquid refrigerant to the direct storage tank. The refrigerant is directly mixed with water to extract the heat. The pressures and temperatures are recorded after and before all components. The temperature of the tank is measured during the charging process with six thermocouples located at different locations around the storage tank. After the clathrate formation inside the storage tank, the compressor is shutdown. The cold energy is stored for some time and then utilized. A discharging unit is used where water passes through the tank through direct copper coils to melt the clathrate and extract the energy. The following sections discuss the modeling of the system's main components.

3.2 System Modeling and Assumptions

The direct thermal energy storage system is modeled using the components of refrigeration units such as a compressor, condenser, evaporator and expansion valve. The thermal storage system behaves like the evaporator of the refrigeration unit but it is modeled to have a direct contact heat transfer between the refrigerant and stored load. The following assumptions are made to model the components using the thermodynamic properties of refrigerants:

(1) Steady state operation of the system is assumed.

(2) Efficiency of the compressor is assumed to be 80%.

(3) Heat transfer to the surrounding is assumed to be negligible.

(4) Pressure drops in connections and copper coils are assumed to be negligible.

(5) All the components are assumed to be insulated.

Besides the previous assumptions, the following assumptions are made for the thermal analysis for the direct storage tank of the cold thermal energy storage system

(6) The density of the refrigerants hydrate stored is independent of the temperature.

(7) The sensible energy of refrigerant hydrates is small, thus neglected in both the liquid and solid phases.

(8) The heat transfer is modeled as a direct contact heat transfer.

For the analysis of the thermal storage system, there are four points used before every component through which the properties of the refrigerant are studied and analyzed during the charging time. State 1 is considered to be before the compressor. State 2 is considered to be before the water cooled condenser. State 3 is before the expansion valve and the last state, State 4, is before the storage tank. Figure 4 shows all the points analyzed for the thermal storage system. Note that all modeling points are shown similar to the single stage refrigeration unit with some assumptions discussed in this section to describe the energy storage system.

Figure 4 shows the Temperature-Enthalpy diagram of a single stage thermal energy storage system. All points shown in figure are based on the idea of operating compression refrigeration unit and used the evaporator as a thermal energy storage tank. The compression efficiency and the pressure drop in connection and pipes are assumed within the modeling of system. EES software is used to model the thermal energy storage system. The software uses the properties of the two tested refrigerant to get the cooling load and values of enthalpies that is required for the analysis of the two refrigerants. The collected modeling results of the system are then compared to the experimental results for verification.

For State 1: the pressure (P_1) is saturation pressure at the temperature of the storage tank. The enthalpies at state 1 (h_1) are found using the storage tank outlet temperature and the saturated pressure at the storage tank temperature. The entropy (s_1) is also found using the pressure and temperature at State 1.

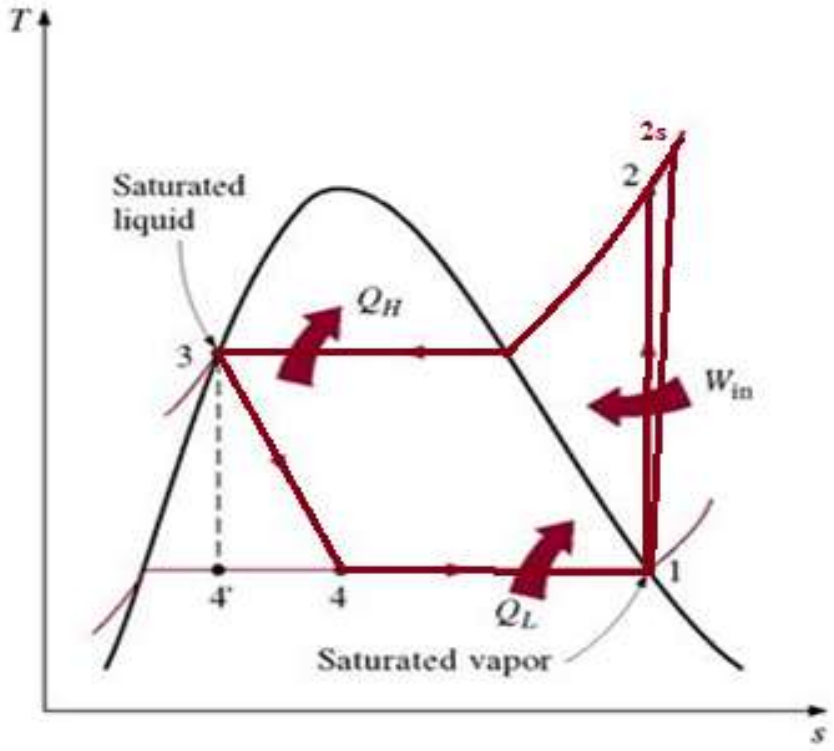

Figure 4: Temperature-Entropy diagram of single stage refrigeration system

For State 2: ideal compression is considered thus the entropy at State 2 is similar to the entropy at state 1. State 2s is found with a compression efficiency of 80% and (h_2). The pressure at State 2 is found using the compression ratio across the compressor. For State 3: the pressure is considered the same as (P_2) with 5% drop in pressure due to the condenser coils and the phase change of refrigerant. The entropy and enthalpy at state 3 are found by using (P_3) and the liquid saturated properties at (P_3) with saturated liquid quality. For State 4: the quality of refrigerant is first found using the enthalpies of the saturated liquid and the saturated gas at the storage tank temperature. The enthalpy at State 4 is found using the quality at State 4 and the saturated vapor and saturated liquid at the storage tank pressure line. All the codes and values generated for refrigerant R134a and R404a are shown in the Appendix C. A program is developed with the Engineering Equation Solver program (EES) to model of the thermal storage system.

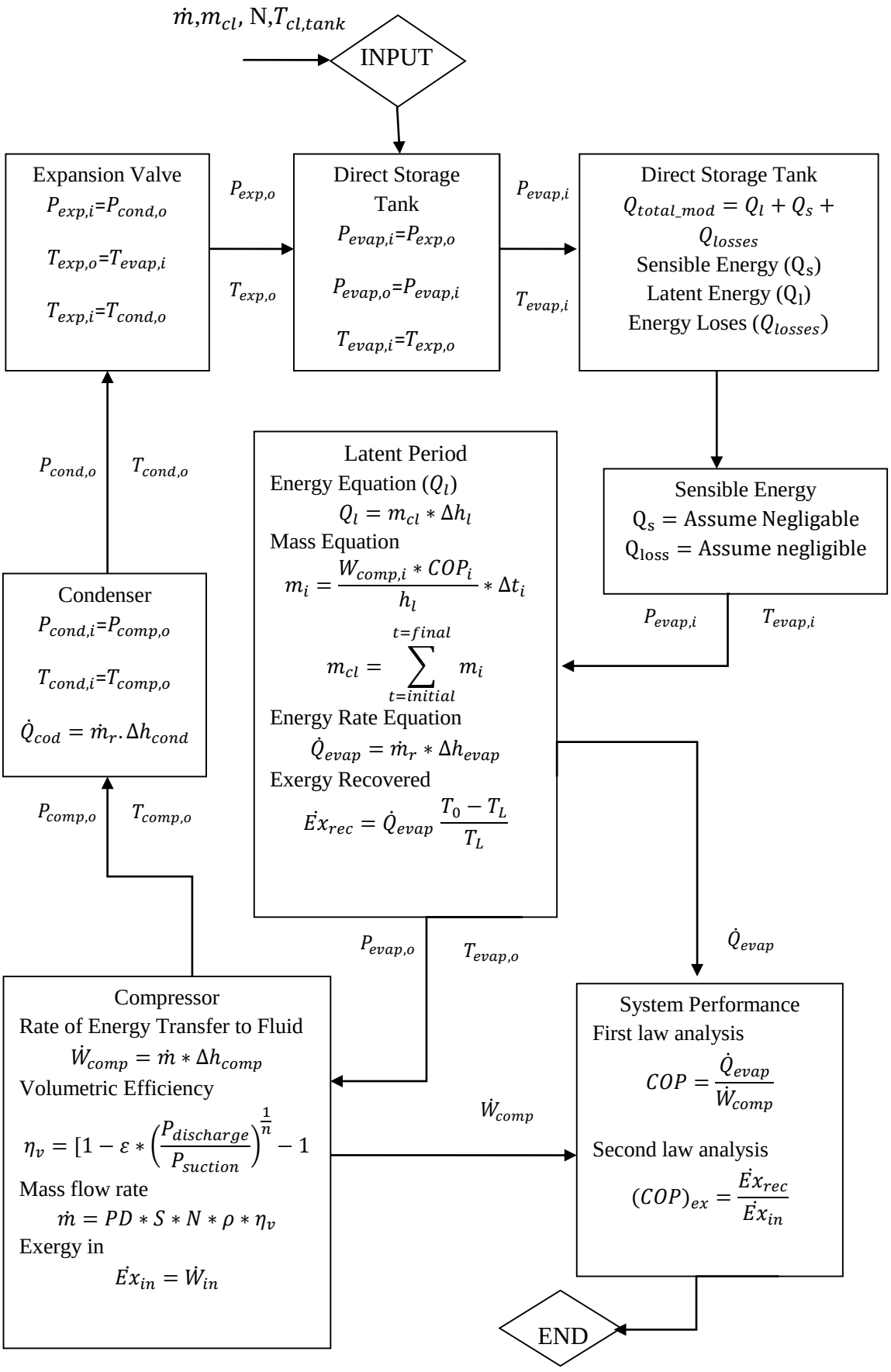

Figure 5: Flow chart for modeling the thermal energy storage system

3.3 Direct Storage Tank Modeling

The system used to form refrigerant clathrate hydrate has been given the name *"*direct thermal storage system" due to the direct mixing between water and refrigerant. The direct thermal storage system consists of four main components namely the direct storage tank, condenser, compressor and expansion valve. The processes used in the experiment are charging and discharging. In the charging process, heat is removed from the thermal direct tank through the vapor refrigeration unit. The storing and the discharge part will be discussed in Chapter 5. The following section discusses the modeling of each component through different operations.

The total energy inside the direct thermal energy storage tank can be modeled using the following equation

$$Q_{total\_mod} = Q_l + Q_s + Q_{losses} \tag{3.1}$$

where the term (Q_l) represents the total latent heat of the storage medium inside the storage tank in kJ/kg. The term (Q_s) represents the sensible heat of the storage medium in kJ/kg. The term (Q_{losses}) represents the total heat losses from the storage tank. Due to the minor losses from the storage tank and due to the short period of the sensible heat of the storage medium, the two terms are canceled from the analysis of the energy inside the storage tank. Therefore, the total energy is modeled using the latent heat stored inside the tank and shown by Equation 3.2:

$$Q_l = \left(m_{water} + m_{ref,tank}\right) * \Delta h_l \tag{3.2}$$

where the terms $\left(m_{water} + m_{ref,tank}\right)$ represent the total mass of water and refrigerant 134a or 404a filled in the storage tank. The term (Δh_l) represents the latent heat of refrigerant clathrate in kJ/kg : (i.e. 358(kJ/kg) for R134a, and ~ 380(kJ/kg) for R404a). The rate of heat removal inside the tank is represented by

$$\dot{Q}_{evap} = \dot{m}_r * \Delta h_{evap} \tag{3.3}$$

As shown in the energy equation inside the tank (Equation 3.2), the quantity of energy stored mainly depends on the mass of water and the mass of refrigerant injected into the system.

The modeling of the total storage medium or total mass of clathrate formed is shown in Equation 3.4a and 3.4b, where the summation of clathrate mass (m_i) at

instantaneous time (Δt_i) gives the total mass of clathrate formed inside the thermal storage tank (m_{cl}).

$$m_i = \frac{\dot{W}_{comp,i} * COP_i}{h_l} * \Delta t_i \tag{3.4a}$$

$$m_{cl} = \sum_{t=initial}^{t=final} m_i \tag{3.4b}$$

where the terms ($\dot{W}_{comp,i}$) represent the instantaneous work to the compressor at time in (kW) at a specific time (Δt_i), (COP, i) represents the instantaneous coefficient of performance of the system using the energy transfer to the fluid equation at time (Δt_i), and the term (h_l) represents the latent heat of fusion of clathrate hydrate as per Table 6. The limits in Equation 3.4b represent the initial and the final time during the thermal charging process.

3.4 Compressor Modeling

During the cold storage of refrigerants hydrate, the compressor model could be characterized using the following equations. The work to the compressor can be modeled using the enthalpies across the compressor.

$$\dot{W}_{comp} = \dot{m}_r * \Delta h_{comp} \tag{3.5}$$

The volumetric efficiency equation can be expressed by the pressure ratio and the clearance volume percentage $\varepsilon = 0.04$ as follows

$$\eta_v = [1 - \varepsilon * \left(\frac{P_{discharge}}{P_{suction}}\right)^{\frac{1}{n}} - 1 \tag{3.6}$$

The volumetric efficiency of the compressor can also be expressed in term of mass flow rate and piston displacement by using the actual mass flow rate compressed by the compressor divided by the piston displacement at the suction point.

$$\eta_v = \frac{\dot{m} * v_{suction}}{V * N} \tag{3.7}$$

where the terms (V) represent the cylinder displacement volume (m^3/s), ($\dot{m}$) is the mass of refrigerant, and the term (N) represent the speed of the compressor.

Combining the volumetric efficiency using the pressure ratio and the clearance volume, the following equation for the modeled mass flow rate is derived;

$$\dot{m} = PD * S * N * \rho * \eta_v \tag{3.8}$$

where the terms (PD) represents the cylinder displacement volume, (N) is the number of revolutions per minute, (S) is the number of cylinders, and (ρ) is the density of the saturated vapor at the compressor inlet. The term (η_v) represent the volumetric efficiency of the compressor shown in Equation 3.7. Figures 6 and 7 show the modeling of the compressor power at different compressor speeds. It is clearly shown that the compressor will consume more power when operating with R404a refrigerant. The cooling load for R134a and R404a system is modeled using equation 3.2 and shown in table13 and 14. The ratio of water to refrigerant used for refrigerants R134a and R404a are 2.23:1 and 1.84:1 respectively.

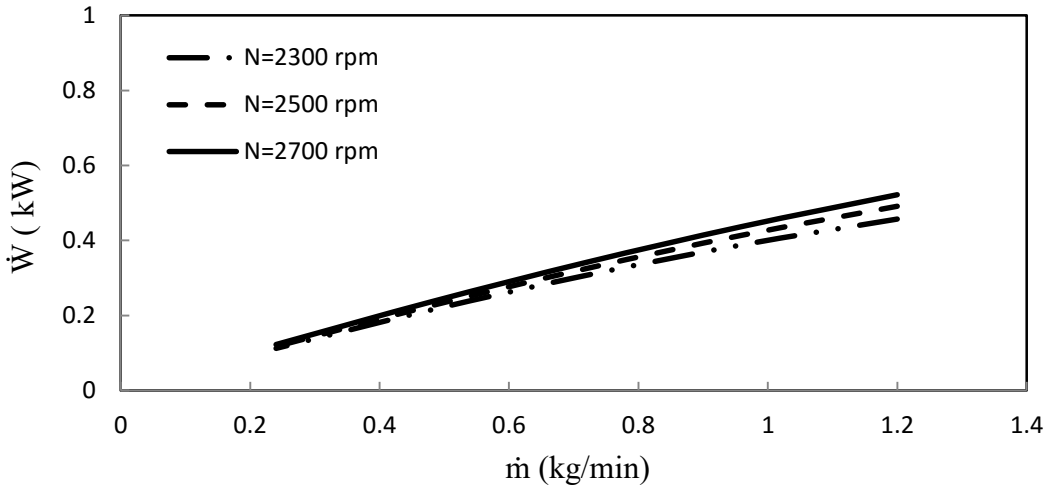

Figure 6: Effect of R134a refrigerant mass flow rates on compressor power at different compressor speeds

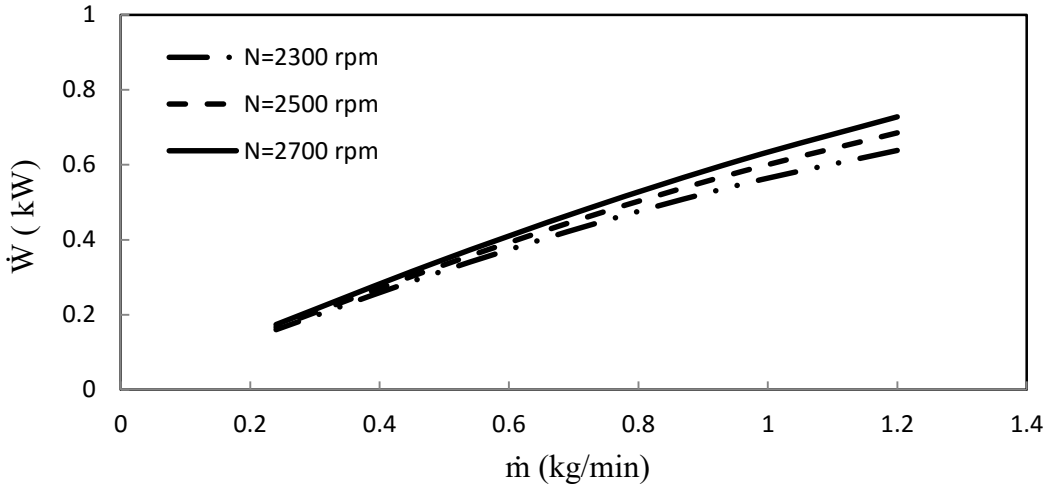

Figure 7: Effect of R404a refrigerant mass flow rates on compressor power at different compressor speeds

3.5 System Performance

The coefficient of performance of the system during the charging process can be modeled by using the energy transferred to the refrigerant (R134a or R404a) using Equation 3.5 and the rate of heat extracted from the direct tank using Equation 3.3 .Therefore, the COP of the system can be found using the following equation:

$$COP = \frac{\dot{Q}_{evap}}{\dot{W}_{comp}} \tag{3.9}$$

While modeling the performance of the thermal energy storage system, it is found that R134a has a better performance than R404a, therefore, R134a shows a better COP at the modeled variables. Figures 8 and 9 show the modeling of the coefficient of performance of the storage system at different compressor speeds and variable refrigerant mass flow rates. These figures show that as the mass flow rate increase, the coefficient of performance will increase. In addition, figures 8 and 9 also show that high compressor speed has lower COP when compared to runs of low compressor speed. The cooling load of R134a system is modeled using equation 3.2 and has a value of 5703 KJ/kg, while the cooling load for system R404a is 6452 kJ/kg. The cooling load for both refrigerants is modeled based on a fixed quantity of water equal to 11 kg.

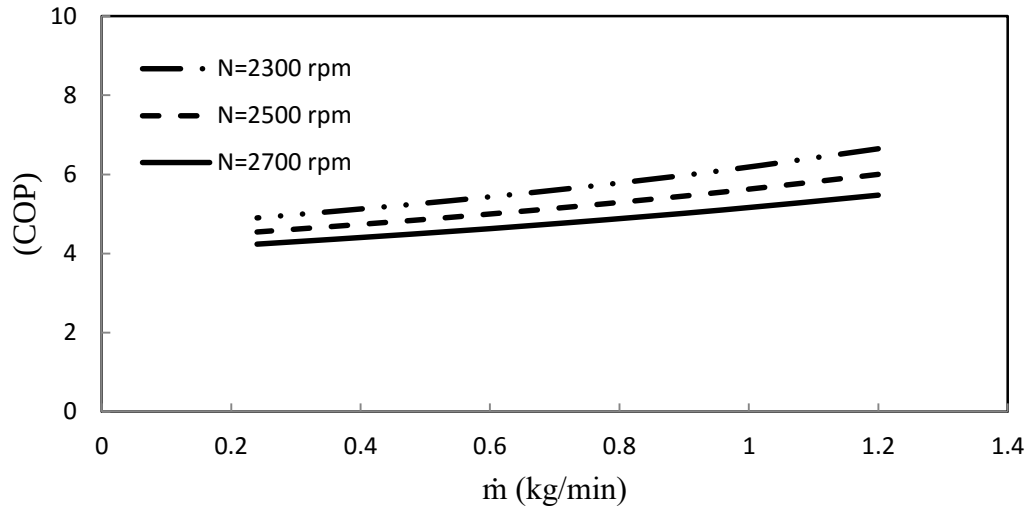

Figure 8: Effect of R134a refrigerant mass flow rate on system energetic efficiency at different compressor speeds

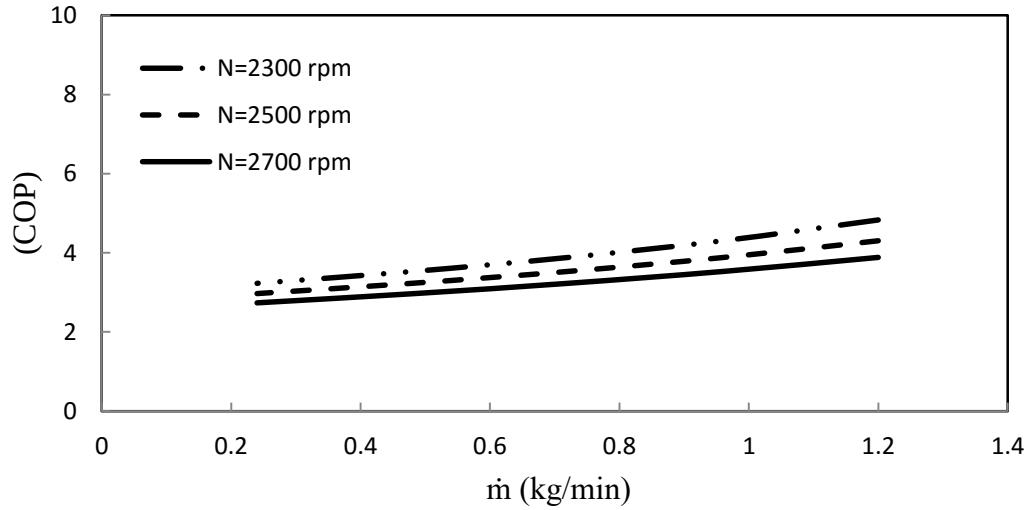

Figure 9: Effect of R404a refrigerant mass flow rates on system energetic efficiency at different compressor speeds

The second law analysis of thermal storage systems is very distinct from the first law analysis as it introduces new concept to evaluate the system. Therefore, the analysis based on the second law needs to be discussed and modeled for the experimental evaluation.

The second law of the system can be modeled using two ways; Firstly, by using the coefficient of performance shown by the following equation:

$$(COP)_{exe} = \frac{COP_{cycle}}{COP_{ideal}} \tag{3.10}$$

Secondly, it can be modeled by using the exergy recovered and the exergy supplied equation as follows:

$$(COP)_{exe} = \frac{\dot{E}x_{rec}}{\dot{E}x_{in}} \tag{3.11}$$

where the exergy recovered can be calculated by equation 3.12, and the exergy input can be calculated by Equation 3.13. The term T_L represents the temperature inlet to the direct tank

$$\dot{E}x_{rec} = \dot{Q}_{evap}\,\frac{T_0 - T_L}{T_L} \tag{3.12}$$

$$\dot{E}x_{in} = \dot{W}_{in} \tag{3.13}$$

Therefore, the exergy analysis or the second law analysis of the system is modeled to give a clear idea about the performance of the storage process. Figure 10 and 11 shows the performance of the system based on the exergy analysis for direct thermal storage systems with refrigerant R134a and refrigerant 404a. It is noted that the exergetic efficiency at low compressor speed will be higher than high compressor speed. Furthermore, it is noted that R134a has higher exergetic efficiency than R404a at the same modeling conditions. The relation in Figures 10 and 11 shows the relation between the mass flow rate of the working fluid and the exergetic efficiency. The relation shows that as the mass flow rate of refrigerant increase, the exergetic efficiency of the system will also increase. This relation is verified experimentally in this research.

The flow chart of modeling the thermal energy storage system is shown in Figure 5. The energetic and exergetic efficiencies of the system are modeled. The work to compressor and the cooling load are used for energetic efficiency. The exergy in and the exergy recovered are used for exergetic efficiency of the system The input variables to the systems are the mass flow rate of refrigerant, the clathrate hydrate mass of different refrigerant, the speed of the compressor, and the initial temperature of mixtures of water and refrigerant inside storage tank.

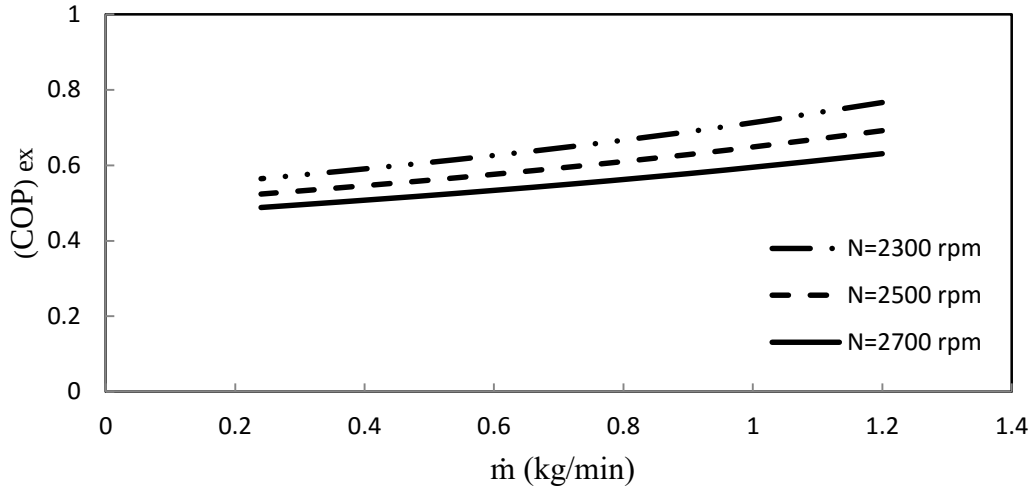

Figure 10: Effect of R134a refrigerant mass flow rate on system exergetic efficiency at different compressor speeds

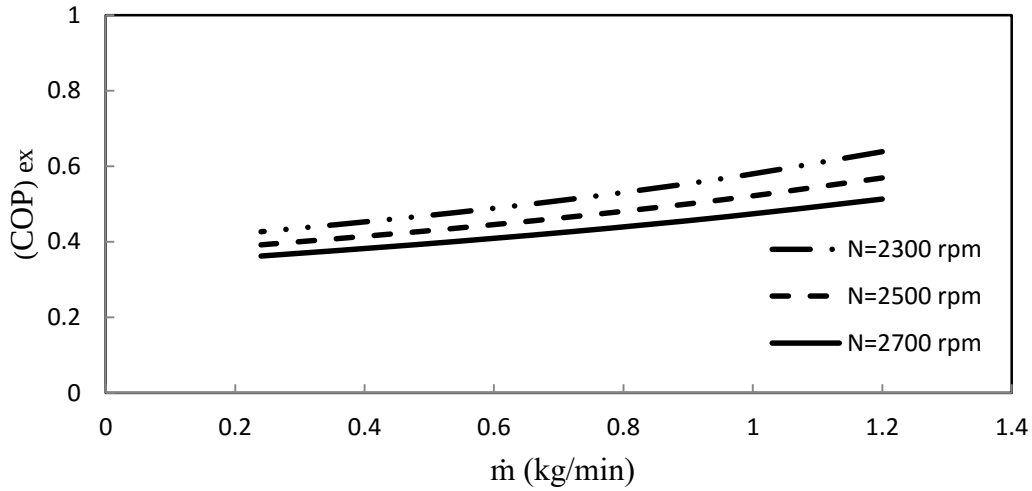

Figure 11: Effect of R404a refrigerant mass flow rate on system exergetic efficiency at different compressor speeds

Chapter 4: Experimental Test Facilities

4.1 Introduction

The system used to form refrigerant clathrate hydrate consists of different components. These components are divided in this research into three categories: main components, complementary components, and data acquisition components. The main components are the thermal storage tank or evaporator, compressor, condenser and expansion valve. The complementary components are the refrigerant receiver, oil separator, sight glass, and charging connection. Other complementary components are integrated into the system to ensure its safety; such as pressure safe switch, relief valve, suction line accumulator. The system is connected to discharging unit which consists of a fan coil unit, condenser pressure regulator, cooling tower, and circulation water pump. Figure 12 shows the experimental apparatus of thermal energy storage. The following chapter will examine the function of each component separately. Further, the system is designed to work in two different operation stages such as single stage and multi stage operation. The following chapter will further discuss the different operational stages of the system. All the experimental data collected are set with single stage operation. More discussion about system operation modes such as single and multi-stage operation of direct storage system is presented in this chapter.

Figure 12: Picture view of the experimental direct thermal energy storage test rig

4.2 Experimental Test Facility

In this thesis, an experimental system is designed and built to support the formation of clathrate hydrate of different types of refrigerants. Further, the system is designed to work at different operation stages, namely single-stage and multi-stage, and for different thermal storage namely indirect and direct storage system. The schematic diagram of the experimental test rig is shown in Figure 13. The system is designed to have the following operating conditions

I. Single-stage operation with a single direct storage system
II. Multi-stage operation with a single direct storage system
III. Single-stage operation with a single indirect storage system
IV. Multi-stage operation with a multi storage systems

Within this research, only one operating condition is discussed: single stage operation with direct storage system. The direct system is supported by pressure gauges and thermocouple before and after all components. All the data collected from the system is then sent to the data acquisition.

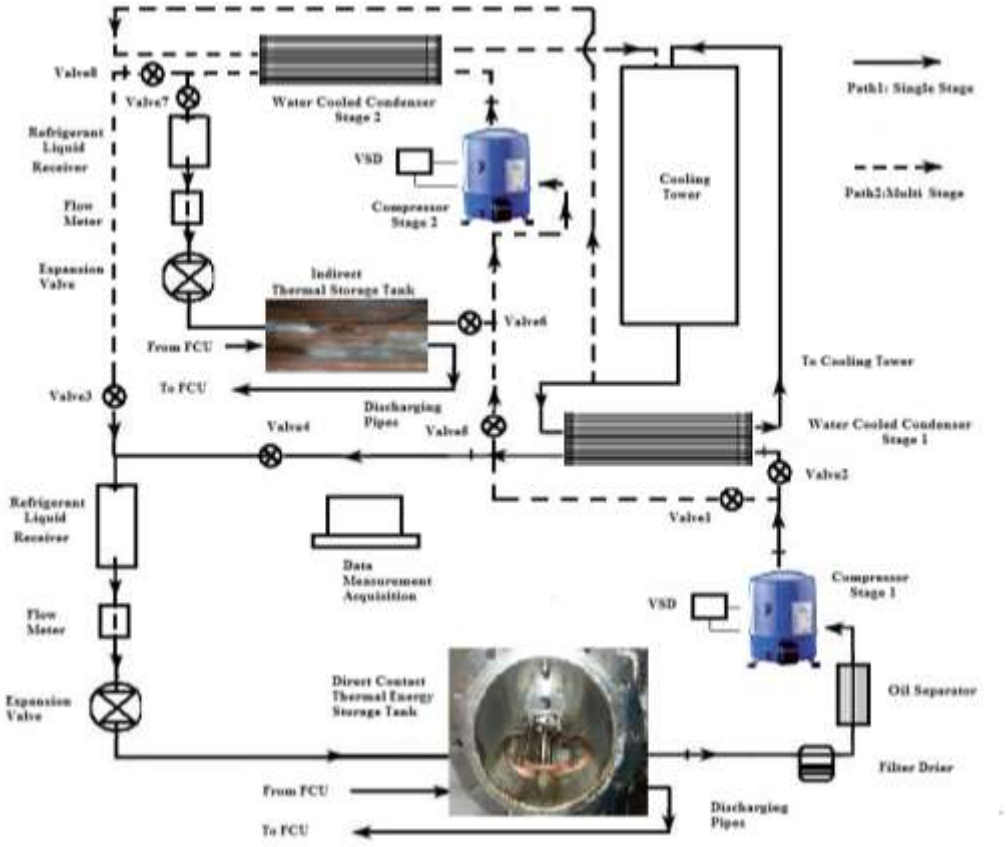

Figure 13: Detailed experimental schematic apparatus used for thermal storage

The system shown in Figure 13 consists of different thermal storage cycles combined in one system. The system is capable of storing energy in two different operations: direct and indirect operation. A system that stores energy directly is called a “direct thermal energy storage system”. The direct thermal storage system consists of two main stages: a single-stage and a multi-stage stage. Each stage is designed to work separately or as a dual operation. During the operation of the single stage, some valves are closed (valve 1 and valve 3) to allow the refrigerant to pass through the required components (i.e. path 1). Similarly, for multi-stage operation, valve 2 and valve 4 should be closed to run the system (i.e. path 2). Vales 5, 6, 7, and 8 are always closed during the operation of the direct thermal energy storage system. The common part in both stages is the direct thermal storage tank. The storage tank is designed to exchange heat with internal discharging coils connected with a fan coil unit. Normal tape water is used to pass through the discharging coils inside the storage tank to exchange heat and return back to the fan coil unit. The fan coil unit further exchanges the cold released to cool the surrounding air. The process of discharging the thermal storage tank is explained in section 4.3.1 under the title “Experimental Apparatus and Procedure”.

4.2.1 Single stage operating mode with single direct storage system

The single stage system used in this work is illustrated in Figure 14. The system consists of a vapor compression cycle with a direct mixing evaporator. The evaporator of the system directly mixes the refrigerant and the water to form new cold compound called clathrate or refrigerant clathrate hydrate. Since the refrigerant is injected directly into the water to extract the heat it is called “a direct contact thermal energy storage system”. Such a direct system requires some extra auxiliaries added to the normal refrigeration unit such as filters driers, oil separator, sight glasses, and refrigerant receivers. Filter driers are added to the system to capture any moisture that might be carried by the refrigerant vapor to the compressor. Therefore, a filter drier is placed after the storage tank and another is placed before the compressor to insure complete dryness and removal of moisture for longer time.

A refrigerant receiver is located after the condenser to ensure a continuous liquid refrigerant supply to the expansion valve. This will ensure a stability of the mass flow through the whole running process. To ensure a liquid flow of refrigerant through the expansion valve, a sight glass is placed in the liquid line, before the expansion valve,

to observe the refrigerant flow. The sight glass has two levels from which the refrigerant level can be monitored. Bubbles seen through the sight glass indicate a shortage in refrigerant in the system. The presence of bubbles or a decrease in the level of refrigerant seen in the sight glass indicates that the rate of energy across the storage tank is reduced, or there is a shortage in refrigerant. More description of the system's component is presented in the following section. Figure 14 shows the main components of the single stage system used experimentally in this thesis. The specifications of the direct storage system components are illustrated in Table 7.

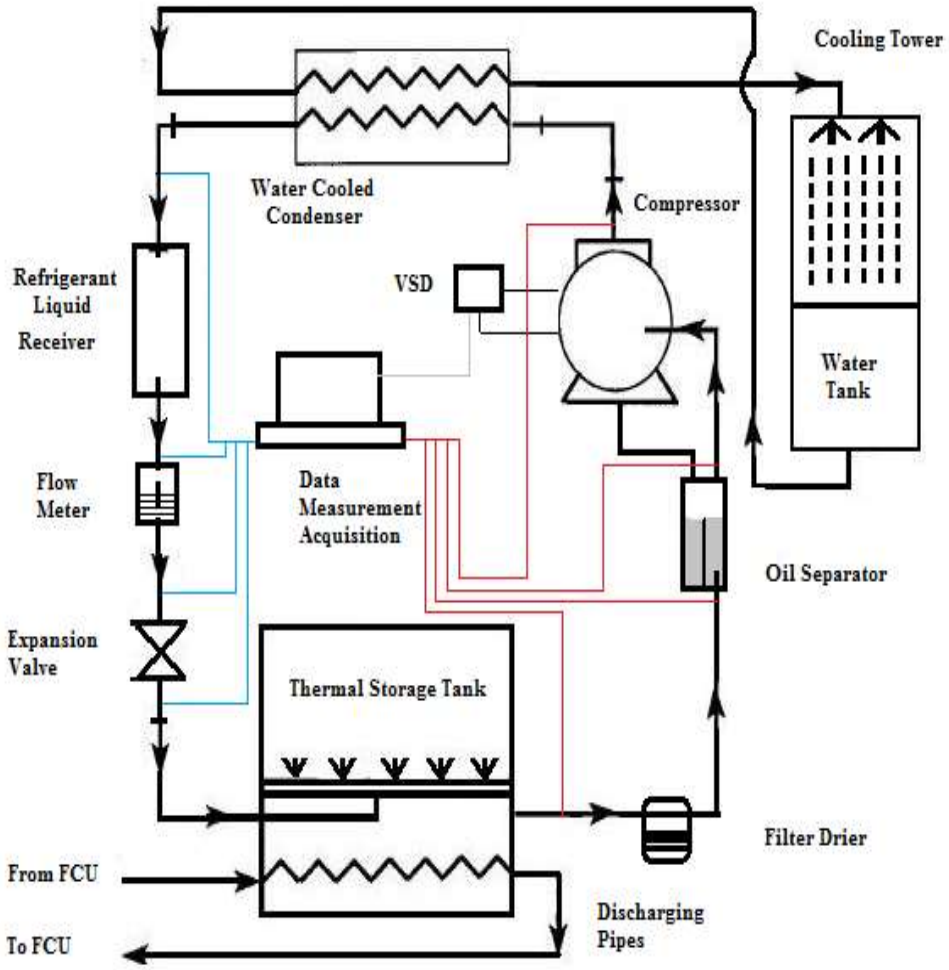

Figure 14: Rig components for direct thermal energy storage system

Table 7: Rig components used for single-stage direct TES system

Component	Specification
Compressor	MTZ Hermetic Reciprocating (Danfoss Maneurop Compressor)
	Capacity:1.5Hp, Nominal speed 3600 rpm
Condenser	Water-cooled brazed plate heat exchanger. Load:2.2kW
	Parallel flow, 30 plates
Expansion Valve	Manual expansion valve
Flow meter	Normal refrigerant flow meter. Range (0-1.5LPM)
	Platon made flow meter
Receiver	Refrigerant receiver for liquid refrigerants
	Danfoss receivers
Oil Separator	Normal refrigeration cycle oil separator
	Danfoss oil separator
Evaporator	Stainless steel direct mixing heat exchanger. (Inner diameter 40 cm),
	(Tank length 90 cm)
Filter Dryer	Normal filter dryer .Type DCR. Volume 2.350 L

4.2.2 Multi stage operating mode with single direct storage system

The multi stage direct thermal energy storage system consists of five main components: a direct storage tank, two compressors, a condenser, and an expansion valve. The components of the multi-stage direct thermal system is almost the same as the single stage direct thermal system with a difference in the number of compressors used. In multi stage thermal storage two compressors were used to achieve the cooling process. The thermal energy storage system used in this experiments are able to work in two separate stages; single and double stage. The schematic diagram in Figure 66 (Appendix B) shows the multi-stage cycle. Table 21 (Appendix B) shows the characteristics of the components in a multi-stage direct thermal storage system.

4.3 Single Stage Experimental Apparatus and Procedure

4.3.1 Experimental apparatus

The experimental direct thermal energy storage system used in this research to form refrigerant clathrate hydrate is shown in Figure 15.

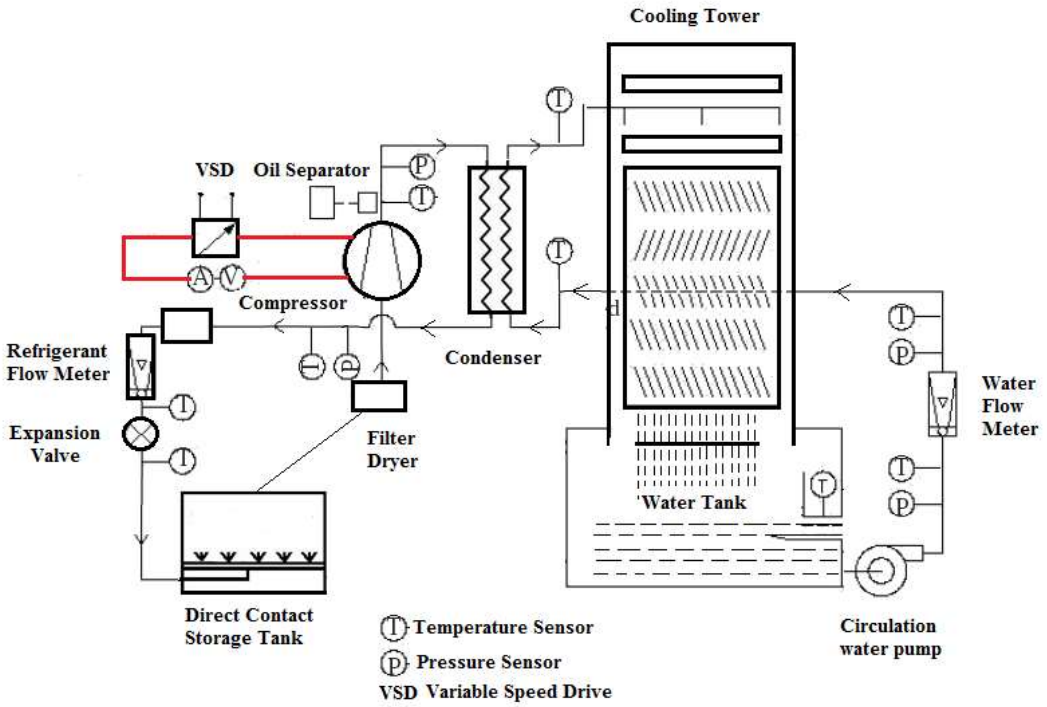

Figure 15: Experimental apparatus for direct thermal energy storage system

The system in Figure 15 shows a direct thermal energy storage system with a direct storage tank and an interior refrigerant distributer connected to a fan coil unit. Cold thermal load is formed inside the stainless steel cylinder tank (storage tank) with a diameter of 40cm and length of 90 cm. The tank is supported with an inner refrigerant distributer to enhance heat transfer inside the tank. Figure 16 shows the stainless refrigerant distributer inside the storage tank.

Figure 16: Refrigerant distributer inside the direct storage tank

The inner stainless refrigerant distribution was designed to centralize the storage tank where refrigerant bubbles flow from the bottom side of the distributer to the top. The stainless refrigerant distributer has one main inlet and 64 exit holes. The holes are arranged in two neighboring pipes to ensure the temperature in the tank is even. Red copper heat exchanger coils are mounted inside the storage tank for the discharging function. A water discharge valve is equipped at the bottom of the storage tank for cleaning the tank and replacing the water. A safety valve is mounted at the top of the storage tank with a maximum pressure of 15bar. The refrigeration unit connected to the storage tank consists of a compressor, water coolant condenser, oil separator, refrigerant receiver, driers, and a manual expansion valve.

The storage tank used in this experiment has two flanges with centralized glass on both sides, which makes it possible to view the refrigerant clathrate formation during the charging process. The cold clathrate forming inside the tank is recorded and observed through two glass vision windows mounted at both sides of the storage tank. Figure 16 shows the flanges for the direct thermal storage system.

A feed water tank is placed on the top of the storage tank to make it possible for water and refrigerant to be fed to the tank while running the experiments. Furthermore, the cold storage tank is supported with six temperature measurement points: three at the bottom and three at the center. The temperature sensors are distributed equally where two are placed at the left and right of the upper part, and two at the left and right of the bottom part of the storage tank. Two sensors are located at the center bottom and center of the tank. Pressure transducers are also mounted at the inlet and exit of the storage tank. The flow rate was measured using a PLATON rotameter with range of 0.2-1.5 LPM. The details of the compressor, condenser and expansion valve used in the experimental apparatus will be discussed in details in the experimental component section.

4.3.2 Experimental procedure

The experimental procedure for the direct storage system is listed as follows: 1)- System preparation, 2)- Refrigerant changing process, 3)- Cold charging process, 4)- Cold release process.

a) System preparation

Before using the rig for direct thermal energy storage, the following valves should be closed (valve #3, 5, 10, 9, 7) and the following valves should be open to allow refrigerant to flow (valve #1, 4, 6, 8).

b) Refrigerant charging process:

Before running the system or filling the refrigerant inside the system, the storage tank should be cleaned and vacuumed. The cold storage tank is cleaned by tap water before all tests. The valve for discharging is located at the bottom of the direct tank. The system is then vacuumed using a vacuum pump for the removal of air from the system. The gauge should read 29 Hg in. The calculated amount of liquid water and liquid refrigerant is charged into the tank through the valve at the top of the direct tank. The ratio of water to refrigerant is shown in the setup process in Chapter 5.

c) Cold charging process:

After the charging of water and refrigerant inside the tank, the system is turned on to start the charging process. The expansion valve should be open to allow the refrigerant to flow in a closed loop. All the pressure gauges should be monitored to avoid high pressure at any component. If high pressure occurs in one of the gauges, this is due to a closed valve of less refrigerant in the system. For the current test rig, the pressure gauge before the evaporator might shows as high reading above 90 psig. This is due to the choking of refrigerant in the refrigerant distributer inside the tank. It is highly recommended to stop the system if pressure before the direct tank exceeds 50 psig. The charging cycle of the direct thermal storage system is shown in Figure 17

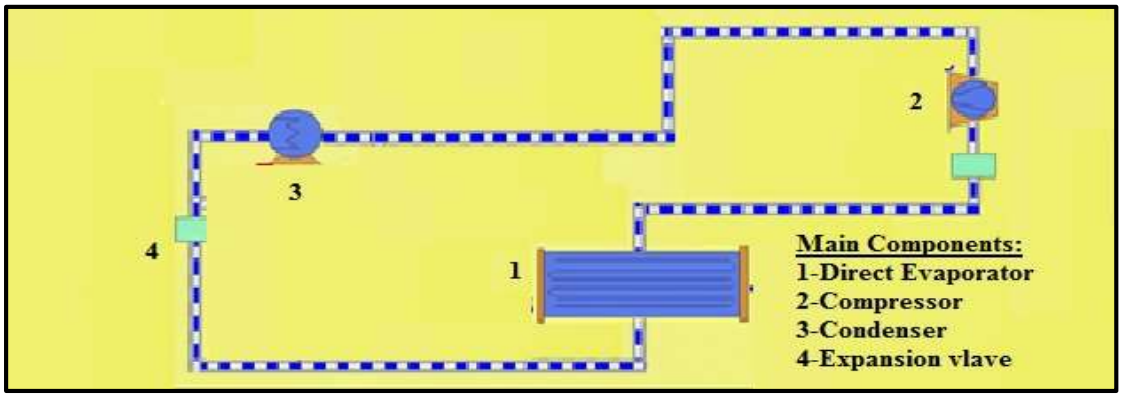

Figure 17: Vapor compression cycle during charging process of direct storage tank

After forming the clathrate hydrate, the storage tank is kept for some time. The tank is completely insulated such that no heat across the tank is allowed (Figure 18).

Figure 18: Picture view of thermal energy storage tank

d) **Cold release process:**

After the storage period, the system is ready for discharge or release of cold energy. The discharge process occurs using a fan coil unit connected to the storage tank. The cold storage tank temperature decreased during the discharging process, which indicates that the cold release process has been started. The system is discharged until the temperature of the tank goes back to its initial state. While discharging the thermal tank, cold storage valves before and after the direct tank are closed and cold release valves are opened; in addition, the fan coil unit and injection pump are turned on to release cold energy.

4.4 Experimental Components

4.4.1 Direct storage tank

The direct storage tank is supported with an inner refrigerant distributer to enhance heat transfer inside the tank as shown in Figure 16. Red copper heat exchanger coils with a diameter of 5/8” are mounted inside the storage tank for the discharging function. A water discharge valve is equipped at the bottom of the tank for cleaning the tank and replacing the water. A safety valve is mounted at the top of the storage tank with a maximum pressure range of 15bars. The direct storage tank used in this experiment has two flanges with centralized glass which make it possible to view the clathrate formation during the charging process. The two glass vision windows are mounted at both sides of the flanges and have a diameter of 12cm each. The cold

refrigerant clathrate forming inside the tank is recorded and observed through these two glass vision windows mounted on the side of the tank. Further, the cold storage tank is supported with six temperature measurement points: three at the bottom and three at the center.

4.4.2 Compressor

The compressor used in the direct thermal storage system is considered as a hermetic reciprocating compressor. As named by manufacturer, the compressor is positive displacement Maneurop MTZ compressors. The purpose of the compressor in this system is to raise the low pressure of refrigerant coming from the storage tank to a high pressure that of the condenser. Usually such compressors capacity ranges from 1/12 HP to 30 BG in household refrigeration [64]. The hermetic compressor used within the experiment is a 1.5 hp reciprocating compressor with a separate variable speed control. The nominal speed at 50Hz is given by the manufacturer as 2900 rpm while at 60Hz, it reaches to 3600 rpm. All the experimental process carried in this research uses a range of 2300 to 3000 rpm. The maximum pressure from the low pressure side is given by manufacturer as 25 bars, while the maximum from the high pressure side is 30 bars. The compressor used has a charging limit of 3 kg of refrigerant. The charging limit of oil is around 1 liter. For the energy efficiency of this experiment, the data from the compressor is collected and analyzed. The compressor characteristics are shown in Appendix B. The compressor ratio during the experiments varies with mass flow rate and type of refrigerant used. It is important to know the compressor ratio during the experiment because the compressors are rated in terms of how much flow they produce at a given ratio. The compressor ratio is defined as discharging pressure divided by suction pressure in absolute pressure. From the experiments, it is noted that the compressor performance is influenced by compressor ratio, suction, and discharge temperature and compressor speed. The type of refrigerant used also has an effect on the compressor performance.

4.4.3 Water-cooled condenser

There are many condensers to be considered when making a selection for a direct thermal storage system. The famous condensers types are air cooled and water cooled. The condenser used in this experiment is water-cooled condenser with cooling capacity of 2.2 kW. The purpose of the condenser is to cool the hot refrigerant coming from the compressor at high pressure. The heat of the refrigerant is exchanged with

water coming from the cooling tower. During the experimental process, the refrigerant passes through the condenser and undergoes latent and sensible stages. In addition, the liquid refrigerant is slightly sub cooled during this process. The total heat removed or rejected depends on the capacity of the condenser. The capacity of the system is shown in Table 8. The condensers selection depends mainly on the following consideration; size of the cooling load, refrigerant used, temperature of circulated water, and the amount of the circulated water. The load used within the experiments varies depending on the parameters used and the quantity of energy stored. The temperature of the water leaving the cooling tower to the condenser is between 20℃ and 23℃. The circulated quantity of water to the condenser varies from 0 to 35 LPM based on the temperature and pressure of the condenser. The condenser and the cooling tower are connected with the condenser pressure regulator, which allows water to flow through the condenser based on the temperature and pressure of the condenser.

4.4.5 Cooling tower

The purpose of the cooling tower is to provide cold water to the condenser. Cold water leaving the tower is supplied to the condenser by a water pump used in this experiment. The cold water is then passed through the hot plates of the condenser to exchange heat with the refrigerant indirectly. Warm water is then passed back to sprays or distribution troughs at the top of the tower to fall to the bottom part of the tower. Evaporization of heat takes place, which therefore cools the water again.

4.4.6 Expansion valve

The expansion valve used in the experiment is a manual expansion valve. Due to the limitations of such manual valves, it is made to control the flow and thus control the quantity of refrigerant entering the storage tank. The purpose of the expansion valve is to control the flow of refrigerant passing from the high pressure line of the condenser to the low pressure line of the storage tank. It is used to drop the pressure before it enters the storage tank.

4.5 Subsystem components

4.5.1 Pressure safe switches

The purpose of the pressure switch used in the experiment is to set the maximum safe operating pressure in the system. There are two pressure safe switches: a high pressure safe switch and a low pressure safe switch. The high pressure safe switch or the pressure cut-off switch is placed after the compressor with a set point of 230 psig.

The mechanism of the safe switch works to stop the compressor if the adjustable spring exceeds the set range. The cut-off point is usually set to be higher than the expected operating pressure, which in this case ranges between 100-200 psig for both tested refrigerants. The mechanism of the low pressure safety valve is almost the same. A spring is adjusted to match the required pressure. It is placed at the suction part of the compressor. During the experiments the high safe pressure cut-off point is set to 230 psig, while the low cut-off switch is set to around 20 inches of mercury (Hg in vac).

4.5.2 Condenser pressure regulator

The system is designed to work satisfactorily during maximum operating conditions. The condenser was sized to operate under maximum conditions of pressure and temperature. But when the load is reduced, the temperature and pressure of the condenser drops, resulting in a lower pressure difference across the high and low pressure which may lead to a malfunction of the system. Therefore, the purpose of condenser pressure regulator is to control the water-regulating valve that is operated by the condenser pressure. In other words, if the pressure of the condenser drops, the valve will gradually close to regulate the amount of water entering the condenser. The condenser pressure regulator can be fitted with a directly controlled water regulator valve controlled by the condenser pressure.

4.5.3 Evaporator relief valve

To prevent over pressure within the storage tank, a relief valve is placed in the evaporator to stop the system in case the pressure exceeds the limited pressure. The pressure is set to be 70 psig. The difference between the pressure safe switch and the evaporator relief valve is that the pressure safe switch cut-off or stops the system in case the pressure exceeds the limited pressure. However, in the relief valve, it only opens to release some of the pressure for safety while the system is operating.

4.5.4 Sight glass

The purpose of the sight glass is to show that the refrigerant is present in the pipe which should be in liquid phase. The main application of the sight glass in the thermal storage system is in the liquid line from the receiver to the expansion valve. Normal sight glass is used during the experiments. Furthermore, the sight glass is used to identify the quantity of refrigerant in the thermal storage system.

In case of a shortage, the refrigerant level monitored from the sight glass will be in a mixture phase (gas and liquid phase).

4.5.5 Charging connection

The purpose of a charging connection is to add refrigerant to the system when needed. The safest place to charge refrigerant is before the expansion valve, in the liquid receiver.

4.5.6 Oil separator

Since circulated refrigerant will be carrying oil, and this oil must be returned to the compressor, an oil separator is placed in the system. An oil separator is also called as suction line accumulator

4.6 Measurement Devices

In addition to the main components, several instruments are connected to the system. These instruments are connected to either improve performance plus monitor the system, or to ensure the safety of the system's operation.

4.6.1 Pressure gauges and transducers

The system is equipped with different pressure gauges and pressure transducers to measure the pressure. All pressure gauges and transducers are placed at the inlet and outlet of each component. The main use of the pressure gauges and transducers is to monitor the system's behavior and ensure the safety of operation. Pressure gauges show the measured value of the pressure on a scale, while the pressure transducer detects the pressure variation and sends it to data acquisition to digitalize it and send it to a computer in order to view it, store it, and analyze it. Omega pressure transducer PX240A series are mounted in the storage system. The data sheet for the pressure transducer used is shown in Appendix B.

4.6.2 Thermocouples

All the components of a direct storage system are linked to data acquisition system. Temperature thermocouples are used during the experiment to measure the temperature before and after each component. They are also placed around the storage tank to measure the temperature distribution inside the storage tank. Thermocouples are connected to the data acquisition system so it can be viewed on a computer. K type thermocouples were chosen to be installed in the system.

Chapter 5: Experimental Results and Discussion

5.1 Introduction

The modeling for direct thermal storage shows that high thermal capacity and high system performance is possible by using cold thermal energy storage with clathrate hydrate of different refrigerants. However, without an experimental assessment for clathrate hydrate storage technology, the potential of storage hydrate is not clear. Therefore, the following sections describe a number of experiments at different operating conditions that show the capability of such thermal technology to store cold energy. Further sections will compare between two refrigerants used to form clathrate hydrate in this research. In the open literature, only a limited number of detailed experimental studies are reported. Thus, clathrate hydrate experimental assessments are reported in this chapter in order to:

I. Verify the mathematical equations used to model the thermal storage system,
II. Determine the conditions under which refrigerant clathrate hydrate forms,
III. Evaluate the temperature at which refrigerant clathrate hydrate forms
IV. Evaluate the time at which refrigerant clathrate starts and ends,
V. Study system performance while forming different clathrate hydrates.

Different parametric studies are carried out for the storage system to investigate the effect of the selected parameters on the behavior of the storage system. The studied parameters used in this research are; flow rate of refrigerant, compressor speed and type of refrigerant. The mass of water used in this research is fixed. Therefore, the ratio of refrigerant to water in the storage tank is fixed. The variables used while conducting the experiments are shown in Table 8.

Table 8: Experimental operating conditions for clathrate R134a and R404a

Run set #	Mass of water inside tank (kg)	Type of Refrigerant	Compressor Speed (RPM)	Flow rate of ref. (kg/min)
Exp. #1	11	R134a	2700	0.96/0.72/0.48
Exp. #2	11	R134a	2500	0.96/0.72/0.48
Exp. #3	11	R134a	2300	0.96/0.72/0.48
Exp.#4	11	R404a	2700	0.96/0.72/0.48
Exp.#5	11	R404a	2500	0.96/0.72/0.48
Exp.#6	11	R404a	2300	0.96/0.72/0.48

5.2 Setup Process

A direct thermal energy storage apparatus is operated for three main processes: *charging*, *storing* and *discharging*. For the charging process of direct a thermal energy storage apparatus, refrigerant R134a and R404a are used inside the tank as a working fluid separately. The ratio of refrigerant to water set within the experiments is studied with a constant temperature bath apparatus to determine the exact ratio of mixing between refrigerant (guest molecules) such as R134 and host molecules (water). For clathrate hydrate formation of refrigerant 134a, the ratio was reported to be (1:2.23). Therefore, one kilogram of water corresponds to (1/ 2.23) (i.e. 0.448 kilograms of refrigerant R134a). On the other hand, the approximate ratio of refrigerant R404 is approximated by (1:1.84). Thus, one kilograms of water needs (1/ 1.84) (i.e. 0.54 kilograms of refrigerant R404a) to form clathrate hydrate. The charging process of refrigerant R134a or R404a requires the system to be evacuated from all air. The storing process for clathrate hydrate requires the system to be insulated from the surrounding temperature to minimize the heat losses.

A direct thermal energy storage system can be operated and charged based on the need of energy used. For a direct thermal energy storage system, the water is kept at a certain quantity inside the tank where it mixes with refrigerant. The refrigeration unit is used to charge the thermal storage tank. The amount of energy stored inside the storage tank in (kJ) is modeled by the water mass and refrigerant mass in (kg), and heat of fusion of refrigerant in (kJ/kg) as shown in modeling Equation 3.2.

Different refrigerants will have different latent heats of fusion as shown in Table 6.

The following calculations (Table 9) are used to find the experimental quantity of refrigerant needed to form refrigerant clathrate hydrates for both refrigerant R134a and refrigerant R404a.The quantities mentioned are approximate and they are measured in Kg. Table 9 shows that for refrigerant R134a, the ratio of R134a is about 0.448 Kg for every 1 Kg of water. While for refrigerant R404, the ratio is 0.543Kg of R404 for every 1 Kg of water. For all experiments with the given ratio shown in Table 9, it is noted that when the cold storage process starts, bubbles start to form on the top layer of the storage medium water.

Table 9: Ratio of water to refrigerant based on mass fraction

Specification	R134a	R404a
Total charged refrigerant (kg)	8.702	9.747
Total charged water (kg)	11	11
Total refrigerant needed for the refrigeration unit (kg)	~3.77	~3.77
Mass of refrigerant available to form clathrate	4.932	5.977
Ratio	1:2.23	1:1.840
Refrigerant needed per one kg of water (kg)	~0.448	~0.543
Expected mass of clathrate (kg)	~15.93	~16.97

The experimental results of forming refrigerant clathrate hydrate show that at the beginning of the experiment, the bubbles coming out from the refrigerant distributor are milky because of the mixture of water and refrigerant as shown in Figure 19 (part a). During the initial stage, cloudy gases will appear inside the tank. this clouds are due to the mixing of refrigerant and water. When reaction proceeded rapidly, a foam-like substance appears on the top side of the storage medium as shown in Figure (19, part b). Foam will appear at the top surface of the water. The foam represent the initial stage of forming the clathrate hydrate. While the progress of refrigerant clathrate formation is continued, the white foam surface starts to float over the water surface and foam increase gradually. The formed foam then goes down and the refrigerant clathrate hydrate becomes compact as shown in Figure (19, part d & e). At the end of the hydrate formation process, a crystal structure form is visible from the sight glass Figure (19 part f). The crystal structure are scattered all over the formed clathrate hydrate. All temperature readings inside the storage tank are recorded by thermocouples during the charging process and formation of clathrate hydrate. The variation of the eight thermocouples located on the storage tank is discussed in the storage tank behavior section. The temperature variations inside the storage tank are shown for both R134a and R404a refrigerants from figure 40 to figure 63 in Appendix A.

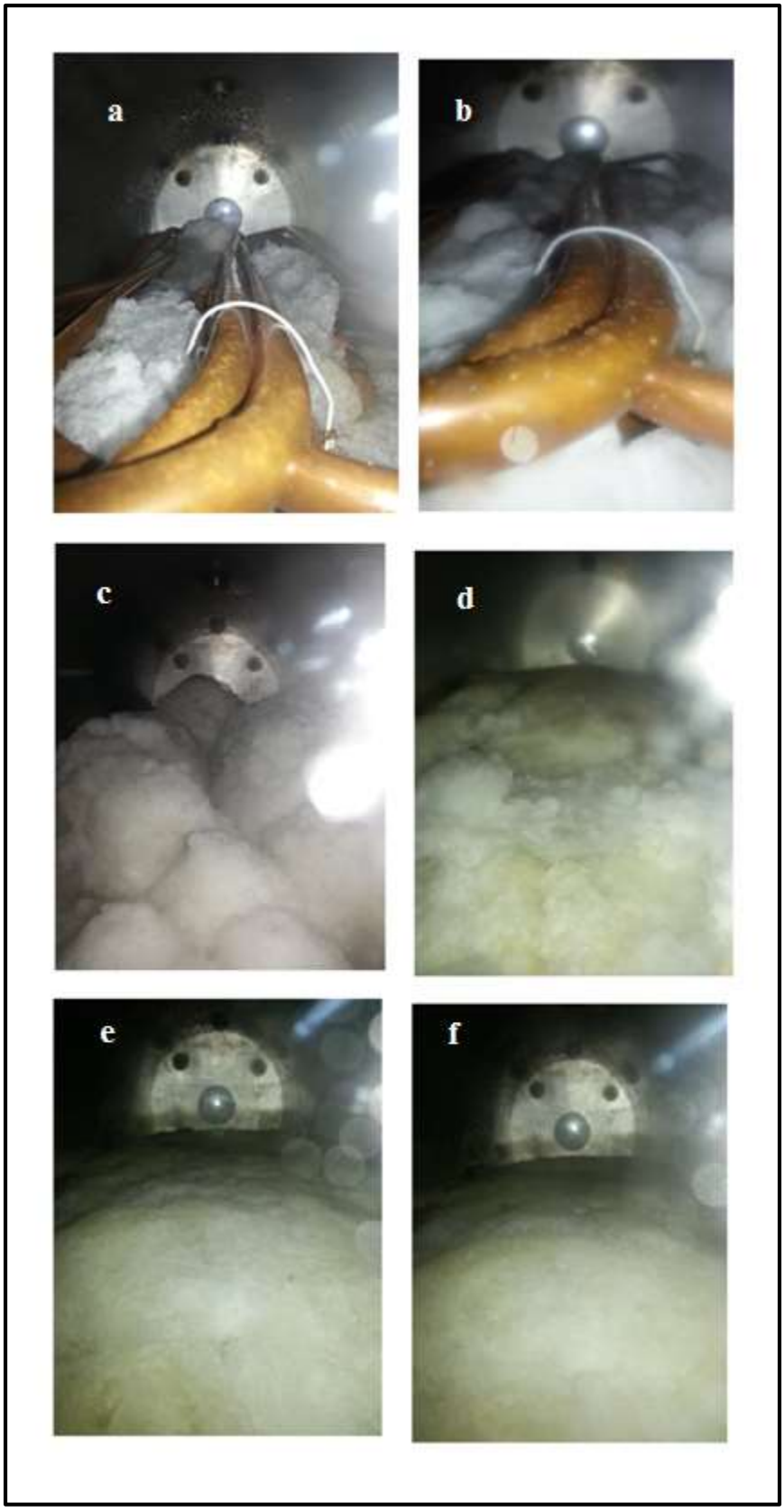

Figure 19: Formation of R134a clathrate hydrate during charging process

5.3 Direct Storage Tank Behavior

The behavior of the direct thermal energy storage tank includes; the variation of the temperature inside the tank, the pressure variation of the refrigerant inlet and the outlet from the storage tank, the quantity of refrigerant clathrate hydrate formed and the operational processes of charging and discharging. The behavior of the system is conducted by measuring the temperature and pressure of the refrigerant used and the temperature of the storage medium. Many experimental tests are studied for both refrigerants, the results are summarized in this chapter. This section will discuss the behavior of the storage tank and the compressor used. Further results related to the clathrate formed are disused in the discussion of results section.

5.3.1 Direct storage tank temperature variation

For clathrate hydrate to be used in thermal storage, it should be formed at storage temperature ranges between 5℃ and 12℃. It is experimentally noted that for different refrigerants, there is a certain time needed before clathrate hydrate starts to form. This period is the sensible period for the storage material. Figures 21 to 23 show the variation of the average temperature inside the direct storage tank for refrigerant R134a clathrate hydrate. It is experimentally noted that in almost all experimental runs, the temperature of the tank with R134a will converge in the range of 4℃ and 6℃ as shown in Figures 21 to 23. For the case of R404a clathrate hydrate, the temperature inside the direct storage tank will converge to a higher temperature than that of R134a which is between 10℃ and 7℃ as shown in figures 24 to 26.

At the beginning of the charging process, the temperature of the storage medium inside the storage tank ranges between 17 ℃ and 20 ℃. The temperature and pressure of the mixed water and refrigerant will decrease gradually with time while charging the direct storage tank. It is noticed that the inlet temperature varies based on the pressure of the storage tank and the mass flow rate of the refrigerant. The inlet temperature of the storage tank varies between -8 ℃ and -2 ℃ for refrigerant R134a. The experimental results show that the inlet temperature of refrigerant R404a is lower than that of R134a. Thus clathrate hydrate with R404a forms at a higher temperature than R134a clathrate hydrate.

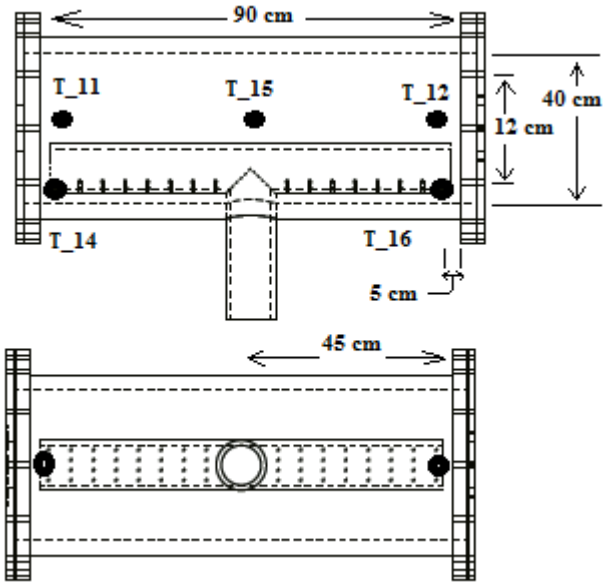

Figure 20: Location of the temperature sensors around the storage tank

The inlet temperature of R404a varies between -17℃ and -8 ℃. This also shows that refrigerant R404a can reach to a lower temperature than refrigerant R134a at the same pressure line. At the end of the charging period, almost all of the storage medium inside the thermal storage tank form clathrate hydrate. Table 10 shows the experimental operation condition of refrigerant R134a under different variables of compressor speed and different refrigerant mass flow rate. The mass of initial mass of water and initial mass of refrigerants charges is also shown. The ratio throughout the charging process is calculated based on the initial quantities of charged water and charged refrigerant.

Tables 10 and 11 summarize the experimental runs carried out for refrigerant R134a and R404a. Different temperature sensors are used to measure the variation of temperature inside the storage tank. The initial temperature inside the storage tank is measured before all experiments. For refrigerant R134a, the experiment average ending temperature inside the storage tank is in the range of 4 ℃ and 5.7℃. On the other hand, the average ending temperature inside the storage tank for R404a is in the range of 6.8 ℃ and 8.4℃. Total of 5 main temperature sensors are located in the outer surface of the tank as shown in Figure 20.

Table 10: Experimental operating conditions for refrigerant R134a

Fig #	Comp. Speed (rpm)	Mass flow Rate (kg/min)	Charging Time (min)	Average Initial Temperature of Storage Tank (℃)	Average Final Temperature of Storage Tank (℃)	Mass of Storage Medium (kg)	Ratio of water to refrigerant
40	2300	0.48	48	18.02	5.6	11kg of water: 4.93 kg of R134a	2.23:1
41	2300	0.72	40	18.37	5.7	11kg of water: 4.93 kg of R134a	2.23:1
42	2300	0.96	21	17.55	4.1	11kg of water: 4.93 kg of R134a	2.23:1
43	2500	0.48	50	17.08	4.4	11kg of water: 4.93 kg of R134a	2.23:1
44	2500	0.72	38	19.42	4	11kg of water: 4.93 kg of R134a	2.23:1
45	2500	0.96	25	17.12	4	11kg of water: 4.93 kg of R134a	2.23:1
46	2700	0.48	48	20	5.2	11kg of water: 4.93 kg of R134a	2.23:1
47	2700	0.72	39	19.8	4.2	11kg of water: 4.93 kg of R134a	2.23:1
48	2700	0.96	22	18.8	4.0	11kg of water: 4.93 kg of R134a	2.23:1

Table 11: Experimental operating conditions for refrigerant R404a

Fig #	Comp. Speed (rpm)	Mass Flow Rate (kg/min)	Charging Time (min)	Average Initial Temperature of Storage Tank (℃)	Average Final Temperature of Storage Tank (℃)	Mass of Storage Medium (kg)	Ratio of water to refrigerant
49	2300	0.48	55	20.1	7.9	11kg of water: 5.9 kg of R404a	1.84:1
50	2300	0.72	40	21.73	7.8	11kg of water: 5.9 kg of R404a	1.84:1
51	2300	0.96	30	19.3	7.2	11kg of water: 5.9 kg of R404a	1.84:1
52	2500	0.48	52	16.9	8.31	11kg of water: 5.9 kg of R404a	1.84:1
53	2500	0.72	40	22.63	8.4	11kg of water: 5.9 kg of R404a	1.84:1
54	2500	0.96	30	18.95	8.4	11kg of water: 5.9 kg of R404a	1.84:1
55	2700	0.48	50	23	6.8	11kg of water: 5.9 kg of R404a	1.84:1
56	2700	0.72	41	22	7.3	11kg of water: 5.9 kg of R404a	1.84:1
57	2700	0.96	30	19.43	7.5	11kg of water: 5.9 kg of R404a	1.84:1

As described previously, Figures 21 to 23 represent the effect of refrigerant mass flow rate on the average temperature inside the tank during R134a clathrate formation. It is noticed that the charging time is not fixed, and this is because of the variation of the mass flow rate inlet to the tank. . It is also experimentally noticed that the temperature will converge to 4℃ or 6℃ for refrigerant R134a. Figures 24 to 26 show the variation of temperature during R404a clathrate formation. It is experimental noticed that the average temperature will converge between 7℃ and 10℃ . This shows that clathrate with refrigerant 404a forms at a higher temperature than clathrate R134a. Additional results presenting the instantaneous temperature inside the storage tank are presented in Appendix A (Figures 58 to 63)

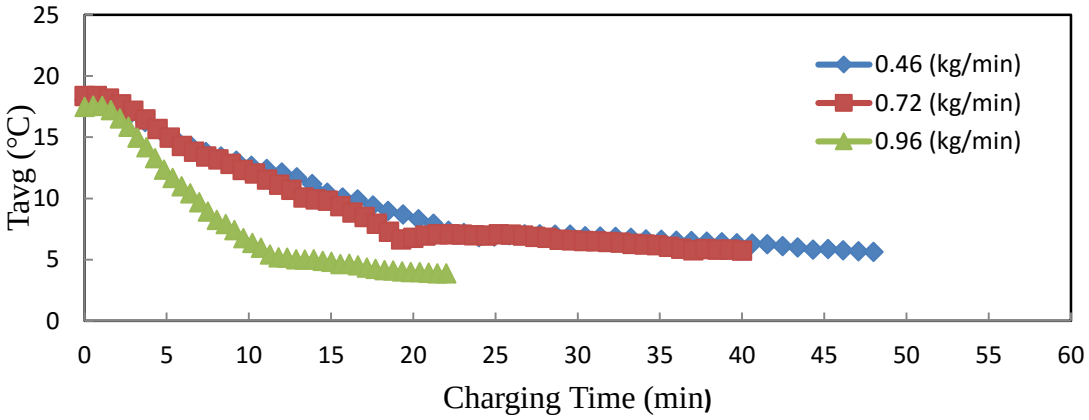

Figure 21: Variation of average R134a clathrate temperature inside the storage tank during charging process at N= 2300 rpm

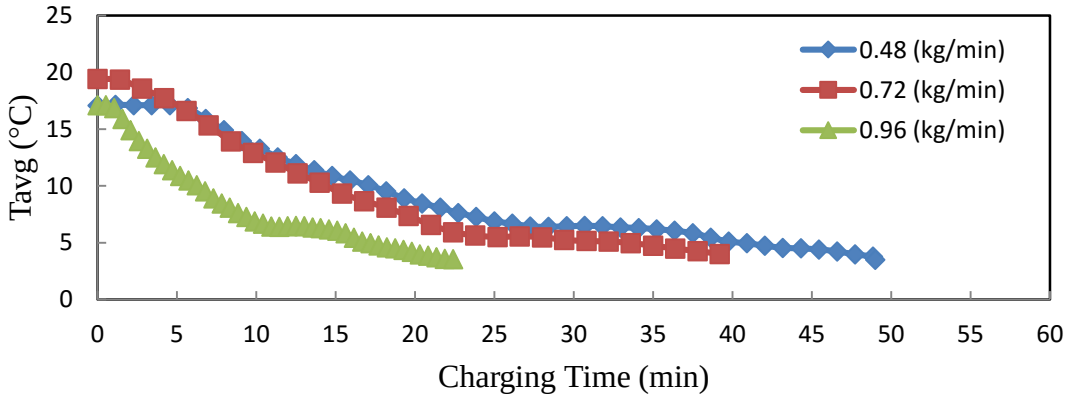

Figure 22: Variation of average R134a clathrate temperature inside the storage tank during charging process at N= 2500 rpm

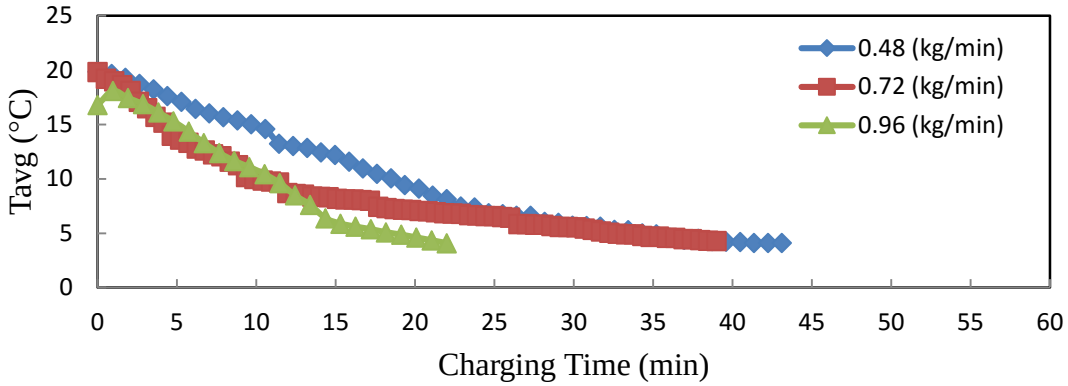

Figure 23: Variation of average R134a clathrate temperature inside the storage tank during charging process at N= 2700 rpm

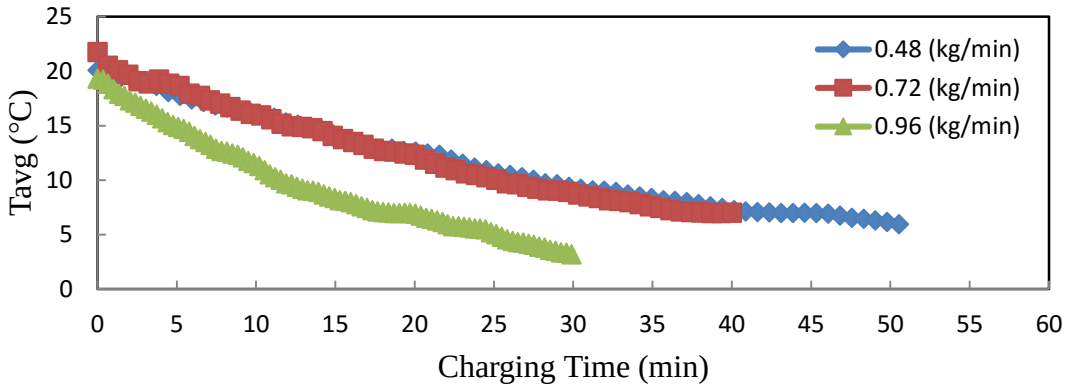

Figure 24: Variation of average R404a clathrate temperature inside the storage tank during charging process at N= 2300 rpm

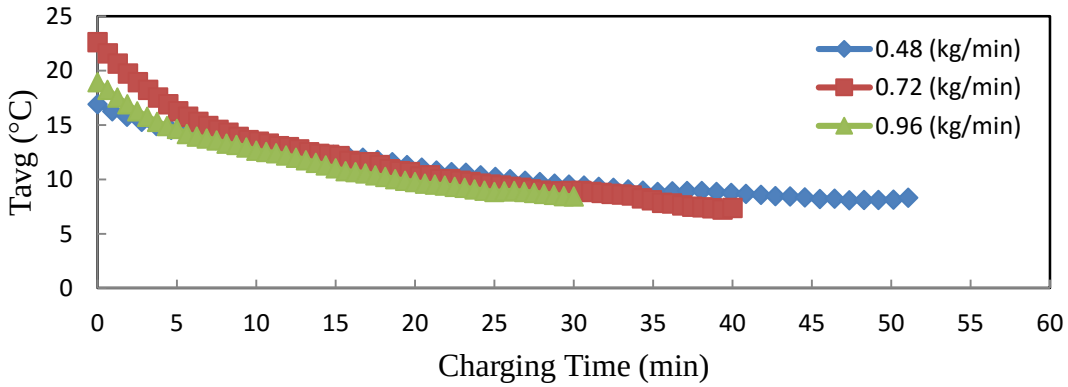

Figure 25: Variation of average R404a clathrate temperature inside the storage tank during charging process at N= 2500 rpm

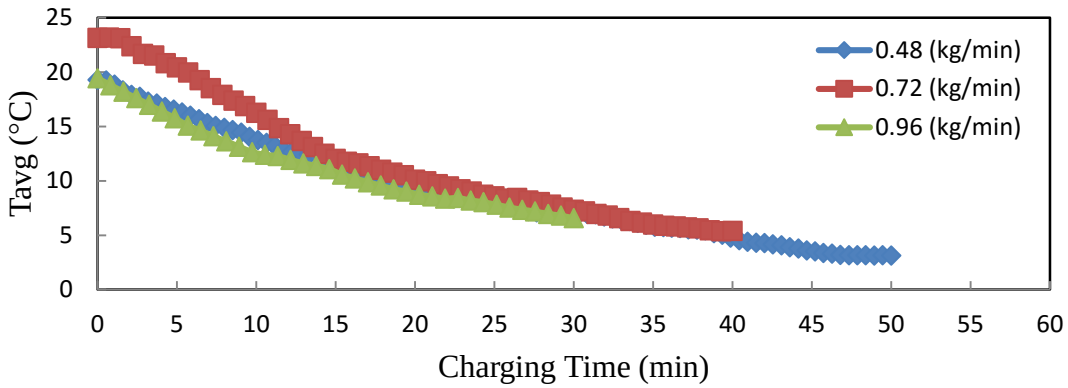

Figure 26: Variation of average R404a clathrate temperature inside the storage tank during charging process at N= 2700 rpm

5.3.2 Direct storage tank pressure variation

The behavior of the direct storage tank is carried out by measuring the pressure and temperature across the tank. Throughout this research, several experiments were conducted to study the behavior of the system during the charging process of the direct thermal energy storage system. The pressure transducers readings located on the inlet and the exit of the storage tank are used to generate mathematical equations which can predict the behavior of the system used for storage purposes. Table 12 shows the variation of pressure during the charging process of R134a hydrate with a mass flow rate of 0.96 (kg/min). It is noted that the pressure outlet will remain at a constant rang during the charging process. The pressure inlet will vary based on the mass flow rate of refrigerant entering the compressor. At the end of the charging process, the mass flow rate of refrigerant will decrease which will lead to high pressure ratio. The pressure ratio across the compressor is shown in Figures 32 and 33 for refrigerant R134a and R404a respectively. Figures 27 to 29 are the graphical representation of the mathematical polynomials shown in Table 12. These figures show the pressure at the suction and discharge section of the compressor used. In addition, they show the pressure line at the inlet of the thermal storage tank. The charging process ends when the pressure ratio starts to increase. This is an indication that the mass flow rate is decreased due to clathrate hydrate solid blockage.

Table 12: Variation of the pressure readings during R134a clathrate formation

Compressor Speed	System Mathematical Relation (Fourth Degree Polynomials)
2700 rpm	P_{comp_in}= -0.0003 t^4 + 0.0403 t^3 - 1.3067 t^2 + 7.7639 t + 199.53
	P_{comp_out}= 3E-06 t^4 + 0.0113 t^3 - 0.4952 t^2 + 5.5075 t + 705.84
	P_{tank_out}= -0.0003 t^4 + 0.0403 t^3 - 1.3067 t^2 + 7.7639 t + 199.53
	P_{tank_in}= = -0.001 t^4 + 0.0712 t^3 - 1.6084 t^2 + 8.0667 t + 163.82
2500 rpm	P_{comp_in}= -0.0032 t^4 + 0.1508 t^3 - 2.3373 t^2 + 9.6845 t + 234.24
	P_{comp_out}= 0.0019 t^4 - 0.085 t^3 + 1.2163 t^2 - 2.6878 t + 483.45
	P_{tank_out}= -0.0032 t^4 + 0.1508 t^3 - 2.3373 t^2 + 9.6845 t + 234.24
	P_{tank_in}= -0.0016 t^4 + 0.0681 t^3 - 0.8787 t^2 - 0.3618 t + 214.84
2300 rpm	P_{comp_in}= -0.0005 t^4 + 0.029 t^3 - 0.6169 t^2 + 5.7174 t + 188.72
	P_{comp_out}= -0.0002 t^4 + 0.0123 t^3 - 0.3069 t^2 + 3.0702 t + 570.54
	P_{tank_out}= -0.0005 t^4 + 0.029 t^3 - 0.6169 t^2 + 5.7174 t + 188.72
	P_{tank_in}= 0.0002 t^4 - 0.0142 t^3 + 0.2741 t^2 - 3.1199 t + 142.97

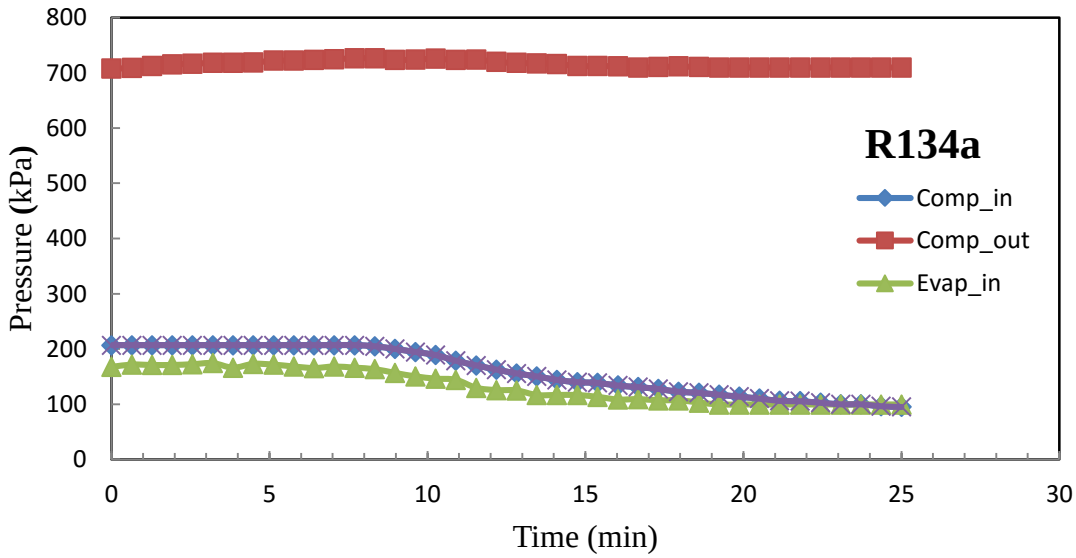

Figure 27: Pressure variation of storage tank during charging process at N=2700 rpm and ṁ= 0.96 (kg/min)

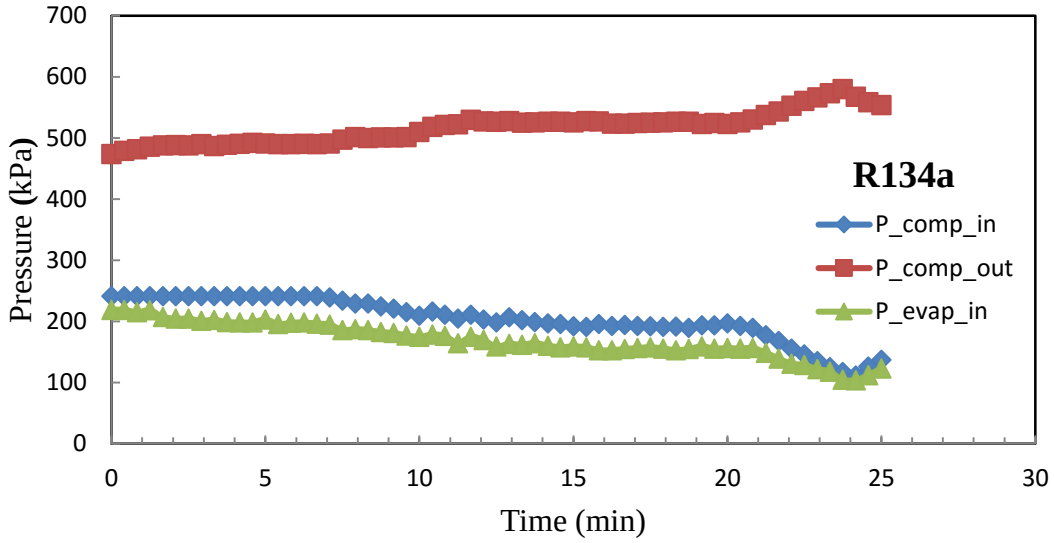

Figure 28: Pressure variation of storage tank during charging process at N= 2500 rpm and ṁ= 0.96 (kg/min)

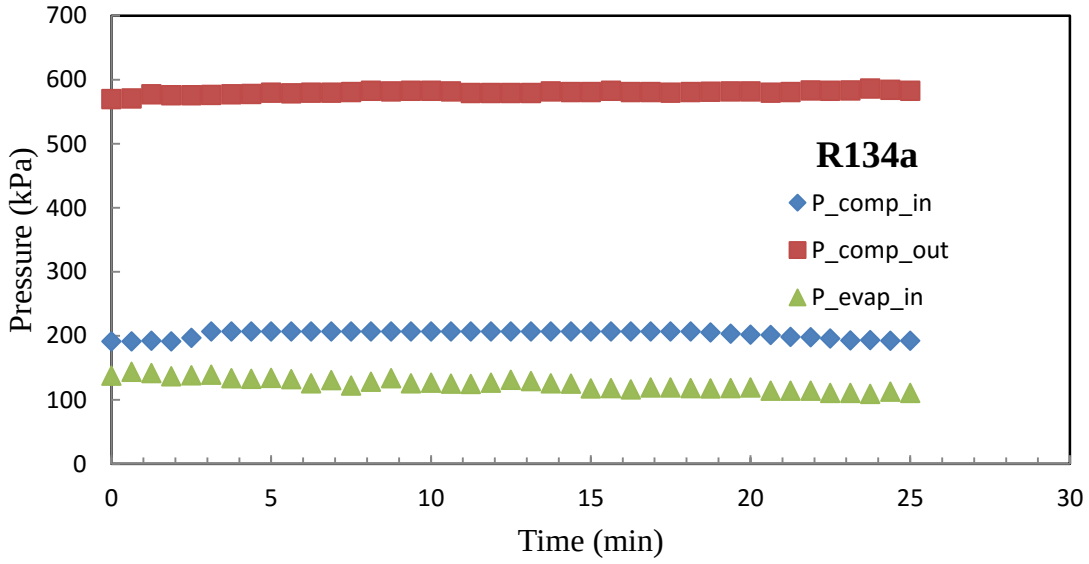

Figure 29: Pressure variation of storage tank during charging process at N= 2300 rpm and ṁ= 0.96 (kg/min)

5.3.3 Uncertainty analysis

All experimental readings were collected to data measurement system. The measurement systems include two data acquisition: one with 20 input channels, 12 thermocouple K-types, and 8 pressure transducers. The other data acquisition collects temperature reading at different locations around the storage tank. All temperature sensors are calibrated using ice bath with temperature accuracy of $\pm 0.01℃$. Calibration results shows the accuracy for the first data acquisition thermocouples K-types is with in $\pm 0.2℃$,while the accuracy of the second data acquisition Carel thermocouples is $\pm 0.1℃$. All experimental readings were collected every 60 seconds for data acquisition 1 and every 30 seconds for data acquisition 2.

5.4 Compressor Behavior

The behavior of the compressor can be analyzed by studying the temperature and pressure across the compressor. The enthalpy values generated from the pressure and temperature reading for refrigerant R134a and R404a are recorded for different experimental sets. It is noticed that the pressure at the inlet of the compressor is not similar to that at the exit of the storage tank. The difference between the pressures is about 5% losses. This loss in pressure is due the pipe connections and the filter driers between the storage tank and the compressor. It is also noticed that the pressure at the outlet of the compressor remains as a constant line throughout the charging process as shown in Figure 27 and 29. At the end of the storage process, the mass flow rate passing through the compressor decreases which leads to a decrease in the electrical current consumed by the compressor. Also, it is noticed that the compressor starts to vibrate at the end of the storing process due to blockages inside the storage tank. This blockage occurs when all water and refrigerant turn to clathrate, which blocks the entrance of the storage tank.

5.4.1 Compressor power

The actual power consumed by the compressor is presented by multiplying the voltage supplied to the compressor and the electrical current across the compressor. The electrical power consumed by the compressor is divided into two stages. The first stage is before and while forming the clathrate hydrate.

The second stage is after forming the clathrate hydrate. The results show that the compressor consumes a certain power during clathrate hydrate formation, while the power consumption decreases after the formation of the clathrate. This decrease in power consumption is directly affected by the current passing across the compressor. The current passing during the formation stage is more than the current passing after the clathrate formation stage. Furthermore, the high current consumed by the compressor is directly related to the mass flow rate of the refrigerant passing through. The voltage during the charging process remains constant at a constant compressor speed. The only factor which affects the voltage across the compressor is the speed of the compressor. The values of the electrical power during the charging process show that the current across the compressor reduces from 2.1 (A) to 1.8 (A) when the mass flow rate reduces from 0.96 kg/min to 0.24 kg/min. It is also noted that the voltage consumed by the compressor remains constant for a certain speed. For example, for 2700 RPM, the voltage supplied to the compressor is 404V and the voltage consumed is 332.3V. Similarly, the volt consumed with compressor speed 2500 rpm is 308.3V and with compressor speed 2300 rpm is 284.4 V.

Another way to calculate the power consumed by the compressor is to use the value of energy transferred to the working fluid during the experiments. Figures 6 and 7 show the modeling of the compressor power used at different compressor speeds. It is clearly shown that the compressor consumes more power when operating with R404a refrigerant. Furthermore, the modeling shows a direct relation between the compressor speed and the consumption of power. It is also shown that at low mass flow rate, less power will be consumed.

Figures 30 and 31 show the experimental values of compressor power based on the energy transfer to the working fluid for clathrate formation of R134a and R404a. It is experimentally noted that the power needed for refrigerant R404a is higher than the power needed for refrigerant R134a. The experimental relation between the compressor speed and the consumption of power matches the modeling of the system. Furthermore, the experimental relation between the mass flow rate of the working fluid and compressor power is also noted as modeled

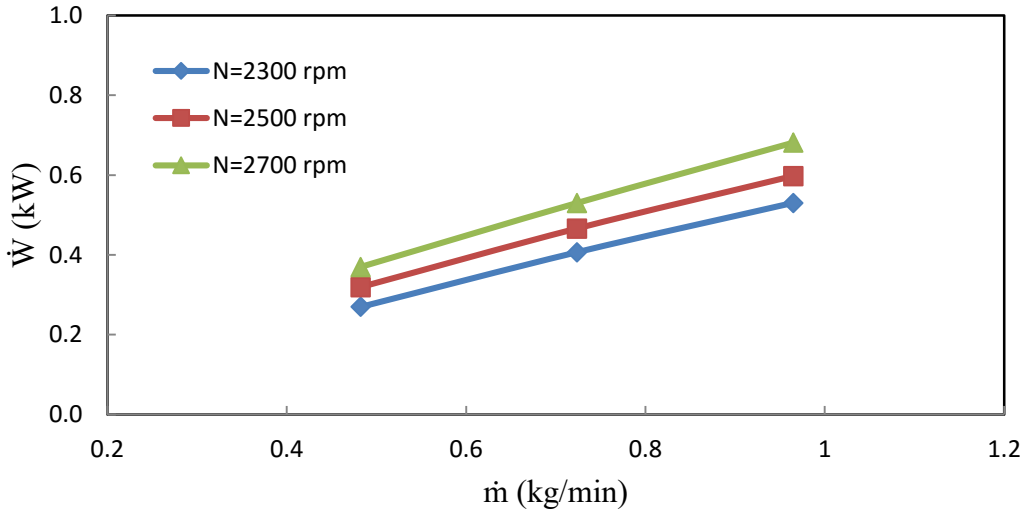

Figure 30: Effect of refrigerant R134a mass flow rate on input compressor power during charging process

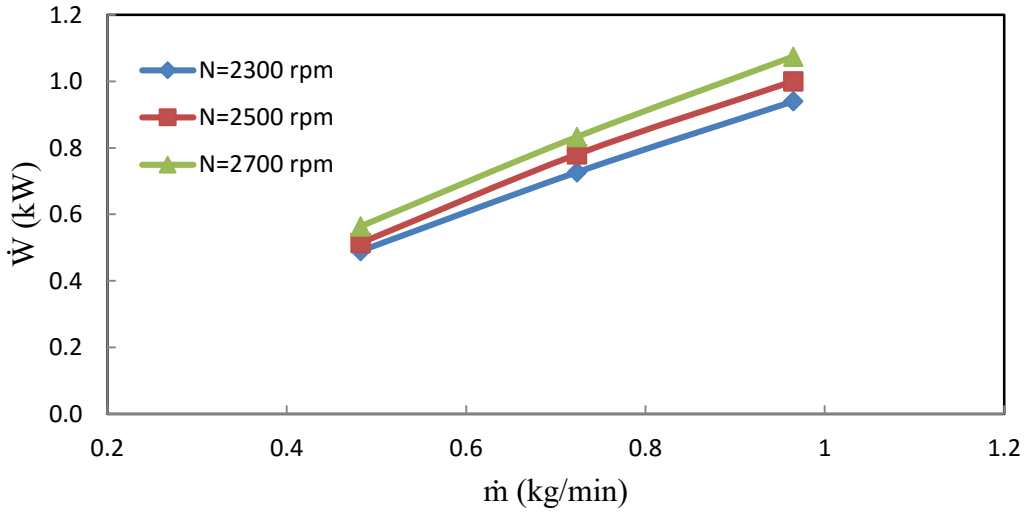

Figure 31: Effect of refrigerant R404a mass flow rate on input compressor power during charging process

5.4.2 Compressor Pressure ratio

The compressor pressure ratio is one of the most important parameters in studying the clathrate formation of different refrigerants. It is noted that the pressure ratio is affected by the mass flow of refrigerant injected inside the storage tank and the

compressor speed. The compressor pressure ratio varies with different speeds according to the following equation for R134a.

$$(Po/Pi)_i = (-0.0472\,\dot{m}_r^2 - 3.3568\,\dot{m}_r + 6.3591)*[1 + (N_i - 2700)] - (1.5663\dot{m}_r^2 - 0.6217\dot{m}_r + 4.9727)*[1 + (N_i - 2500)] + (5.1258\dot{m}_r^2 - 10.084\dot{m}_r + 7.8748*[1 + (N_i - 2300)] \quad (5.1)$$

The variation of the compressor pressure ratio for refrigerant R134a is shown in Figure 32. The results show that the highest compression ratio occurs at high compressor speeds and lower refrigerant mass flow rate. On the other hand, all pressure ratios at high mass flow rates converge to lower compression values at all compressor speeds.

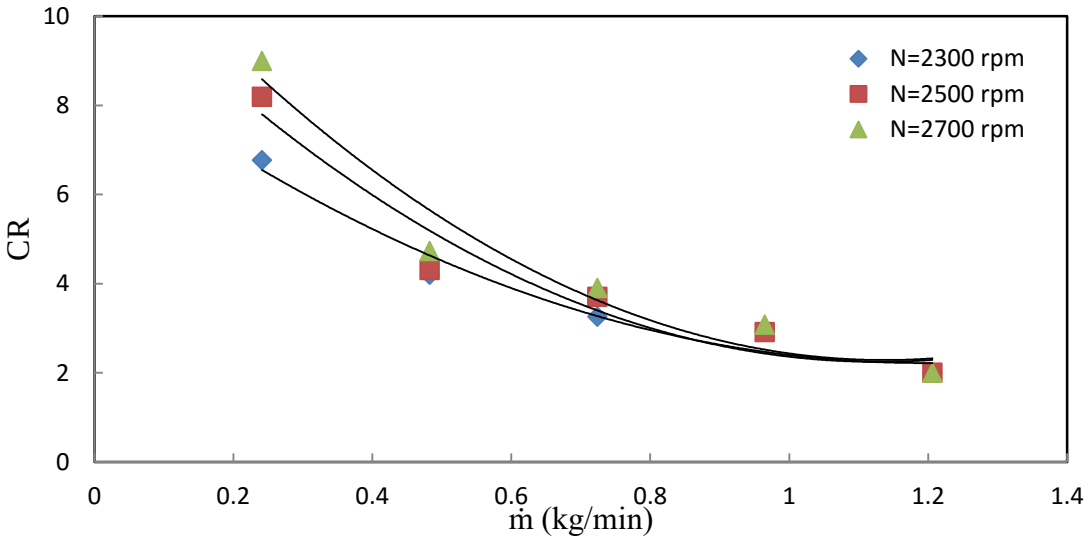

Figure 32: Effect of R134a mass flow rate on compressor ratio at different compressor speed during charging process

On the other hand, the compressor pressure ratio for refrigerant R404a varies with different speeds according to the following equation;

$$(Po/Pi)_i = (4.6173\,\dot{m}_r^2 - 10.208\,\dot{m}_r + 10.593)*[1 + (N_i - 2700)] - (0.1891\,\dot{m}_r^2 + 2.4933\,\dot{m}_r + 7.3695)*[1 + (N_i - 2500) + (1.4404\,\dot{m}_r^2 - 3.5249\,\dot{m}_r + 6.9719)*[1 + (N_i - 2300)] \quad (5.2)$$

From the results, it is noted that the compression ratio of refrigerant R404a is higher than R134a. This also affects the power consumed for R404a clathrate formation. Figures 32 and 33 shows the effect of mass flow rate on the system compression ratio during clathrate formation of R134a and R404a. At a certain compressor speed, Equation 5.1 and 5.2 shows the variation of compressor pressure ratio at different mass flow rates. The bracket term shown in Equations 5.1 and 5.2 indicate that if the value in bracket is not equal to 1 at a specific rpm (N_i), then the whole term is set equal to zero.

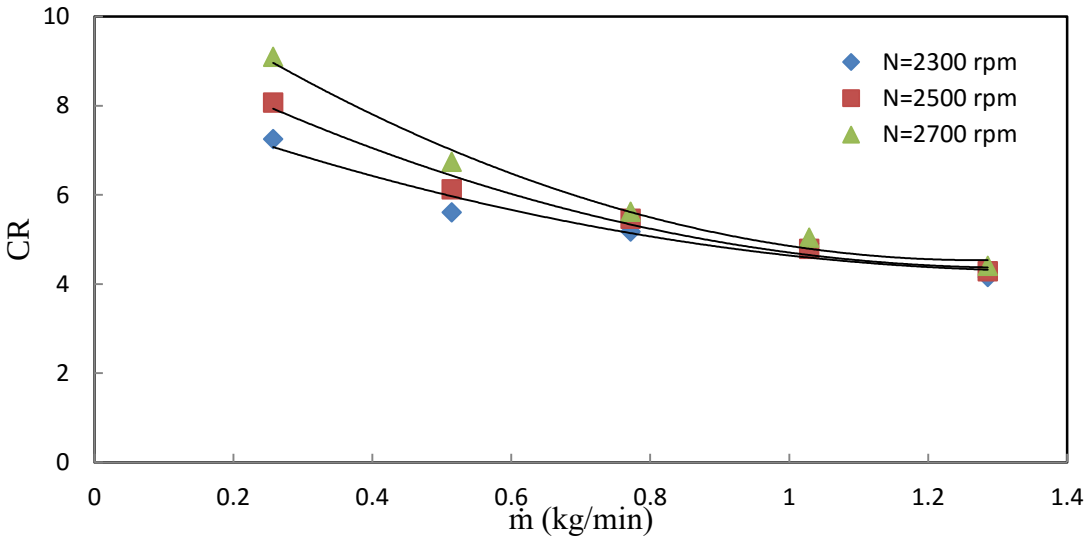

Figure 33: Effect of R404a mass flow rate of refrigerant R404a refrigerant on the system at different compressor speeds

5.5 System Performance Evaluation

Thermodynamics analyses such as energy and exergy analyses are conducted in this section to evaluate the charging efficiency using different refrigerants to form clathrate hydrate. To perform the thermodynamic analysis during the experiments, the temperature and pressure readings are taken and used to determine the properties of the refrigerants. The pressure and temperature records are noted before and after the thermal storage equipments shown in Figure 17. Furthermore, the temperature inside the storage tank is recorded at different location for all runs as shown in Figure 20.

In this study, energetic and exergetic analyses of different refrigerants are performed for the charging period. The energy analysis gives us only the quantity of energy stored. On the other hand, the exergetic analysis (second law analysis) gives us the quality of the stored energy.

Therefore, energy and exergy analyses have been carried out for the experimental runs at different parametric conditions to evaluate the direct thermal energy storage system. Tables 13 and 14 summarize the comparative results between the model and the experiments obtained for refrigerant R134a clathrate hydrate. Tables 15 and 16 summarize the comparative results obtained for refrigerant R404a clathrate hydrate. The model equation of total energy stored inside the storage tank is shown in equation 3.2. The total energy stored inside the storage tank can be represented experimentally by the following equation:

$$Q_{total-exp} = \dot{m}_r * \Delta h_{avg} * t_{total} \quad (5.3)$$

where the term ($\dot{m}_r$) represents the mass flow rate of refrigerant during the charging process in (kg/min), and the term (Δh_{avg}) is the average enthalpy change during the charging process in (kJ/kg). It is represented by the following equation:

$$\Delta h_{avg} = \sum \frac{\Delta h_i * \Delta t_i}{t_{total}} \quad (5.4)$$

where the terms (t_{total}) represent the total charging time, Δh_i represent the change of enthalpy at a specific time across the direct evaporator, and the term Δt_i represent the period between two points (Δt) of the charging process.

The exergy recovered during the charging period is modeled using equation 3.12, and the exergy supplied during the charging period is modeled using equation 3.13.

Table 13: Comparison of storage time between model and experiment data for different operation conditions for R134a

Variables		Modeling				Experiential				
Comp. Speed	Mass Flow Rate	Total Mass of Clathrate	Hydrate Fusion R134a	Total Load Stored	Total Charging Time	Mass of Clathrate Formed	Total Energy Stored	Total Charging Time	Average Enthalpy	Rate of Heat Absorbed
(RPM)	(kg/min)	(kg)	(kJ/kg)	(kJ/kg)	(min)	(kg)	(kJ)	(min)	(kJ/kg)	(kJ/s)
2300	0.4824	15.93	358	5703	62	12.4	4439	48	191.7	1.541
2300	0.7236	15.93	358	5703	41	15.5	5540	40	191.4	2.308
2300	0.9648	15.93	358	5703	31	10.8	3856	21	190.3	3.060
2500	0.4824	15.93	358	5703	62	12.9	4631	50	192	1.544
2500	0.7236	15.93	358	5703	41	15.5	5546	40	191.6	2.311
2500	0.9648	15.93	358	5703	31	11.4	4221	22	192.7	3.099
2700	0.4824	15.93	358	5703	62	12.2	4372	48	188.8	1.518
2700	0.7236	15.93	358	5703	41	14.8	5305	39	188	2.267
2700	0.9648	15.93	358	5703	31	11.3	4037	22	190.2	3.058

Table 14: System performance with refrigerant R134a clathrate hydrate at different flow rates and different compressor speed

Comp. Speed	Mass Flow Rate	Rate of heat absorbed	Power Input	COP	Exergy Recovered	Total Exergy Distracted	Second Law Efficiency
(RPM)	(kg/min)	(kJ/s)	(kJ/s)		(kJ/s)	(kJ/s)	%
2300	0.4824	1.54	0.27	5.62	0.167	0.103	62
2300	0.7236	2.31	0.41	5.68	0.262	0.145	64
2300	0.9648	3.06	0.53	5.77	0.350	0.180	66
2500	0.4824	1.54	0.32	4.83	0.195	0.134	58
2500	0.7236	2.31	0.47	4.96	0.280	0.186	60
2500	0.9648	3.10	0.60	5.19	0.367	0.230	62
2700	0.4824	1.52	0.37	4.10	0.186	0.184	50
2700	0.7236	2.27	0.53	4.28	0.282	0.248	53
2700	0.9648	3.06	0.68	4.49	0.387	0.294	57

Table 15: Comparison of storage time between model and experiment data for different operation condition for R404a

Variables		Modeling				Experiential				
Comp. Speed	Mass Flow Rate	Total Mass of Clathrate	Hydrate Fusion R404a	Total Load Stored	Total Charging Time	Mass of Clathrate Formed	Total Energy Stored	Total Charging Time	Average Enthalpy	Rate of Heat Absorbed
(RPM)	(kg/min)	(kg)	(kJ/kg)	(kJ/kg)	(min)	(kg)	(kJ)	(min)	(kJ/kg)	(kJ/s)
2300	0.4824	16.98	380	6452	65	14.2	5093	51	207	1.664
2300	0.7236	16.98	380	6452	44	16.9	6044	40	208.8	2.518
2300	0.9648	16.98	380	6452	33	16.4	5881	30	203.2	3.267
2500	0.4824	16.98	380	6452	66	14.2	5067	52	202	1.624
2500	0.7236	16.98	380	6452	44	16.3	5847	40	202	2.436
2500	0.9648	16.98	380	6452	33	16.3	5850	30	202.1	3.250
2700	0.4824	16.98	380	6452	66	13.7	4899	50	203.1	1.633
2700	0.7236	16.98	380	6452	44	16.8	6008	41	202.5	2.442
2700	0.9648	16.98	380	6452	33	16.3	5850	30	202.1	3.250

Table 16: System performance with refrigerant R404a clathrate hydrate system at different flow rates and different compressor speed

Comp. Speed	Mass Flow Rate	Rate of heat absorbed	Power Input	COP	Exergy Recovered	Total Exergy Distracted	Second Law Efficiency
(RPM)	(kg/min)	(kJ/s)	(kJ/s)		(kJ/s)	(kJ/s)	%
2300	0.4824	1.66	0.49	3.40	0.253	0.253	52
2300	0.7236	2.52	0.73	3.46	0.401	0.327	55
2300	0.9648	3.27	0.94	3.48	0.550	0.390	58
2500	0.4824	1.62	0.51	3.16	0.226	0.288	44
2500	0.7236	2.44	0.78	3.12	0.387	0.393	49
2500	0.9648	3.25	1.00	3.25	0.520	0.480	51
2700	0.4824	1.63	0.56	2.90	0.214	0.350	38
2700	0.7236	2.44	0.83	2.93	0.341	0.492	41
2700	0.9648	3.25	1.07	3.03	0.493	0.581	46

The following Figures 34 to 37 present the experimental results of the system performance based on the first law and the second law. It is noticed that the system will perform better with refrigerant R134a than refrigerant R404a. The experimental results conducted for the system performance show similar trends as the modeling results shown in Figures 7 to 10.

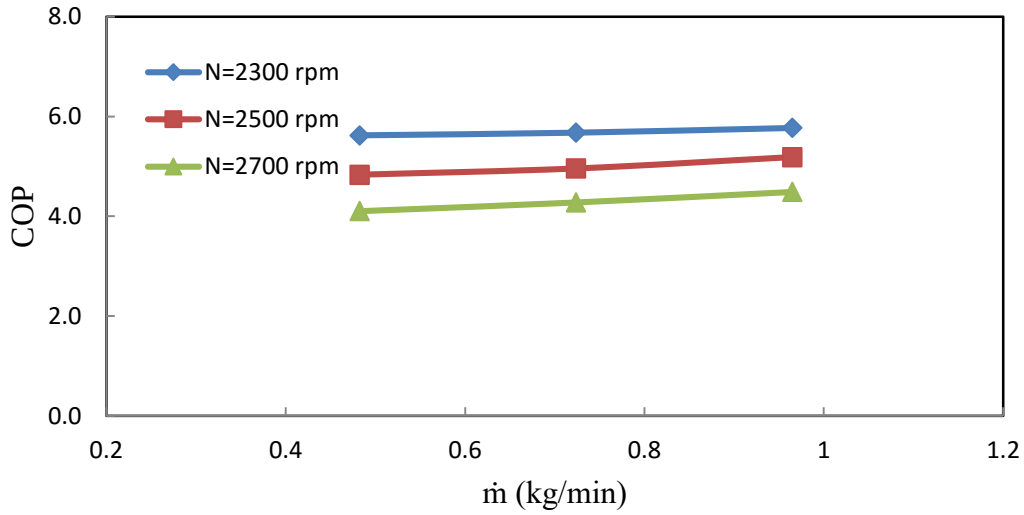

Figure 34: Effect of R134a mass flow rate on COP during charging process based on first law analysis

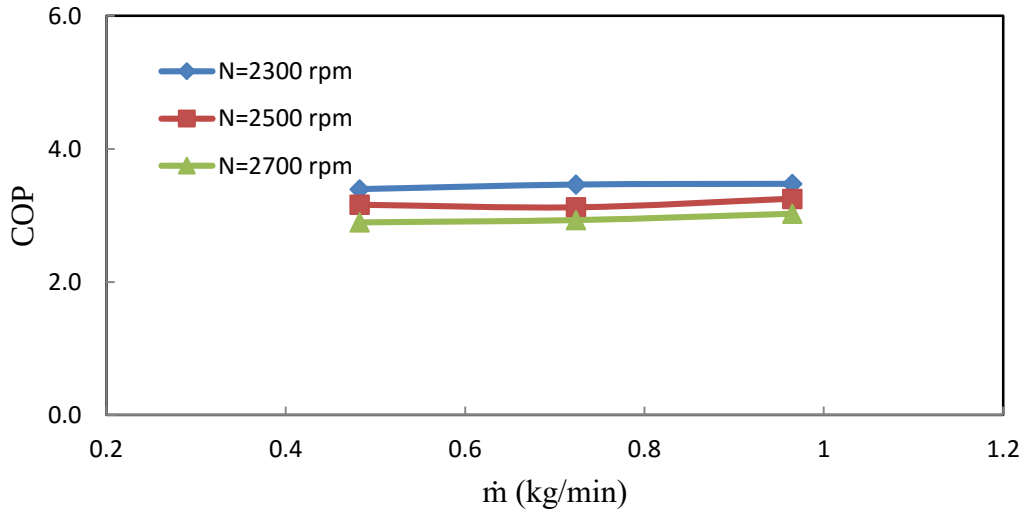

Figure 35: Effect of R404a mass flow rate on COP during charging process based on first law analysis

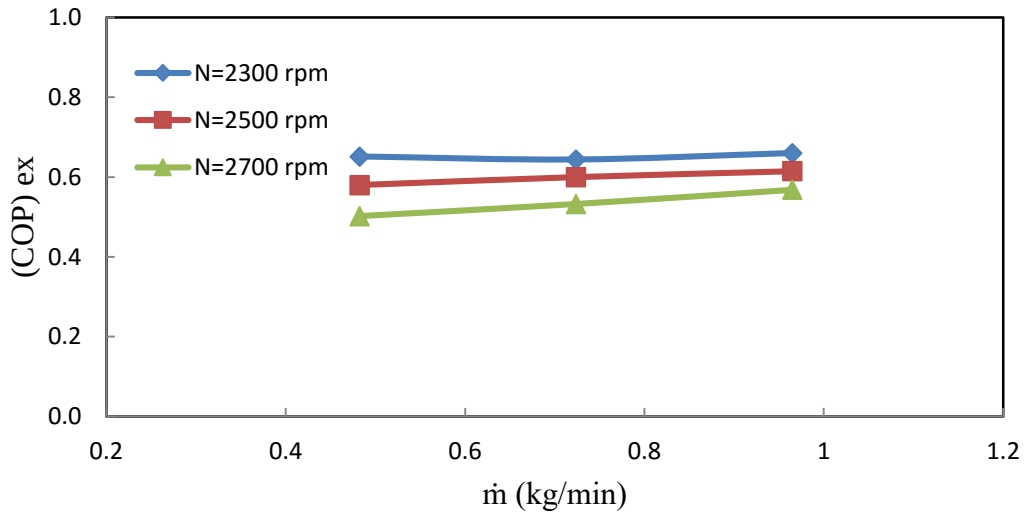

Figure 36: Effect of R134a mass flow rate on COP during charging process based on second law analysis

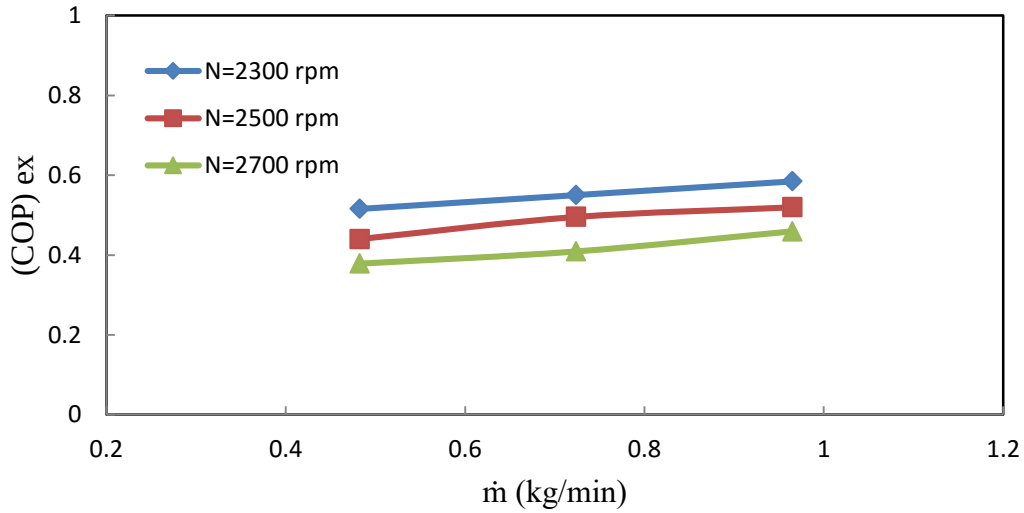

Figure 37: Effect of R404a mass flow rate on COP during charging process based on second law analysis

The periodic coefficient of performance and second law efficiency can be found by using the real experimental reading for R134a as shown in Figures 38 and 39. The results here are obtained every minute for different compressor speeds and a fixed mass flow rate of 0.96 (kg/min). The first law analysis shows that the system will reach a steady state with a coefficient of performance of around 5 as shown in Figure 48.

The second law analysis shows that the efficiency of the system is very high at the beginning of the charging process. However, at a steady state, the efficiency converges to around 60 % as shown in Figure 39. For almost all experimental data, the system performance is very high at the beginning of the charging process and this is due to the high rate of removal of heat in the storage tank during the sensible period.

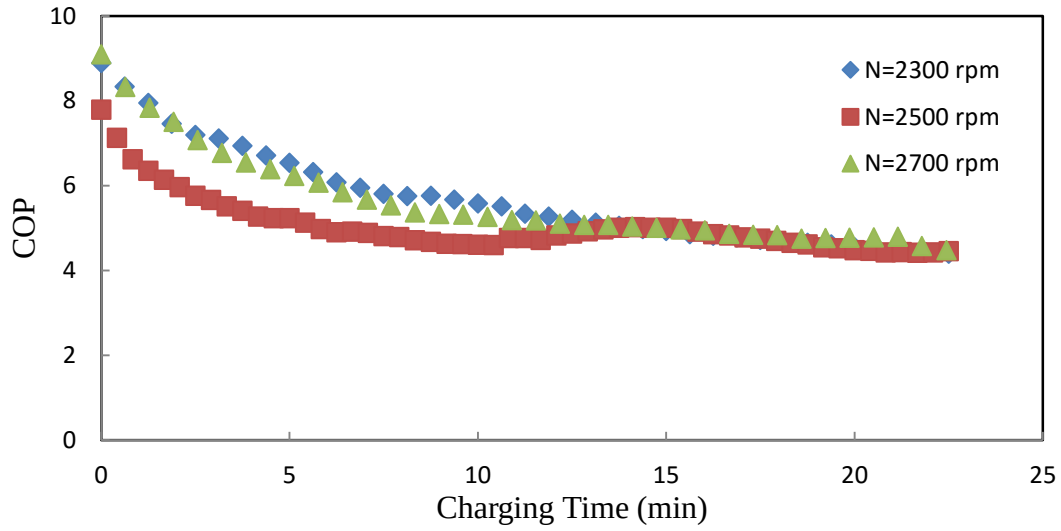

Figure 38: System performance based on first law analysis during clathrate formation of R134a and ṁ=0.96 kg/min

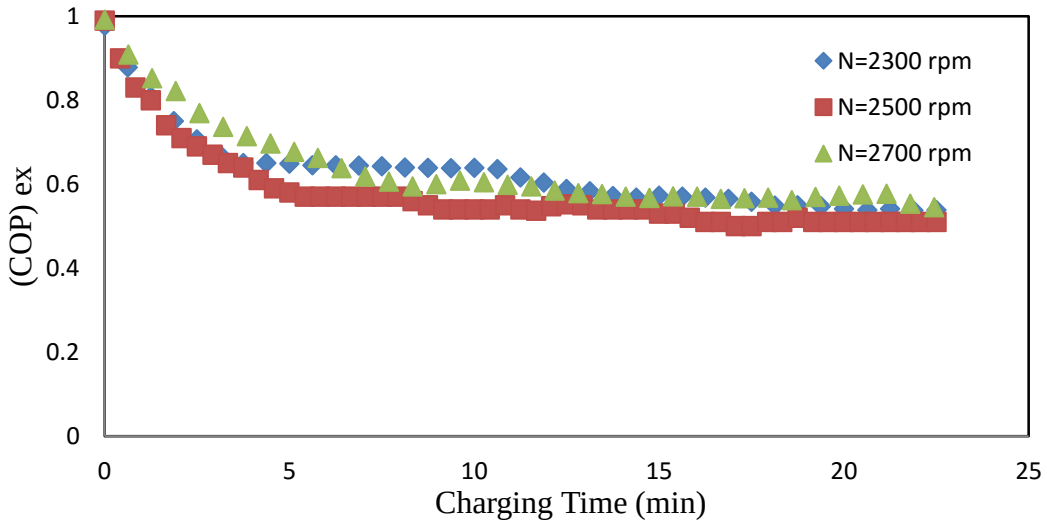

Figure 39: System performance based on second law analysis during clathrate formation of R134a and ṁ=0.96 kg/min

5.6 Comparative analysis between R134a and R404a clathrate

The analysis of the experimental readings for both refrigerants used to form clathrate hydrate shows that forming clathrate hydrate with R134a has more advantage than R404a refrigerant. The comparative analysis presents in this section are in terms of the direct thermal storage system performance, the thermal system compressor power, the compressor pressure ratio and the variation of clathrate hydrate temperature formed inside the direct thermal storage tank during the charging process. For all the experiments conducted in this research, the mass of water is set as a fixed value of 11 kg. Furthermore, the experimental parameters used while conducting the experiments are three different compressor speeds and three different mass flow rate of the working fluid. Table 8 shows the different parameters of the experiments. These parameters aim to experiment the formation of clathrate hydrate of R134a and R404a refrigerants. For clathrate hydrate to form inside the storage tank, the ratio of refrigerant R134a to water used is (1:2.23). This means that for every kg of refrigerant; 2.23 kg of water is used to form clathrate hydrate with R134a. The ratio used for forming clathrate with R404a is around (1:1.84). The quantity of refrigerant can increase or decrease and it can be at different ratio. It depends on the ability of the host molecules of water to interact and absorb the guest molecules of refrigerant.

The power consumed by the compressor while conducting both sets of experiments is found by two ways; one way is by measuring the Voltage and Ampere of the compressor. The other way is by finding the energy rate transferred to the refrigerant across the compressor. It is noted that the value of the energy rate transferred to the working fluid is higher when operating the system with refrigerant R404a. Figures 30 and 31 show the compressor power based on the energy rate transfer to the working fluid for clathrate formation of R134a and R404a respectively. The highest energy rate across the compressor is recorded at operating condition of 2700 rpm and 0.96 kg/min for both refrigerants.

Comparing the two refrigerants in terms of compressor pressure ratio, it is found that the pressure ratio for R404a is higher than R134a. Furthermore, higher pressure ratio is noted when operating at low refrigerant flow rate and high compressor speed for both refrigerants. Table 17 show the highest compression ratio as (4.7) for refrigerant R134a and (6.74) for refrigerant R404a at compressor speed of 2700 RPM.

Similarly, the lowest compression value is recorded while operating at 2300 RPM and high mass flow rate. The effect of R134a and R404a mass flow rate on compressor pressure ratio is shown in Figure 32 and 33 respectively

The performance of the thermal storage system is found by recording the temperature and the pressure reading. Using the reading of temperature and pressure in EES software, the instantaneous enthalpies for the refrigerant used in then noted. The enthalpies readings across the compressor and the storage tank are then used to find the coefficient of performance of the system. Comparing both refrigerants in terms of system performance, it is noticed that the system has higher COP when R134a is used as a working fluid. The COP of the system while forming R134a clathrate hydrate varies between (4.1) and (5.77). The highest record for COP is during operating condition of low compressor speed and high mass flow rate. Table 14 shows the range of operation of different compressor speed and different refrigerant flow rate and the corresponded coefficient of performance. Figure 34 shows the experimental COP results while operating the system with R134a refrigerant. The COP of the system while forming R404a clathrate hydrate varies between (2.9) and (3.48). Figure 35 shows the experimental results recorded for the COP while forming R404a clathrate hydrate. For R134a clathrate hydrate, the best operating condition shows COP of 5.62, 5.68 and 5.77 for compressor speed of 2300 rpm and mass flow rate of 0.48, 0.72 and 0.96 kg/min respectively. For R404a clathrate hydrate, the best operating condition shows COP of 3.40, 3.46 and 3.48 for compressor speed of 2300 rpm and mass flow rate of 0.48, 0.72 and 0.96 kg/min respectively. Comparing the COP of both systems, it is clear that the forming clathrate hydrate with R134a has higher COP than R404a.

The cooling capacity for both refrigerant clathrate hydrate varies based on the operating condition. Tables 13 and 15 show the variation of the cooling capacity at different operating condition. The cooling capacity is directly proportional to the latent heat of fusion of the refrigerant used and the mass of refrigerant and water inside the storage tank. The cooling load for R134a clathrate hydrate is 5703 kJ/kg, while the cooling load for R404a is 6452 kJ/kg.

The temperature inside the storage while forming clathrate hydrate also varies based on the operating conditions. Appendix A shows the temperature variation inside the storage tank for all experimental runs. It is noticed that for refrigerant R134a, less

time is need to form clathrate hydrate when compared to refrigerant R404a. Operating the system with high mass flow rate will require less time to form clathrate hydrate.

This concludes that the compressor speed has less effect than mass flow rate when studying the time needed to form clathrate hydrate. As shown in Table 17, the range of time needed to form clathrate hydrate with refrigerant R134a is around (21) and (50) minutes at different operation of compressor speed and different mass flow rate. Therefore, the formation time for clathrate hydrate will mainly depend on the mass flow rate of the working fluid used. Comparing the results of the two refrigerants, it is noted that R404a takes more time to form clathrate hydrate than R134a at the same operating conditions.

The variation of temperature inside the storage tank during the charging process of R134a clathrate hydrate is shown in Figures 40 to 48 in Appendix A. It is noted that the temperature readings inside the storage tank will start decreasing gradually with time to a certain temperature point, then all the temperature reading will have a constant reading. Figure 40 for example, shows different temperature reading during operating the system at compressor speed of 2300 rpm and mass flow rate of 0.48 kg/min with R134a as a working fluid. Decreasing in temperature inside the storage tank is noted from time (0) to (25) minutes. Later, the temperature readings remain at a certain value as shown from time (25) to (45) minutes. Afterward, the temperature readings curves will further decrease more as shown from time (45) to (50) minutes. The second period, between 25-40 min, represents the latent heat of fusion for R134a clathrate formation. While the third period shows that the clathrate is sub-cooled. Similarly, the variation of temperature inside the storage tank during the charging process of R404a clathrate hydrate is shown in Figures 49 to 57. The formation of R404a clathrate hydration at operating condition of 2300 rpm and 0.48 kg/min is shown in Figure 49. It is noted that more time is needed to form clathrate with R404a at the same operating conditions. Figure 49 shows the variation of temperature reading inside the storage tank for R404 clathrate formation. It is also noted that the latent period for R404a is more than R134a. This is also due to the thermal properties of the guest material of refrigerant hydrate as shown in [65]. All temperature figures in Appendix A are arranged based on the experimental sets shown in Table 10 for R134a clathrate hydrate and Table 11 for R404a clathrate hydrate.

Table 17: Comparative analysis between R134a and R404a clathrate hydrates

Comp. Speed (RPM)	Mass Flow Rate (kg/min)	Average Final Temperature (℃)		Total Charging Time (min)		Rate of Energy absorbed across evaporator (kJ/s)		Rate Transfer to fluid across Compressor (kJ/s)		CR		(COP)en		(COP)ex (%)	
		R134a	R404a	R134a	R404a	R134a	R404a	R134a	R404a	R134a	R404a	R134a	R404a	R134a	R404a
2300	0.4824	5.6	7.9	48	51	1.54	1.66	0.27	0.49	4.2	5.6	5.62	3.40	62	52
2300	0.7236	5.7	7.8	40	40	2.31	2.52	0.41	0.73	3.26	5.17	5.68	3.46	64	55
2300	0.9648	4.1	7.2	21	30	3.06	3.27	0.53	0.94	2.91	4.91	5.77	3.48	66	58
2500	0.4824	4.4	8.31	50	52	1.54	1.62	0.32	0.51	4.3	6.12	4.83	3.16	58	44
2500	0.7236	4	8.4	40	40	2.31	2.44	0.47	0.78	3.7	5.46	4.96	3.12	60	49
2500	0.9648	4	8.4	22	30	3.10	3.25	0.60	1.00	2.91	4.78	5.19	3.25	62	51
2700	0.4824	5.2	6.8	48	50	1.52	1.63	0.37	0.56	4.72	6.74	4.10	2.90	50	38
2700	0.7236	4.2	7.3	39	41	2.27	2.44	0.53	0.83	3.9	5.62	4.28	2.93	53	41
2700	0.9648	4.0	7.5	22	30	3.06	3.25	0.68	1.07	3.07	5.04	4.49	3.03	57	46

5.7 Discussion of Results

The aim of this experimental research is to evaluate the cold thermal energy storage system while forming clathrate with alternative refrigerants. The experiments are conducted to determine the conditions under which clathrate hydrate forms for the tested refrigerants and to study the performance of the thermal storage system. This section discusses the results obtained from the experimental runs during formation of clathrate hydrate with refrigerant R134a and R404a. The results present in this section discuss the cooling load for both refrigerant and the performance of the cold thermal storage system in terms of energy and exergy analysis. The best operation condition is then discussed based on analyzing the experimental data.

The instantaneous enthalpies for both refrigerants are found by measuring the temperatures and pressures readings across the compressor and the storage tank. The rate of heat absorbed inside the storage tank shows different reading based on the operating conditions. For clathrate hydrate with R134a, the rate of heat absorbed shows high rate while operating the system with high mass flow rate. For example, the recorded values for R134a are 1.541 kJ/s, 2.308 kJ/s and 3.060 kJ/s for mass flow rate of 0.48 kg/min, 0.72 kg/min and 0.96 kg/min respectively. Similarly for clathrate hydrate with R404a, the rate of heat absorbed across the storage tank are 1.664 kJ/s, 2.518 kJ/s, and 3.267 kJ/s for mass flow rate of 0.48 kg/min, 0.72 kg/min and 0.96 kg/min respectively. Table 17 presents the comparative analysis between R134a and R404a clathrate hydrate at different running parameters.

Studying the cooling load of both clathrates, results show that clathrate hydrate with R404a has greater cooling load than R134a clathrate. This is due to the fact that refrigerant R134a has less latent heat of fusion of 358 (kJ/kg) when compared to latent heat of fusion of R404a refrigerant. The calculated values of the cooling load stored are noted in Table 13 and 15.

For clathrate hydrate with refrigerant R134a, the system performance varies between (4.10) to (5.77) based on first law analysis. The second law analysis shows the variation between (50%) to (66%) at different operating conditions. This means that the total recovered work by the system is between (50%) to (66%) of the total work supplied.

For refrigerant R134a, it is noted that a high coefficient of performance (5.77) and high system exergetic efficiency (66%) occur at lower compressor speed (2300 rpm) and high mass flow rate of refrigerant (0.948 kg/min). This concludes that running the system with high compressor speed generates more exergetic loss in the system leading to low efficiency. The recorded exergy recovered of R134a system is higher for 2300 rpm than 2700 rpm. For example, for mass flow rate of 0.96 (kg/min) and 2300 rpm, the exergy recovered is 66% of the exergy input. Studying the other mass flow rates 0.72 (kg/min) and 0.48 (kg/min), the exergy recovery is 64% and 62% respectively. This shows that the exergy recovered is high with high flow rate and low compressor speed.

For clathrate hydrate with refrigerant R404a, the system performance shows lower values when compared to R134a clathrate formation. For example, for clathrate hydrate with refrigerant R404a, the coefficient of performance varies between (2.9) to (3.48) based on the first law analysis of thermodynamics at different operating conditions. High system COP of (3.48) occurs while running the system with 2300 rpm and 0.94 (kg/min) mass flow rate. The second law analysis shows variation in exergetic efficiency between (38%) to (58%). The exergetic efficiency of the system is highest when running at low compressor speed and high mass flow rate. For example, running the experiments at compressor speed of 2300 rpm, the exergetic efficiencies are 52%, 55% and 58% for 0.48 (kg/min), 0.72 (kg/min), and 0.96(kg/min) respectively. On the other hand, for high compressor speed of 2700rpm, the exergetic efficiencies are 38%, 41%, 46% for 0.48 (kg/min), 0.72 (kg/min), and 0.96(kg/min) respectively. This shows that the best operating condition found in this research is at compressor speed of 2300 rpm and mass flow rate of 0.96 kg/min.

The tables shown in Section 5.5 are the summary of all experimental results obtained while conducting the experiments to form the clathrate hydrates. These tables summarize the effect of the experimental parameters (compressor speed and mass flow rate) on the thermal system to form clathrate hydrate of two main refrigerants: R134a and R404a. This research shows that the best operating conditions for cold thermal energy storage system are at low compressor speed and at high mass flow rate of the tested operating parameters.

Chapter 6: Conclusion and Recommendations

This research mainly focused on studying clathrate hydrates with different refrigerants. Refrigerant R134a and R404a are used to study the performance of a direct thermal energy storage system with refrigerant clathrate hydrate as a storage medium. The results in this research present the *cold charging process* of refrigerant clathrate hydrates with both refrigerants R134a and R404a. During operation of the direct thermal energy system with refrigerant R134a, it is noted that the clathrate formed temperature readings converge to a temperature range between 4℃ and 6 ℃ inside the storage tank. This indicates that the complete formation of refrigerant R134a clathrate hydrates occurs at these temperature ranges. For refrigerant R134a clathrate formation, it is noted that less time is needed to form the clathrate unlike the case for refrigerant R404a under the same operating conditions of flow rate and compressor speed. Furthermore, it is noted that refrigerant R134a clathrate formation takes more time to dissolve and discharge. This can be explained by the fact that the water molecules forms a stronger cage-like structure around the refrigerant R134a guest molecules which make it takes more time to discharge the refrigerant clathrate structure to start another charging process.

A detailed comparison between R134a and R404a clathrate in terms of mass of clathrate, the energy stored during the charging process, and the coefficient of performance of the system are provided with in this research in Tables 14 to 17. The first and second laws of thermodynamics are used as a tool to evaluate the performance of each refrigerant clathrate formation. The experimental results for system performance are shown in Figures 34 to 39. The experimental study and the mathematical model show that forming clathrate hydrate with refrigerant R134a is more efficient than refrigerant R404a. The coefficient of performance of the thermal energy storage system varies from 4.1 and 5.77 while forming refrigerant clathrate hydrate of R134a. On the other hand, the performance varies from 2.9 and 3.48 while forming clathrate hydrate of R404a at similar experimental conditions. It is noted that a high coefficient of performance occurs at the low compressor speed and high working fluid mass flow rate. The second law efficiency of the R134a system varies between 50% and 66%, while for R404a, the second law efficiency varies between 37% and 58%. Further, the exergy destruction in the R404a thermal storage system is higher than the

exergy destruction in the R134a thermal storage system. Therefore, this thesis proposes the use of R134a refrigerant to form clathrate hydrate for thermal energy storage.

The recommendations for this study can be summarized as follows: according to this research work, refrigerant R134a has more advantage in forming refrigerant clathrate hydrate as a storage medium than refrigerant R404 for a direct thermal energy storage system. Refrigerant R134a shows a better system performance and reasonable stored load compared to R404a clathrate. This work recommends the study of other refrigerants as an alternative for R134a clathrate for thermal storage systems. Also, more research is needed to improve the understanding of the scientific and engineering characteristics of refrigerant clathrate hydrate with thermal energy storage systems. It is also recommended to develop various theoretical and practical aspects related to the performance and implementation of thermal storage system with real HVAC systems. In order to select a thermal energy storage system for real HVAC applications, it is recommended to consider several factors such as; size, operating strategies, environment, economics, and the reliability of such integration.

In this study, the experimental investigation proves that such a system can be reliable in storing thermal energy for short and long periods if used for HVAC systems. A further recommendation is to model thermal system numerically or with ANSYS software to check the reliability of the storage system. In order to improve the designing aspects related to the system performance and real system implementation of the existing direct thermal energy storage system, some recommended developments are presented as follows:

- The size of the storage tank (direct storage tank) is a critical component of such a system; thus, implementing such system in real HVAC systems will require a bigger storage tank.
- The discharging unit is one of the important sub-systems for direct thermal energy storage; thus, improving the efficiency of a fan coil unit (FCU) is strongly recommended.
- The formation of clathrate hydrate inside the tank is almost solid which blocks the discharging coils in most cases; thus, adding a heater inside the tank beside the discharging coils will be of great importance to the system.

- Conducting more experimental test with new refrigerants to form new clathrate hydrates that are suitable for longer thermal storage periods is recommended
- Developing and applying standardized methods to find new refrigerants for better system performance, long lifetime, and safety of the storage system.
- Develop numerical models to understand and optimize the clathrate behavior and the overall storage system before running the system can show a better understanding of the clathrate formation process.

In conclusion, the evaluation of a cold direct thermal energy storage system using alternative refrigerants is the main research topic of this thesis. The evaluation of the multi-stage operation of the existing direct thermal energy storage system needs to be further investigated with current refrigerants and current tested parameters. It would, however, be appropriate to further execute this study using a variety of tested parameters such as lower compressor speeds varying from 700 rpm to 2000 rpm and higher mass flow rate of refrigerant varying between 0.96 kg/min to 3.98 kg/min to conduct the experimental tests. The mass of stored water is also an important parameter and it would be appropriate to conduct experiments using higher mass of water: 22 kg and 33 kg. While the aim in this study is to evaluate thermal energy storage systems, a comparison between direct and indirect thermal energy storage might be a special topic of interest in this field. Hence, further studies with detailed thermal energy storage system behavior can follow with more detail and a wider range of parameters. The development of better cold thermal energy systems will result in a promising contribution to the thermal energy design.

References

[1] T. Kiatsiriroat, P. Siriplubpla, and A. Nuntaphan, "Performance Analysis of a refrigeration cycle using a direct contact evaporator," *Int. J. Energy Res.*, vol. 22, no. 13, pp. 1179–1190, 1998.

[2] T. Kiatsiriroat, S. Vithayasai, N. Vorayos, and a Nuntaphan, "Heat transfer prediction for a direct contact ice thermal energy storage," *Energy Convers. Manag.*, vol. 44, no. 4, pp. 497–508, Mar. 2003.

[3] I. Dincer and M. A. Rosen, *Thermal Energy Storage Systems and Application*, 2nd ed. UK: John Wiley & Sons, 2010, p. 620.

[4] I. Dincer, "On thermal energy storage systems and applications in buildings," *Energy Build.*, vol. 34, no. 2001, pp. 377–388, 2002.

[5] B. Zalba, J. M. Marín, L. F. Cabeza, and H. Mehling, "Review on thermal energy storage with phase change: materials, heat transfer analysis and applications," *Appl. Therm. Eng.*, vol. 23, no. 3, pp. 251–283, Feb. 2003.

[6] A. Sharma, V. V. Tyagi, C. R. Chen, and D. Buddhi, "Review on thermal energy storage with phase change materials and applications," *Renew. Sustain. Energy Rev.*, vol. 13, no. 2, pp. 318–345, Feb. 2009.

[7] M. O. Abdullah, L. P. Yii, E. Junaidi, G. Tambi, and M. A. Mustapha, "Electricity cost saving comparison due to tariff change and ice thermal storage (ITS) usage based on a hybrid centrifugal-ITS system for buildings: A university district cooling perspective," *Energy Build.*, vol. 67, pp. 70–78, Dec. 2013.

[8] L. Perez-lombard and C. Pout, "A review on buildings energy consumption information," *Energy Build.*, vol. 40, pp. 384–348, 2008.

[9] C. Balaras, G. Grossman, C. Ferreira, E. Podesser, L. Wang, and E. Wiemken, "Solar air conditioning in Europe—an overview," *Renew. Sustain. Energy Rev.*, vol. 11, no. 2, pp. 299–314, Feb. 2007.

[10] V. Vakiloroaya, B. Samali, A. Fakhar, and K. Pishghadam, "A review of different strategies for HVAC energy saving," *Energy Convers. Manag.*, vol. 77, pp. 738–754, Jan. 2014.

[11] H. Eldessouky, "Performance analysis of two-stage evaporative coolers," *Chem. Eng. J.*, vol. 102, no. 3, pp. 255–266, Sep. 2004.

[12] M. Salvador and S. Grieu, "Methodology for the design of energy production and storage systems in buildings: Minimization of the energy impact on the electricity grid," *Energy Build.*, vol. 47, pp. 659–673, Apr. 2012.

[13] R. Parameshwaran and S. Kalaiselvam, “Energy conservative air conditioning system using silver nano-based PCM thermal storage for modern buildings,” *Energy Build.*, vol. 69, pp. 202–212, Feb. 2014.

[14] N. Soares, J. J. Costa, a. R. Gaspar, and P. Santos, “Review of passive PCM latent heat thermal energy storage systems towards buildings’ energy efficiency,” *Energy Build.*, vol. 59, pp. 82–103, Apr. 2013.

[15] C. Chaichana, W. W. . Charters, and L. Aye, “An ice thermal storage computer model,” *Appl. Therm. Eng.*, vol. 21, no. 17, pp. 1769–1778, Dec. 2001.

[16] B. a. Habeebullah, “Economic feasibility of thermal energy storage systems,” *Energy Build.*, vol. 39, no. 3, pp. 355–363, Mar. 2007.

[17] O. M. Al-Rabghi and M. M. Akyurt, “A survey of energy efficient strategies for effective air conditioning,” *Energy Convers. Manag.*, vol. 45, no. 11–12, pp. 1643–1654, Jul. 2004.

[18] H. Caliskan, I. Dincer, and A. Hepbasli, “Energy and exergy analyses of combined thermochemical and sensible thermal energy storage systems for building heating applications,” *Energy Build.*, vol. 48, pp. 103–111, May 2012.

[19] A. H. Mohammadi, “Pressure-Temerature Phase Diagrams of Clathrate Hydrates of HFC-134a, HFC-152a and HFC-32,” *AIChE Annual Meeting*, 2010.

[20] Y. Seo, H. Tajima, A. Yamasaki, S. Takeya, T. Ebinuma, and F. Kiyono, “A new method for separating HFC-134a from gas mixtures using clathrate hydrate formation.,” *Environ. Sci. Technol.*, vol. 38, no. 17, pp. 4635–9, Sep. 2004.

[21] D. Liang, R. Wang, K. Guo, and S. Fan, “Prediction of refrigerant gas hydrates formation conditions,” *J. Therm. Scince*, vol. 10, no. 1, pp. 64–68, 2001.

[22] K. Maeda, Y. Katsura, Y. Asakuma, and K. Fukui, “Concentration of sodium chloride in aqueous solution by chlorodifluoromethane gas hydrate,” *Chem. Eng. Process. Process Intensif.*, vol. 47, no. 12, pp. 2281–2286, Nov. 2008.

[23] J. Javanmardi and M. Moshfeghian, “Energy consumption and economic evaluation of water desalination by hydrate phenomenon,” *Appl. Therm. Eng.*, vol. 23, no. 7, pp. 845–857, May 2003.

[24] D. Liang, K. Guo, R. Wang, and S. Fan, “Hydrate equilibrium data of 1,1,1,2-tetrafluoroethane (HFC-134a), 1,1-dichloro-1-fluoroethane (HCFC-141b) and 1,1-difluoroethane (HFC-152a),” *Fluid Phase Equilib.*, vol. 188, pp. 61–70, 2001.

[25] M. Nakaiwa and H. Fukuura, “Formation of CFC alternative R134a gas hydrate,” *Energy Convers. Eng. Conf.*, vol. 4, pp. 269–274, 1990.

[26] Y. Seo, H. Tajima, A. Yamasaki, S. Takeya, T. Ebinuma, and F. Kiyono, “A new method for separating HFC-134a from gas mixtures using clathrate hydrate formation,” *Environ. Sci. Technol.*, vol. 38, pp. pp.4635–4639, 2004.

[27] Z. Li, G. Kaihua, Z. Yongli, S. Bifen, and Z. Jiawei, “Phase equilibrium calculation for refrigerant simple gas hydrates,” *J. Eng. Thermophys.*, vol. 21, no. 1, pp. 31–16, 2000.

[28] A. Eslamimanesh, A. H. Mohammadi, and D. Richon, “Thermodynamic model for predicting phase equilibria of simple clathrate hydrates of refrigerants,” *Chem. Eng. Sci.*, vol. 66, no. 21, pp. 5439–5445, Nov. 2011.

[29] V. Vakiloroaya, B. Samali, A. Fakhar, and K. Pishghadam, “A review of different strategies for HVAC energy saving,” *Energy Convers. Manag.*, vol. 77, pp. 738–754, Jan. 2014.

[30] B. Rismanchi, R. Saidur, H. H. Masjuki, and T. M. I. Mahlia, “Energetic, economic and environmental benefits of utilizing the ice thermal storage systems for office building applications,” *Energy Build.*, vol. 50, pp. 347–354, Jul. 2012.

[31] B. Rismanchi, R. Saidur, H. H. Masjuki, and T. M. I. Mahlia, “Thermodynamic evaluation of utilizing different ice thermal energy storage systems for cooling application in office buildings in Malaysia,” *Energy Build.*, vol. 53, pp. 117–126, Oct. 2012.

[32] Y. Sun, S. Wang, F. Xiao, and D. Gao, “Peak load shifting control using different cold thermal energy storage facilities in commercial buildings,” *Energy Convers. Manag.*, vol. 71, pp. 101–114, Jul. 2013.

[33] M. J. Sebzali and P. a. Rubini, “Analysis of ice cool thermal storage for a clinic building in Kuwait,” *Energy Convers. Manag.*, vol. 47, no. 18–19, pp. 3417–3434, Nov. 2006.

[34] A. Eslamimanesh, A. H. Mohammadi, and D. Richon, “Thermodynamic model for predicting phase equilibria of simple clathrate hydrates of refrigerants,” *Chem. Eng. Sci.*, vol. 66, no. 21, pp. 5439–5445, Nov. 2011.

[35] K. H. Guo, B. F. Shu, and Y. Zhang, “Transient behavior of energy charge-discharge and solid-liquid phase change in mixed gas-hydrate formation,” in *Guangzhou Inst of Energy Conversion, of the Chinese Acad of Sciences*, 1996.

[36] D. Liang, R. Wang, K. Guo, and S. Fan, “Prediction of refrigerant gas hydrates formation conditions,” *J. Therm. Sci.*, vol. 10, no. 1, pp. 64–68, 2001.

[37] Z. Li, G. Kaihua, Z. Yongli, S. Bifen, and Z. Jiawei, “Phase Equilibrium Calculation for Refrigerant Simple Gas Hydrates,” *J. Eng. Thermophys.*, vol. 21, no. 1, pp. 13–16, 2000.

[38] Z. Li, G. Kaihua, Y. ZHAO, and S. Bifen, “Phase Equilibrium Calculation for Binary Refrigerant Gas Hydrates,” *J. Eng. Thermophys.*, vol. 21, no. 2, pp. 269–272, 2000.

[39] F. Nikbakht, A. a. Izadpanah, F. Varaminian, and A. H. Mohammadi, “Thermodynamic modeling of hydrate dissociation conditions for refrigerants R-134a, R-141b and R-152a,” *Int. J. Refrig.*, vol. 35, no. 7, pp. 1914–1920, Nov. 2012.

[40] M. Karamoddin and F. Varaminian, “Experimental measurement of phase equilibrium for gas hydrates of refrigerants, and thermodynamic modeling by SRK, VPT and CPA EOSs,” *J. Chem. Thermodyn.*, vol. 65, pp. 213–219, Oct. 2013.

[41] Y. Bi, T. Guo, L. Zhang, H. Zhang, and L. Chen, “Experimental study on cool release process of gas-hydrate with additives,” *Energy Build.*, vol. 41, no. 1, pp. 120–124, Jan. 2009.

[42] T. Mori and Y. Mori, “Characterization of gas hydrate formation in direct-contact cool storage process,” *Int. J. Refrig.*, vol. 12, no. 5, pp. 259–265, 1989.

[43] R. McCormack, “Use of clathrates for ‘off-peak’ thermal energy storage,” in *Energy Conversion Engineering Conference*, 1900, pp. 300–305.

[44] A. A. Kendoush, K. Joudi, and N. Abid Jassim, “The growth rate of gas hydrate from refrigerant R12,” *Exp. Therm. Fluid Sci.*, vol. 30, pp. 643–651, 2006.

[45] S. Thongwik, N. Vorayos, T. Kiatsiriroat, and A. Nuntaphan, “Thermal analysis of slurry ice production system using direct contact heat transfer of carbon dioxide and water mixture,” *Int. Commun. Heat Mass Transf.*, vol. 35, pp. 756–761, 2008.

[46] J. Wu and S. Wang, “Research on cool storage and release characteristics of R134a gas hydrate with additive,” *Energy Build.*, vol. 45, pp. 99–105, Feb. 2012.

[47] Y. Xie, G. Li, D. Liu, N. Liu, Y. Qi, D. Liang, K. Guo, and S. Fan, “Experimental study on a small scale of gas hydrate cold storage apparatus,” vol. 87, pp. 3340–3346, 2010.

[48] A. Sharma, V. V. Tyagi, C. R. Chen, and D. Buddhi, “Review on thermal energy storage with phase change materials and applications,” *Renew. Sustain. Energy Rev.*, vol. 13, no. 2, pp. 318–345, Feb. 2009.

[49] S. Álvarez, L. F. Cabeza, A. Ruiz-Pardo, A. Castell, and J. A. Tenorio, "Building integration of PCM for natural cooling of buildings," *Appl. Energy*, vol. 109, pp. 514–522, Sep. 2013.

[50] A. Waqas and Z. Ud Din, "Phase change material (PCM) storage for free cooling of buildings—A review," *Renew. Sustain. Energy Rev.*, vol. 18, pp. 607–625, Feb. 2013.

[51] E. Osterman, V. . Tyagi, V. Butala, N. . Rahim, and U. Stritih, "Review of PCM based cooling technologies for buildings," *Energy Build.*, vol. 49, pp. 37–49, Jun. 2012.

[52] W. a. Qureshi, N.-K. C. Nair, and M. M. Farid, "Impact of energy storage in buildings on electricity demand side management," *Energy Convers. Manag.*, vol. 52, no. 5, pp. 2110–2120, May 2011.

[53] S. M. Hasnain and N. M. Alabbadi, "Need for thermal-storage air-conditioning in Saudi Arabia," *Appl. Energy*, vol. 65, no. 1–4, pp. 153–164, Apr. 2000.

[54] M. Ban, G. Krajačić, M. Grozdek, T. Ćurko, and N. Duić, "The role of cool thermal energy storage (CTES) in the integration of renewable energy sources (RES) and peak load reduction," *Energy*, vol. 48, no. 1, pp. 108–117, Dec. 2012.

[55] E. Oró, A. de Gracia, A. Castell, M. M. Farid, and L. F. Cabeza, "Review on phase change materials (PCMs) for cold thermal energy storage applications," *Appl. Energy*, vol. 99, no. 0, pp. 513–533, Nov. 2012.

[56] S. Hunt, "Gas Hydrate Thermal Energy Storage Systems." U.S. Patent 5140824A, Aug. 25, 1992.

[57] G. Li, Y. Hwang, and R. Radermacher, "Review of cold storage materials for air conditioning application," *Int. J. Refrig.*, vol. 35, no. 8, pp. 2053–2077, Dec. 2012.

[58] K. Liu, H. Guven, A. Beyene, and P. Lowrey, "A comparison of the field performance of thermal energy storage (TES) and conventional chiller systems," *Energy*, vol. 19, pp. 889–900, 1994.

[59] S. M. Hasnain, "Review on sustainable thermal energy storage technologies, Part II: cool thermal storage," *Energy Convers. Manag.*, vol. 39, no. 11, pp. 1139–1153, Aug. 1998.

[60] C.-D. Ho, J.-W. Tu, T.-L. Hsien, H. Chang, and T.-C. Chen, "Heat transfer enhancement in cool-thermal discharge systems from ice melting with time–velocity variations," *Int. Commun. Heat Mass Transf.*, vol. 37, no. 7, pp. 815–821, Aug. 2010.

[61] Y. F. Liu and R. Z. Wang, “Method to design optimal scheme for cold storage air conditioning system,” *Energy Convers. Manag.*, vol. 43, no. 17, pp. 2357–2367, Nov. 2002.

[62] H.-J. Chen, D. W. P. Wang, and S.-L. Chen, “Optimization of an ice-storage air conditioning system using dynamic programming method,” *Appl. Therm. Eng.*, vol. 25, no. 2–3, pp. 461–472, Feb. 2005.

[63] S. Ashok and R. Banerjee, “Optimal cool storage capacity for load management,” *Energy*, vol. 28, no. 2, pp. 115–126, Feb. 2003.

[64] I. Dincer and M. Kanoglu, *Refrigeration Systems and Application*, 2nd ed. UK: John Wiley & Sons, 2010, p. 484.

[65] G. Li, Y. Hwang, and R. Radermacher, “Review of cold storage materials for air conditioning application,” *Int. J. Refrig.*, vol. 35, no. 8, pp. 2053–2077, Dec. 2012.

Appendices

Appendix: A (Temperature Readings)

In this appendix, the tables and the graphs for temperature variation inside the storage tank is presented. Thesis graphs of the temperature variations are used to find the energy stored and the temperature distribution inside tank. The order of the graphs are based on run experiments presented in Table 10 and 11**.** The temperature behavior of the direct storage tank of refrigerant R134a and R404a are presented here,

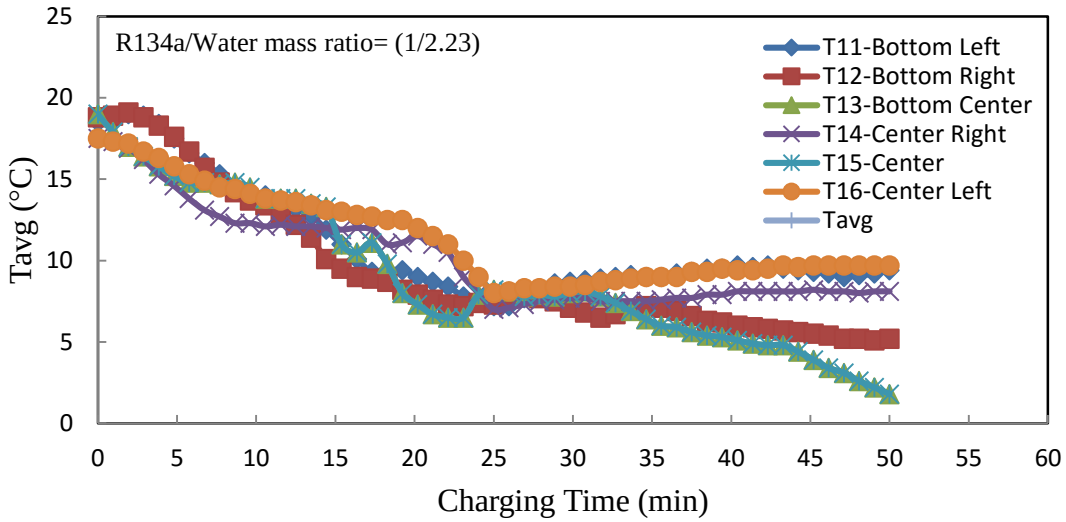

Figure 40: Variation of temperature inside the storage tank during clathrate formation of refrigerant R134a with mass flow rate 0.48 kg/min and N=2300 rpm

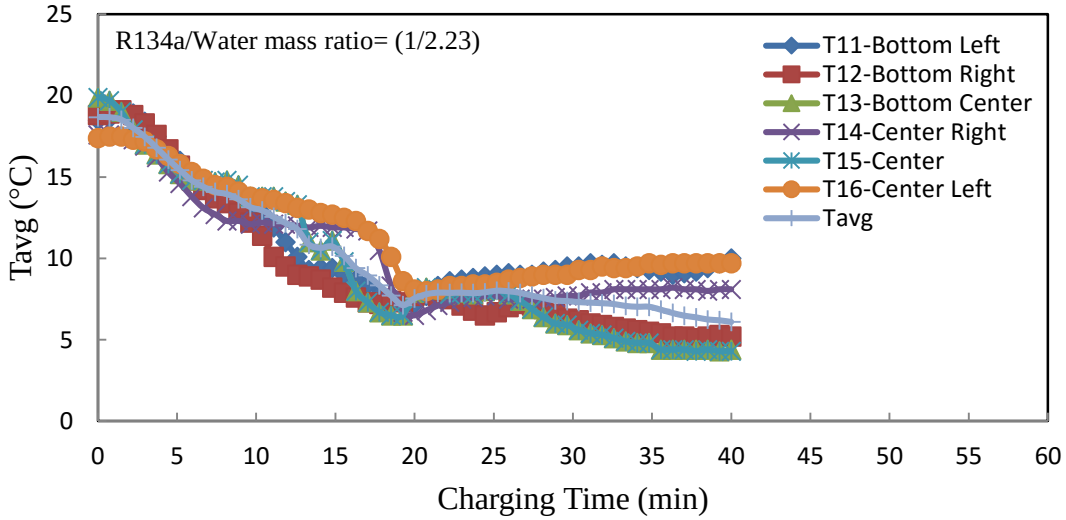

Figure 41: Variation of temperature inside the storage tank during clathrate formation of refrigerant R134a with mass flow rate of 0.72 kg/min and N=2300 rpm

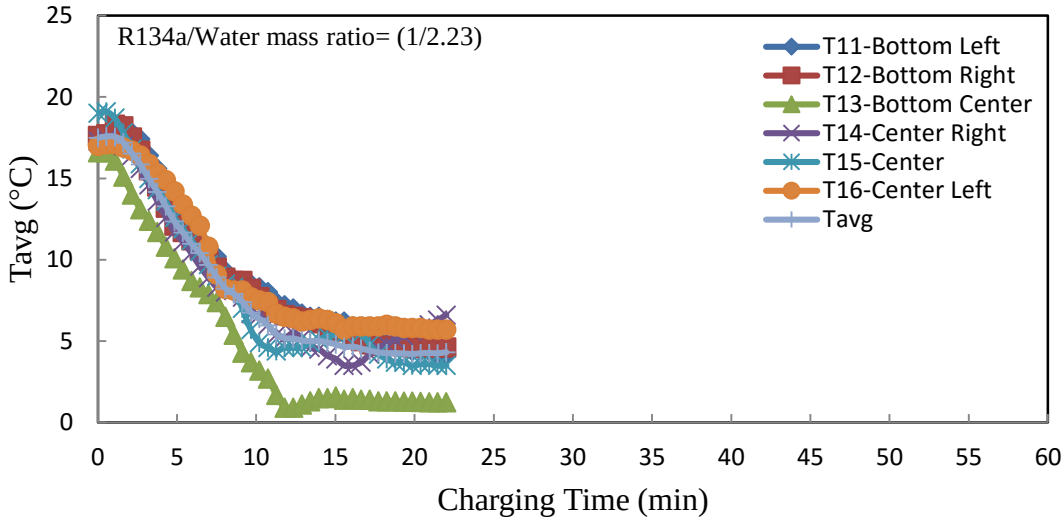

Figure 42: Variation of temperature inside the storage tank during clathrate formation of refrigerant R134a with mass flow rate of 0.96 (kg/min) and N= 2300 rpm

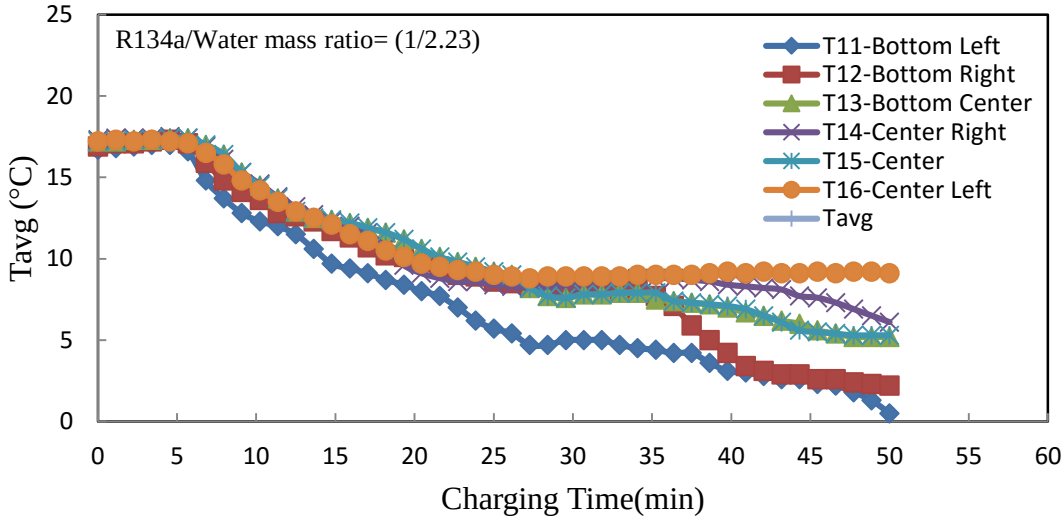

Figure 43: Variation of temperature inside the storage tank during clathrate formation of refrigerant R134a with mass flow rate of 0.48(kg/min) and N=2500 rpm

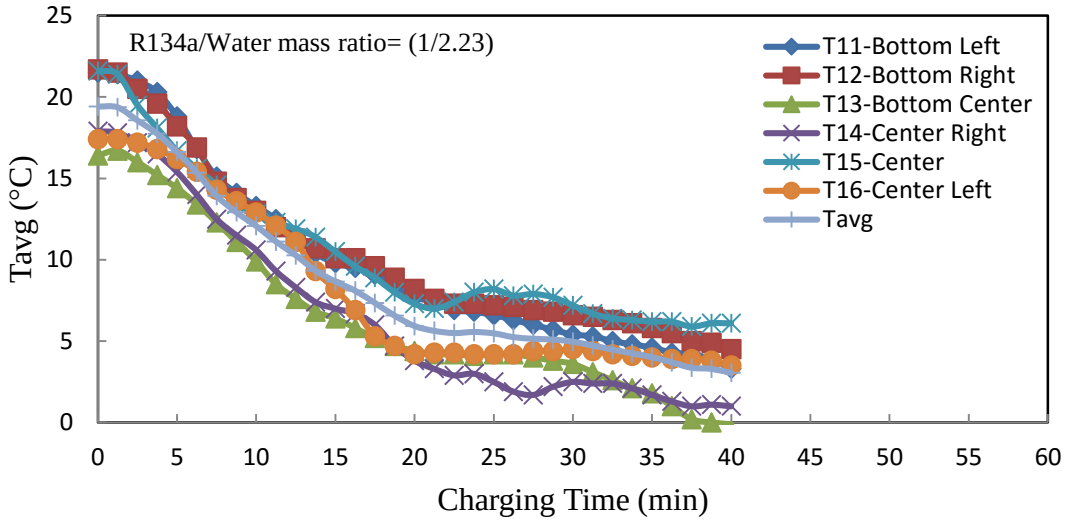

Figure 44: Variation of temperature inside the storage tank during clathrate formation of refrigerant R134a with mass flow rate of 0.72(kg/min) and N= 2500 rpm

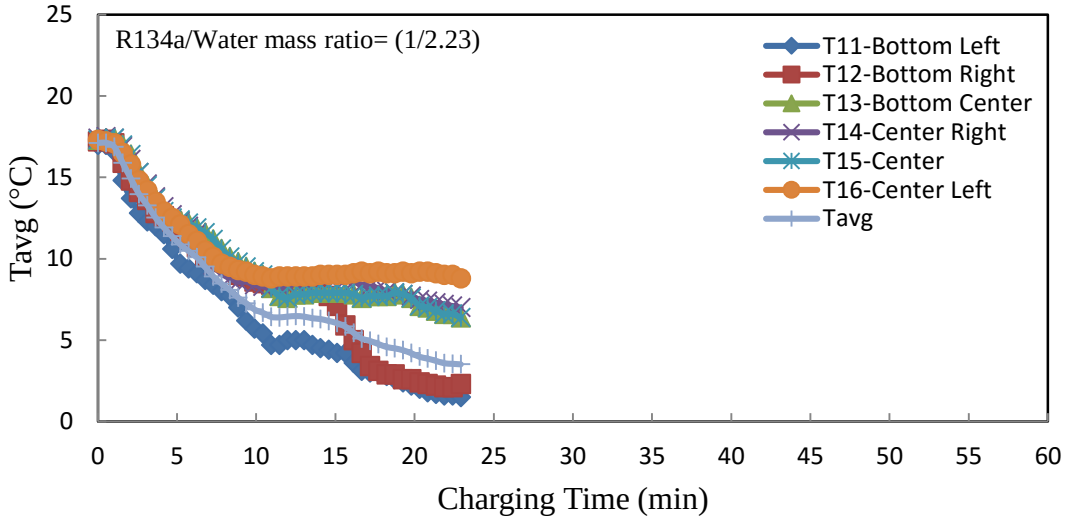

Figure 45: Variation of temperature inside the storage tank during clathrate formation of refrigerant R134a with mass flow rate of 0.96 (kg/min) and N= 2500 rpm

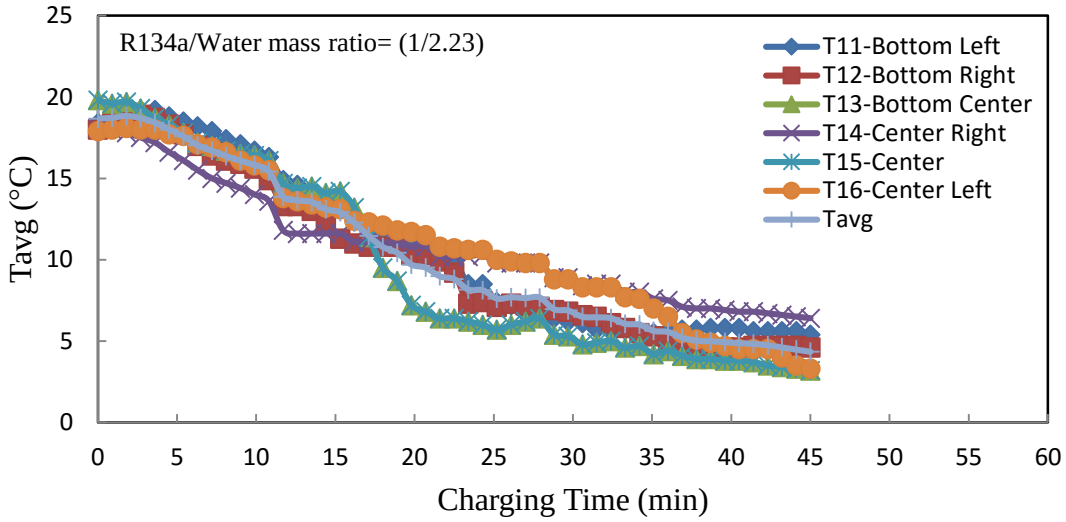

Figure 46: Variation of temperature inside the storage tank during clathrate formation of refrigerant R134a with mass flow rate of 0.48(kg/min) and N= 2700 rpm

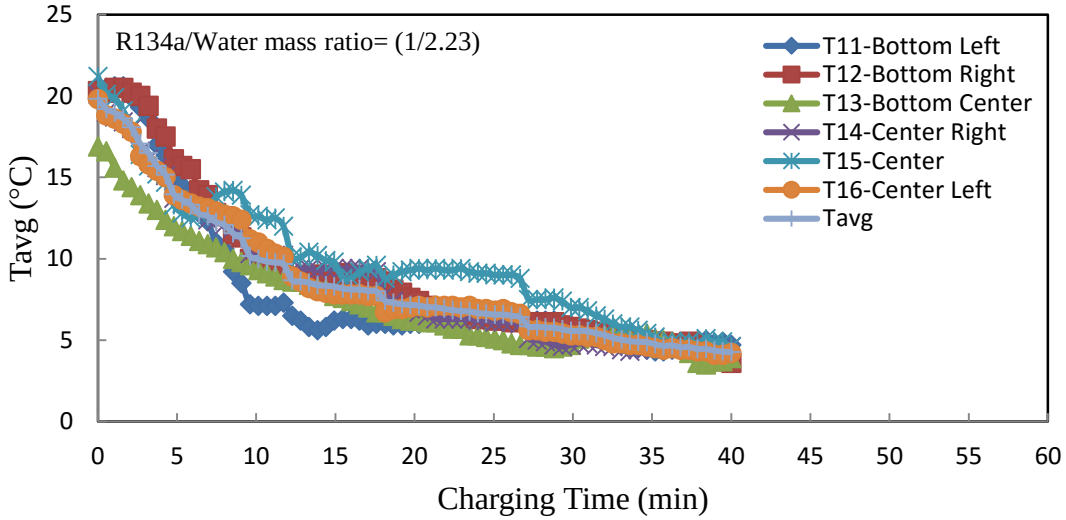

Figure 47: Variation of temperature inside the storage tank during clathrate formation of refrigerant R134a with mass flow rate of 0.72(kg/min) and N= 2700 rpm

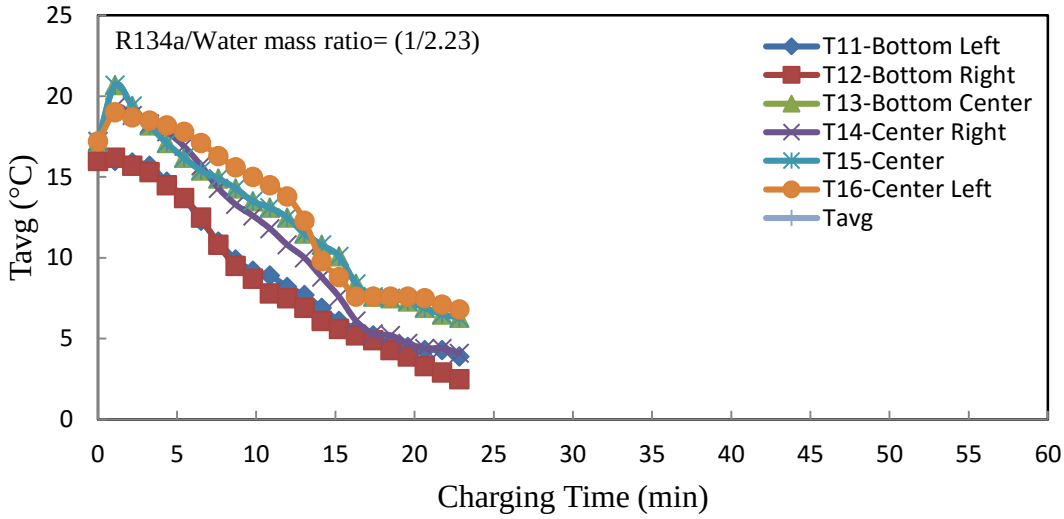

Figure 48**:** Variation of temperature inside the storage tank during clathrate formation of refrigerant R134a with mass flow rate of 0.96(kg/min) and N= 2700 rpm

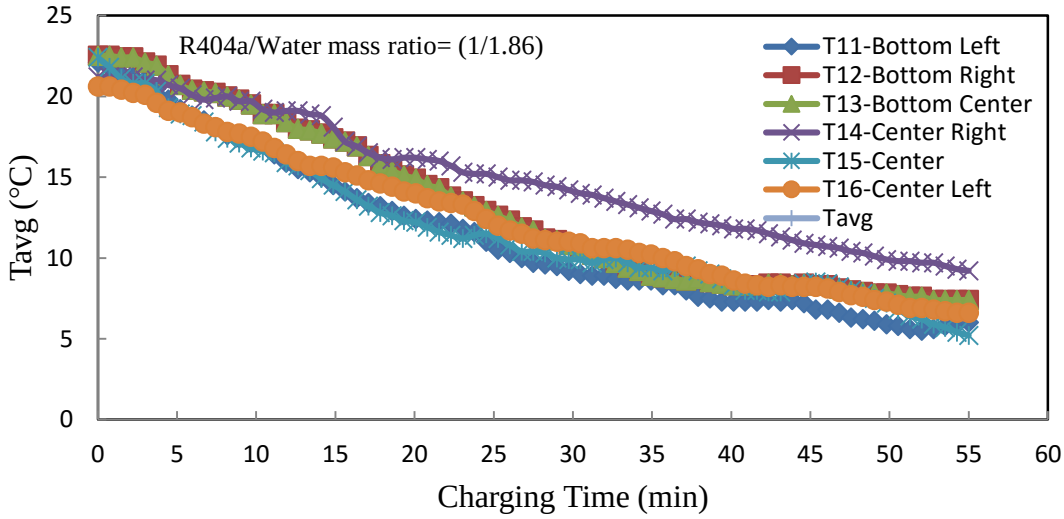

Figure 49: Variation of temperature inside the storage tank during clathrate formation of refrigerant R404a with mass flow rate 0.48 kg/min and N=2300 rpm

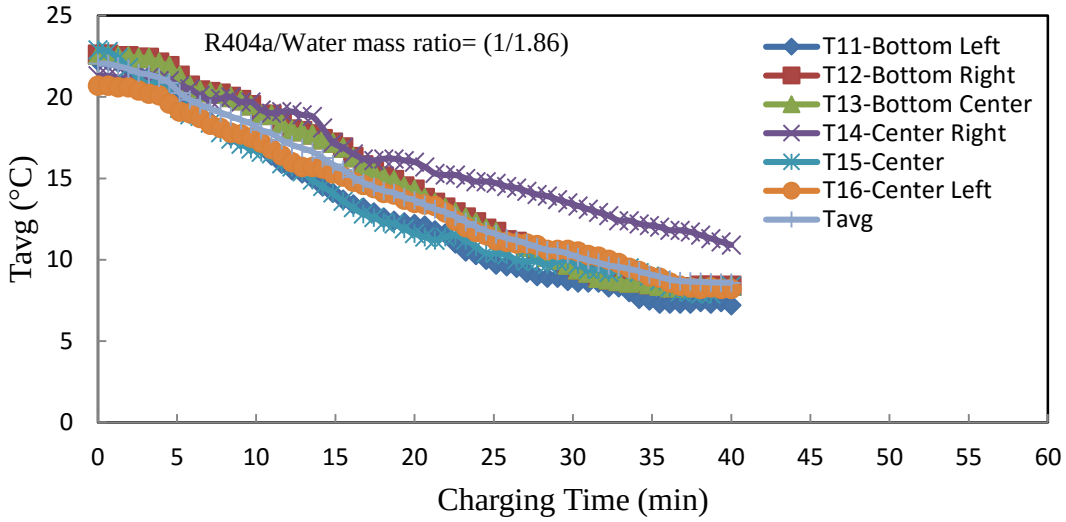

Figure 50: Variation of temperature inside the storage tank during clathrate formation of refrigerant R404a with mass flow rate of 0.72 kg/min and N=2300 rpm

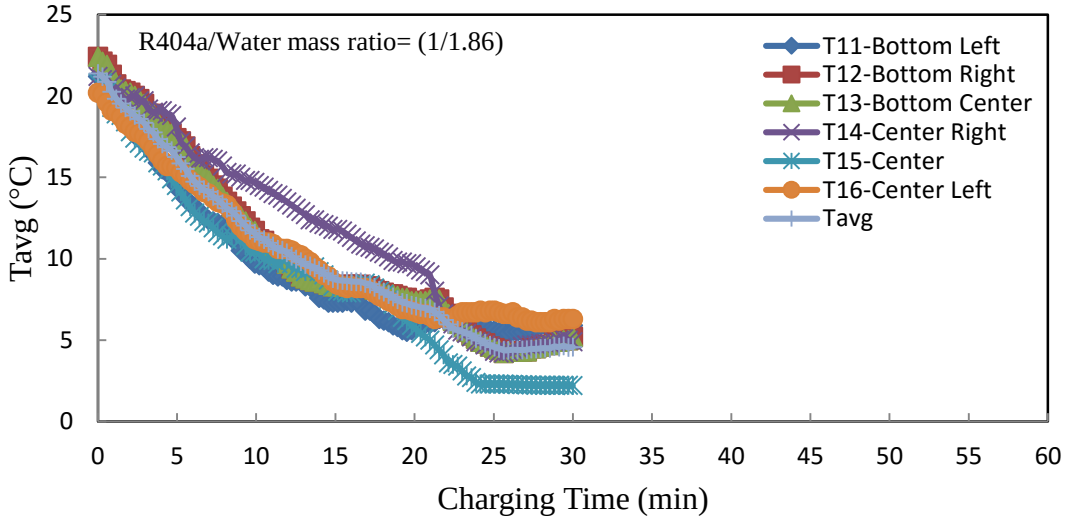

Figure 51: Variation of temperature inside the storage tank during clathrate formation of refrigerant R404a with mass flow rate of 0.96 (kg/min) and N= 2300 rpm

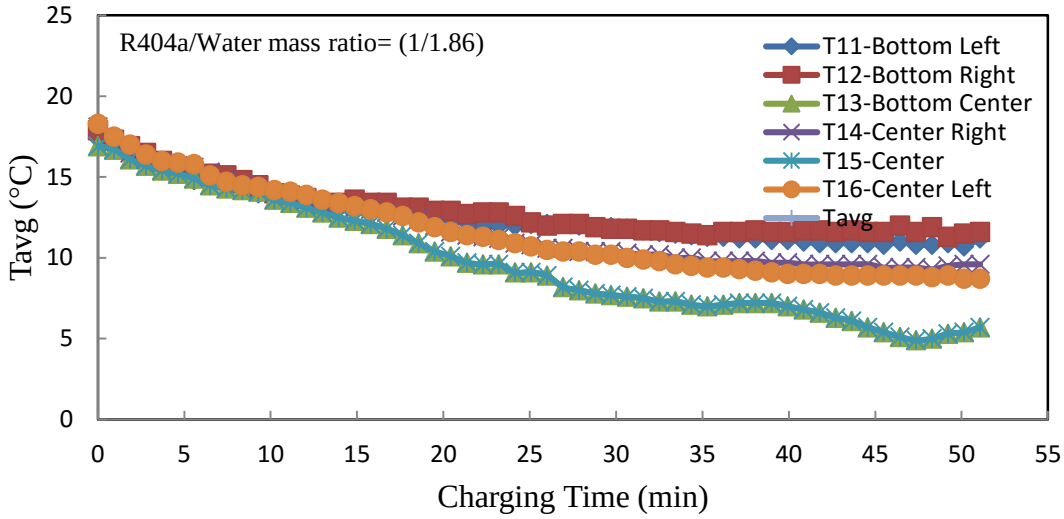

Figure 52: Variation of temperature inside the storage tank during clathrate formation of refrigerant R404a with mass flow rate of 0.48(kg/min) and N=2500 rpm

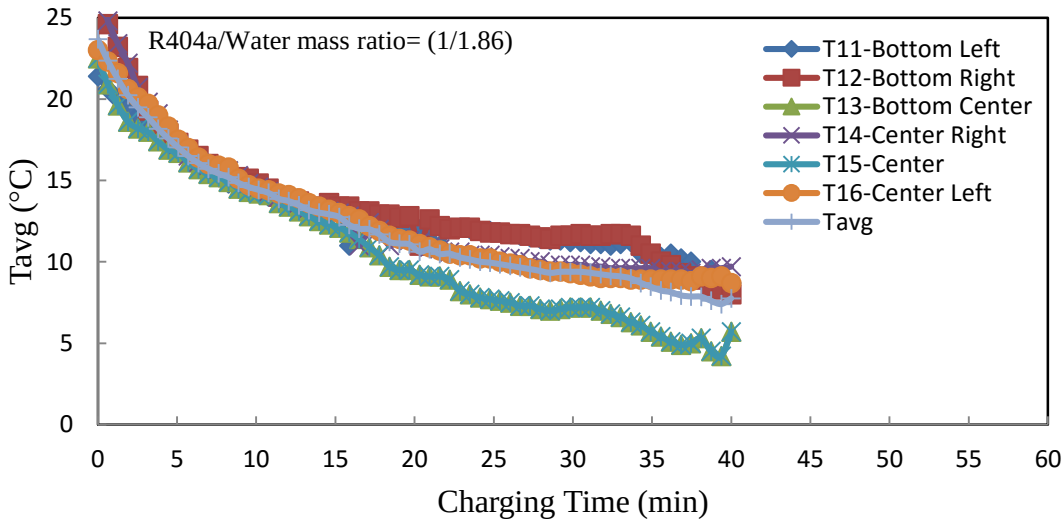

Figure 53: Variation of temperature inside the storage tank during clathrate formation of refrigerant R404a with mass flow rate of 0.72(kg/min) and N= 2500 rpm

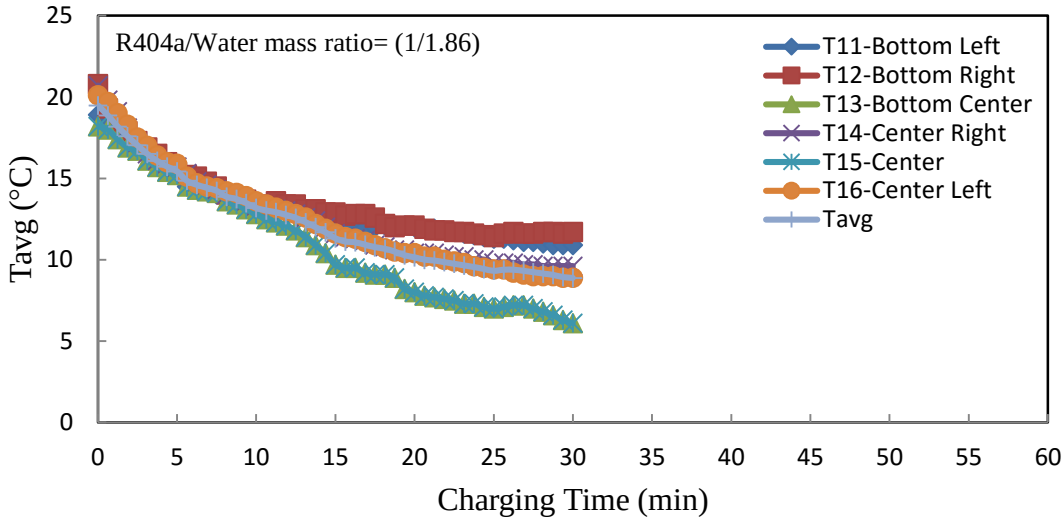

Figure 54: Variation of temperature inside the storage tank during clathrate formation of refrigerant R404a with mass flow rate of 0.96 (kg/min) and N= 2500 rpm

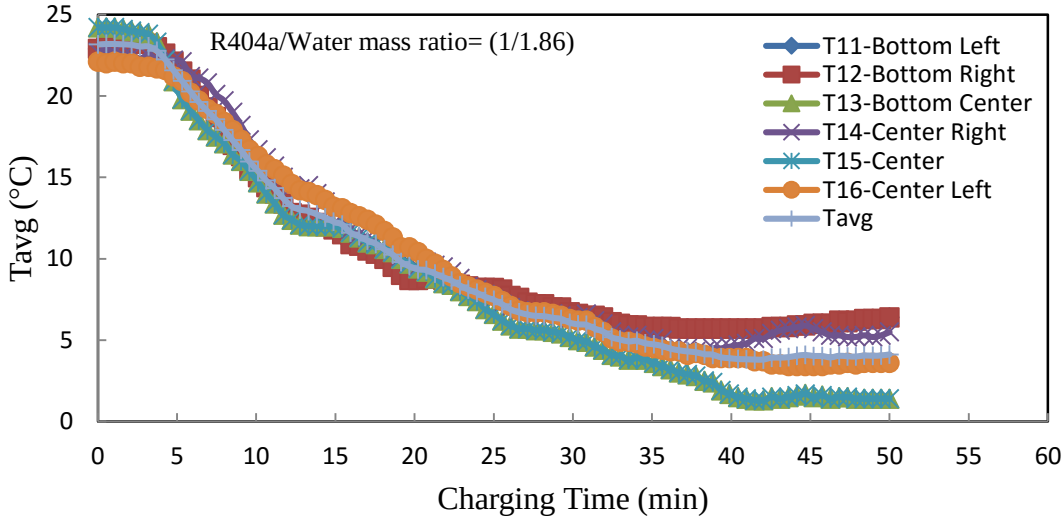

Figure 55: Variation of temperature inside the storage tank during clathrate formation of refrigerant R404a with mass flow rate of 0.48(kg/min) and N= 2700 rpm

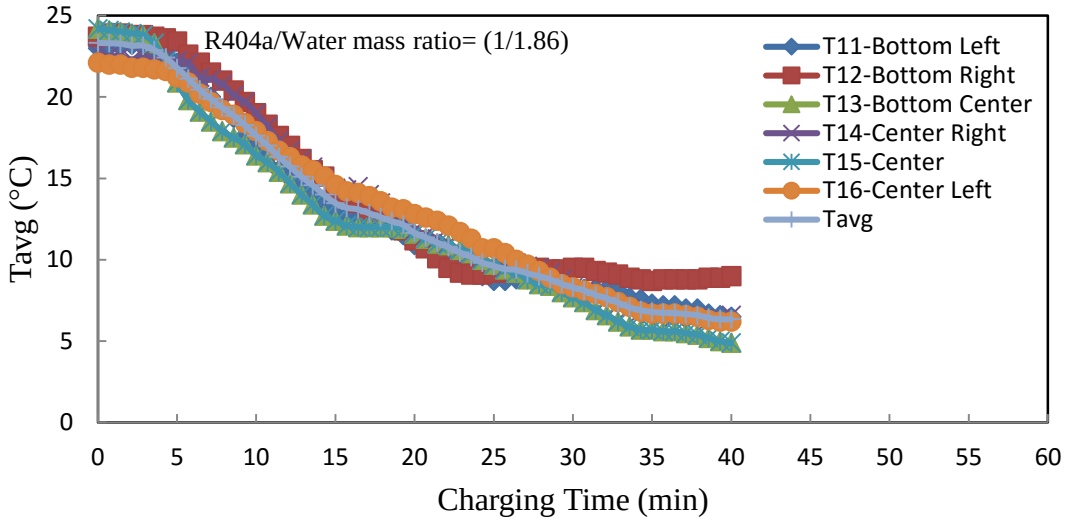

Figure 56: Variation of temperature inside the storage tank during clathrate formation of refrigerant R404a with mass flow rate of 0.72(kg/min) and N= 2700 rpm

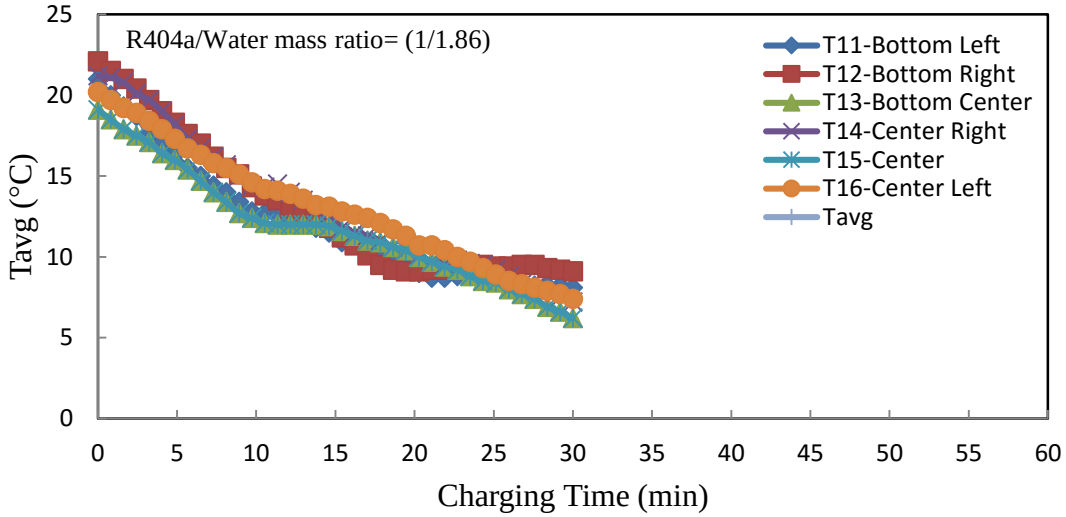

Figure 57: Variation of temperature inside the storage tank during clathrate formation of refrigerant R404a with mass flow rate of 0.96(kg/min) and N= 2700 rpm

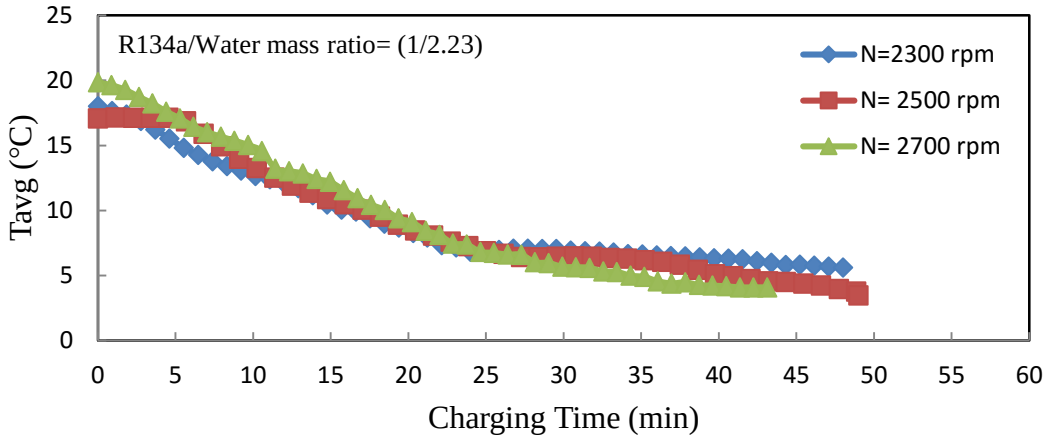

Figure 58: Variation of average R134a clathrate temperature inside the storage tank with change in time at ṁ= 0.48 (kg/min)

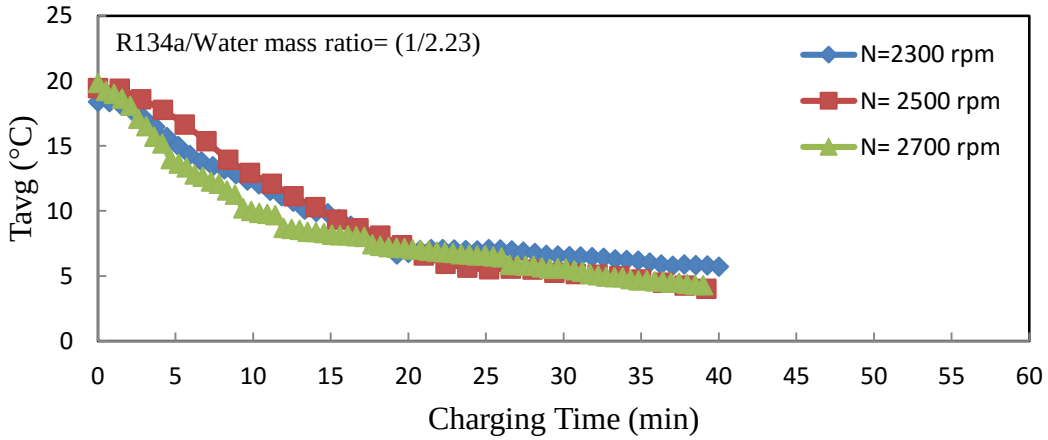

Figure 59: Variation of average R134a clathrate temperature inside the storage tank with change in time at ṁ= 0.72 (kg/min)

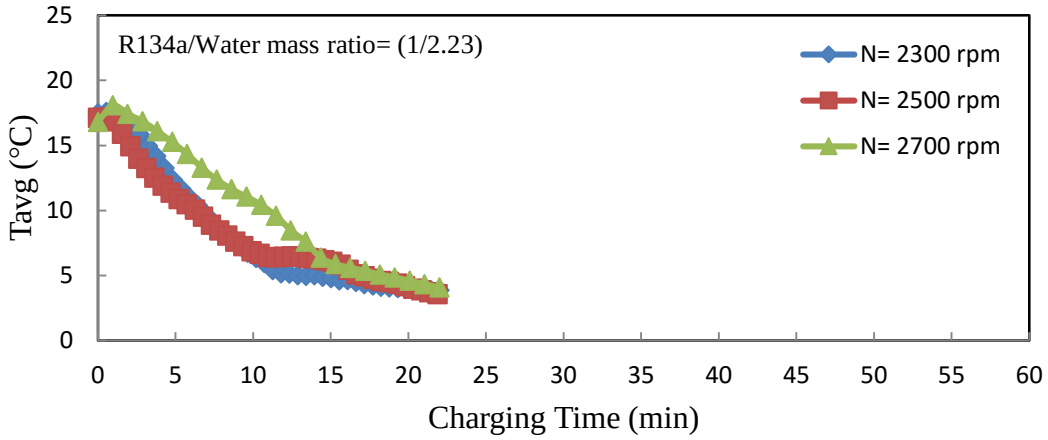

Figure 60: Variation of average R134a clathrate temperature inside the storage tank with change in time at ṁ= 0.96 (kg/min)

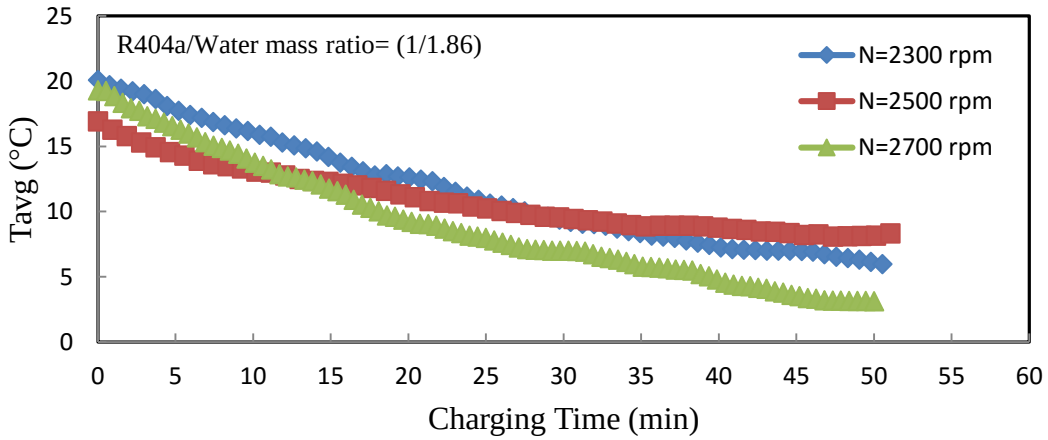

Figure 61: Variation of average R404a clathrate temperature inside the storage tank with change in time at ṁ= 0.48 (kg/min)

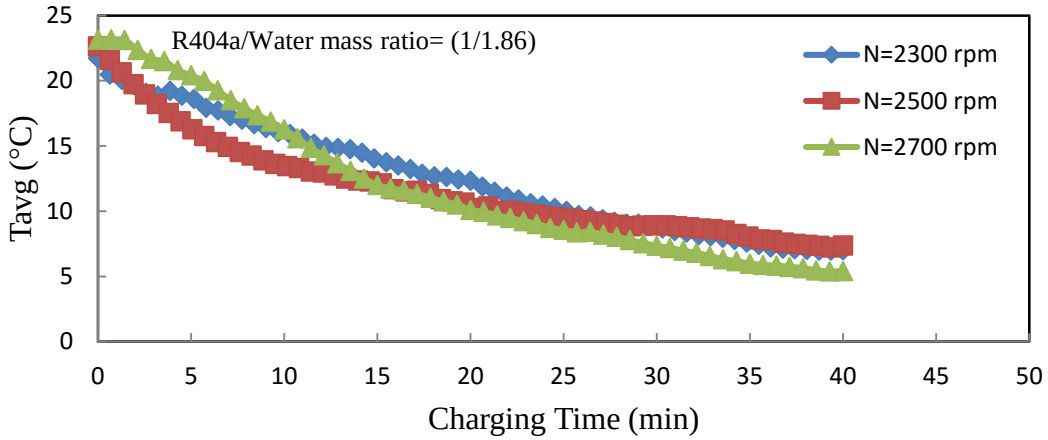

Figure 62: Variation of average R404a clathrate temperature inside the storage tank with change in time at ṁ= 0.72 (kg/min)

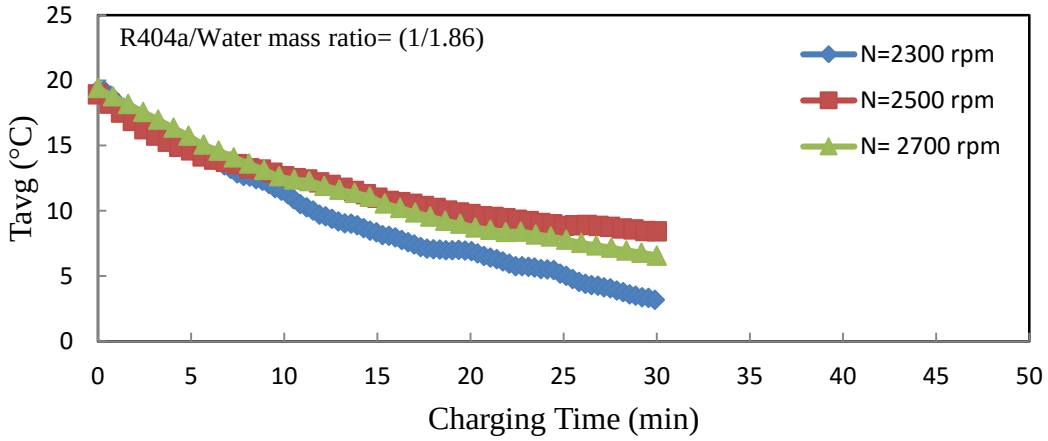

Figure 63: Variation of average R404a clathrate temperature inside the storage tank with change in time at ṁ= 0.96 (kg/min)

Table 18: Relation between pressure ratio and mass flow rate at different compressor speed during refrigerant R134a hydration

Mass flow rate (kg/min)	Comp. Speed 2700 RPM	Comp. Speed 2500 RPM	Comp. Speed 2300 RPM
1.20	2.74	2.69	2.62
0.9648	3.07	2.91	2.91
0.7236	3.90	3.70	3.26
0.4824	4.72	4.30	4.20
0.240	9.23	8.19	6.76

Table 19: Relation between pressure ratio and mass flow rate at different compressor speed during refrigerant R404a hydration

Mass flow rate (kg/min)	Comp. Speed 2700 rpm	Comp. Speed 2500 rpm	Comp. Speed 2300 rpm
1.20	4.40	4.28	4.15
0.9648	5.04	4.78	4.91
0.7236	5.62	5.46	5.17
0.4824	6.74	6.12	5.60
0.240	9.09	8.06	7.25

Appendix: B (Specification of Components)

I. MEASUREMENTS COMPONENTS

1. PRESSURE TRANSDUCERS

The pressure transducer used in the experiments are omega pressure transducer model PX240A which is a gauge type to measure pressures ranging from 0-250 psi with a range of +/- 2.5 psi. The sensor housed is rugged stainless steel body.

SPECIFICATIONS

Excitation: 8 Vdc regulated, 7 to 16 Vdc

Output: 1 to 6 Vdc @ 8 Vdc into 800 Ω min

Linearity: ±0.25% linearity and hysteresis combined

Repeatability: ±0.1%

Zero Balance: 1.0 Vdc ±0.05; 3.5 Vdc ±0.05 for PX243

Compensated Temperature Range: -27 to 63°C (-17 to 145°F)

Operable Overpressure: 2x FS

Response Time: 1 ms

Gage Type: Solid state piezoresistive

Body Material: Stainless steel

Diaphragm Material: 2.5 mm (0.10") square silicon sensor chip with Buna-N O-ring

Media Compatibility: Limited to non-caustic media that will not attack stainless steel, silica, borosilicate glass or Buna-N seal

Pressure Port: 1/8-27 NPT male

WEBSITE LINK

http://www.omega.com/pptst/PX242.html

2. PRESSURE GAUGE

The pressure gauge used within the research is OMEGA's PGUF series liquid fillable utility gauges designed for a wide range of applications. Liquid filled in the field to dampen the gauge pointer movement to avoid vibration. The rated accuracy is ±2.5%.

The gauges used are featured a corrosion resistant 304 stainless steel case and ring, and a durable polycarbonate window with brass movement. Socket connections are standard.

SPECIFICATIONS

Ranges: From 30PSI/2BAR to 1000PSI/70BAR (2000PSI/140BAR and 3000PSI/210BAR ranges on 63 mm (2½") models only)

Accuracy: ±2.5% full scale

Bourdon Tube: Phosphor bronze

Pointer: Galvalume black finish

Movement: Brass

Case & Ring: 304 stainless steel

Connection: ¼ NPTM (1/8 NPTM on 1½" dials)

Seals: Buna-N

Scale: Dual scale psi/Bar

Filling Liquid: Glycerin, silicone oil, or mineral oil

WEBSITE

http://www.omega.com/pptst/PGUF_Series.html

3. THERMOCOUPLES

K type thermocouples were chosen to be installed on the system. The K type thermocouple was purchased from omega engineering company. The specifications of the K-type thermocouples are:

Figure 64: Experimental data measurements system including 12 channels for temperature reading, 8 channels for pressure reading

The flow rate was measured using a PLATON rotameter with range of 0.2-1.5 LPM as shown below.

Figure 65: PLATON refrigerant flow meter

II. MAIN COMPONENTS

4. COMPRESSOR

Table 20: Specification of the compressor used for thermal storage system.

Type	MTZ
Model Number	MTZ 22 JC4AVE
Oil sight glass	Threaded
Oil equalization connection	3/8” flare SAE
Internal pressure relief valve	30bar/ 8 bar
Swept volume	38.1 cm3/rev
Displacement at 50 Hz	6.6 m3/h
Displacement at 60 Hz	8.0 m3/h
Nominal speed at 50Hz	2900rpm
Nominal speed at 60Hz	3600rpm
Nominal voltage at 50 Hz	380-400V /3/50Hz
Nominal voltage at 60 Hz	460V/3/60Hz

Voltage range of 50 Hz	340-440 V
Voltage range of 60Hz	414-506 V
Main wind resistance	-
Wind resistance (between phases)	10.24 Ohm
Wind resistance (between phases 1-2)	10.24 Ohm
Wind resistance (between phases 2-3)	10.24 Ohm
Starting wind resistance	-
Maximum continuous current (MCC)	6 A
Maximum Multi Trip Current (MMT)	-
Oil charge	1 L
Oil type	POE-160PZ
Refrigerant charge limit	3 kg
Maximum pressure LP side	25 bar
Maximum pressure HP side	30 bar
Maximum differential pressure	30 bar

MEASUREMENTS COMPONENTS

5. Filter dryer

Table 21: Specification of filter drier used for thermal storage experiment

Characteristic	Value
Type	DCR 048S
Weight	4 kg
Connection material	COPPER
Connection options	SOLDER, ODF
Solder connection size [in]	5/8 IN
Solder conn. size [mm]	16,00 mm
Connection type	SOLDER, ODF
Core size	48 cu.in.
EAN number	5702428125383
Max. Working Pressure [bar]	46,0 bar
Max. Working Pressure [psig]	667 psig

Net volume [foz US]	79,46 foz US
Net volume [l]	2.350 l
Pressure design	NORMAL PRESSURE
Product description	Refrigerant Filter Drier
Refrigerant(s)	HCFC/HFC
Specification key	DCR 0485s
Temperature range [°C]	-40 - 70 °C
Temperature range [°F]	-40 - 160 °F
Type designation	DCR 0485s

III. MULTI-STAGE COMPONENTS

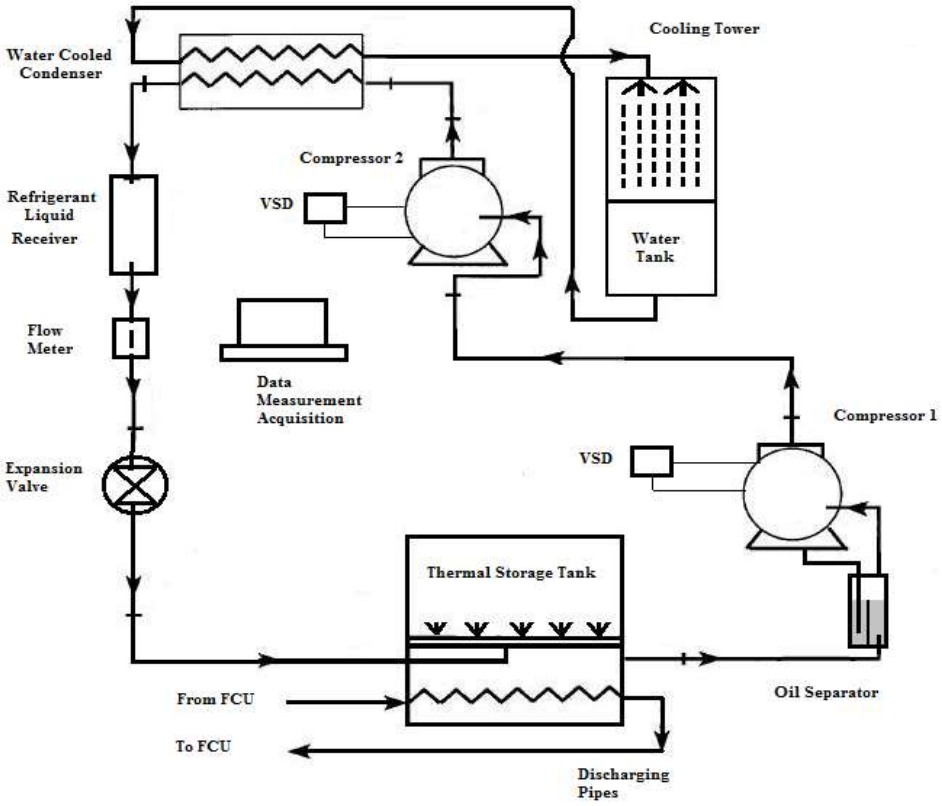

Figure 66: Multi-stage rig components for direct thermal energy storage system

Table 22: Rig components used for direct multi-stage TES system

Component	Specification
Compressor	MTZ Hermetic Reciprocating (Maneurop Model) – (Capacity:1.5Hp each)
Condenser	Water-cooled brazed plate heat exchanger Capacity (Heat Load:2.6KW) Parallel flow, 30 plates
Expansion Valve	Manual expansion valve
Flow meter	Platon~R134aflow meter. Range (0-1.5LPM)
Receiver	Refrigerant receiver for liquid refrigerants
Oil Separator	Normal pressure refrigeration oil separator
Evaporator	Stainless steel direct mixing heat exchanger.
Drier	Normal pressure refrigerant filter drier

Appendix: C (EES CODES)

The EES code used to find the properties of refrigerant R134a and R404a is presented here. All the pressure and temperature values are first copied from data acquisition excel sheet to EES tables

I. R134A EES CODE

```
T0=27
m_ref_LPM=0.8
mass_water_in=11  [kg]
Time_exp_min=25
P_evap_in=P8*6.89
P_evap_out=P9*6.89
P_cond_out=P7*6.89
P_cond_in=P7*6.89
h6=Enthalpy(R134a,T=T6,P=P_cond_in)
h7=Enthalpy(R134a,T=T7,P=P_cond_out)
h9=Enthalpy(R134a,T=T9,P=P_evap_out)
h8=Enthalpy(R134a,T=T8,P=P_evap_in)
del_h_97=h9-h7
"@@@@"
avg_del_h_97= AVGPARAMETRIC('Table 1', 'del_h_97')
"Energy"
avg_m_cl_exp=AVGPARAMETRIC('Table 1', 'm_cl_exp')
"@@@@"
avg_COP=AVGPARAMETRIC('Table 1', 'COP')
avg_W_comp_h=AVGPARAMETRIC('Table 1', 'W_dot_comp_h')
avg_Q_dot_evap=AVGPARAMETRIC('Table 1', 'Q_dot_evap_h')
m_dot_r=m_ref_LPM*(1/60)*(1/1000)*1285
Q_dot_evap_h=m_dot_r*(h9-h7)
Q_dot_cond_h=m_dot_r*(h6-h7)
W_dot_comp_h=m_dot_r*(h6-h9)
COP=Q_dot_evap_h/W_dot_comp_h
X_dot_rec=Q_dot_evap_h*((T0+273)-(T8+273))/(T8+273)
X_dot_dest_total=W_dot_comp_h-X_dot_rec
eta_II=X_dot_rec/W_dot_comp_h
Latent_heat_R134A=358
m_total=(mass_water_in+mass_water_in/R134a_ratio)
m_water_in=11
Total_R134a_in=8.702
mass_system=3.77
R134a_for_Clathrate=Total_R134a_in-mass_system
R134a_ratio=m_water_in/R134a_for_Clathrate
"Energy"
Q_sim=(mass_water_in+(mass_water_in/2.23))*Latent_heat_R134A
Q_exp=m_dot_r*avg_del_h_97*Time_exp_sec
avg_Q_exp=AVGPARAMETRIC('Table 1', 'Q_exp')
Time_sim_min=(Q_sim/Q_dot_evap_h)/60
Time_exp_sec=Time_exp_min*60
m_cl_exp=((W_dot_comp_h*COP)/Latent_heat_R134A)*Time_i
sum_of_cl_mass=SUMPARAMETRIC('Table 1', 'm_cl_exp')
m_cl_formed=(Q_dot_evap_h*Time_exp_sec)/Latent_heat_R134A
W_dot_ele=A*V/1000
COP_ele=avg_Q_dot_evap/W_dot_ele
```

II. R404A EES CODE

The following code is used to get the properties of refrigerant 404a. The term R$ represent the refrigerant R404a. The term (m_ref_LPM) varies and it represents the refrigerant mass flow rate and it is changed based on the actual measured flow rate of refrigerant in LPM. All the pressure and temperature values are read directly from the EES parametric tables. See attached file "ESS-R404a-Temp-Pres-Reading"

```
R$='R404a'
T0=27
m_ref_LPM=0.8
mass_water_in=11  [Kg]
Time_exp_min=30
P_evap_in=P8*6.89
P_evap_out=P9*6.89
P_cond_out=P7*6.89
P_cond_in=P7*6.89
h6=Enthalpy(R$,T=T6,P=P_cond_in)
h7=Enthalpy(R$,T=T7,P=P_cond_out)
h9=Enthalpy(R$,T=T9,P=P_evap_out)
h8=Enthalpy(R$,T=T8,P=P_evap_in)
del_h_97=h9-h8
"@@@@"
avg_del_h_97= AVGPARAMETRIC('Table 1', 'del_h_97')
"Energy"
avg_m_cl_exp=AVGPARAMETRIC('Table 1', 'm_cl_exp')
"@@@@"
m_dot_r=m_ref_LPM*(1/60)*(1/1000)*1285
Q_dot_evap_h=m_dot_r*(h9-h8)
Q_dot_cond_h=m_dot_r*(h6-h8)
W_dot_comp_h=m_dot_r*(h6-h9)
COP=Q_dot_evap_h/W_dot_comp_h
X_dot_rec=Q_dot_evap_h*((T0+273)-(T8+273))/(T8+273)
X_dot_dest_total=W_dot_comp_h-X_dot_rec
eta_II=X_dot_rec/W_dot_comp_h
Latent_heat_R404A=383
m_total=(mass_water_in+mass_water_in/R404a_ratio)
Latent_R404a=383
Total_R404a_in=12.89-3.143
mass_R404a_system=3.77
R404a_inside_tank=Total_R404a_in-mass_R404a_system
R404a_ratio=mass_water_in/R404a_inside_tank
"Energy"
Q_sim=(mass_water_in+(mass_water_in/R404a_ratio))*Latent_R404a
Q_exp=m_dot_r*avg_del_h_97*Time_exp_sec
avg_Q_exp=AVGPARAMETRIC('Table 1', 'Q_exp')
Time_sim_min=(Q_sim/Q_dot_evap_h)/60
Time_exp_sec=Time_exp_min*60
m_cl_exp=((W_dot_comp_h*COP)/Latent_R404a)*Time_exp_sec
sum_of_cl_mass=SUMPARAMETRIC('Table 1', 'm_cl_exp')
m_cl_formed=(Q_dot_evap_h*Time_exp_min)/Latent_R404a
"Time=Time"
```

III. MODELING CODE R134A REFRIGERANT

```
"EES Code generated by Salah Ali"
"This code  solve the model of TES "

T0=20+273
" ********************Energy ***************** "
"evap1"
Q_dot_evap1= m_dot_ref/60* (h_1-h_4x)
"comp1"
W_dot_comp1= m_dot_ref/60*(h_2-h_1)
"cond1"
Q_dot_cond1=m_dot_ref/60*(h_2-h_3)

" ********************Overall System***************** "
eta_comp1_mech=0.8
eta_comp1_mech= (h_2s-h_1)/(h_2-h_1)
COP_act=Q_dot_evap1/W_dot_comp1

" ********************STATE 1***************** "
h_1=Enthalpy(R134a,x=1,P=P_1)
s_1=ENTROPY(R134a,x=1,P=P_1)
P_sat_1=P_sat(R134a,T=T_1)
P_1=P_sat_1
"  ********************STATE 2*****************  "
CR=P_2/P_1
T_sat_2=T_sat(R134a,P=P_2)
h_2s=ENTHALPY(R134a,T=T_2,s=s_2s)
s_2s=s_1
s_2=s_2s
h_2=ENTHALPY(R134a,T=T_sat_2,s=s_2s)
"  ********************STATE 3*****************  "
P_3= P_2-50
h_3=ENTHALPY(R134a,P=P_3,x=x_3)
x_3=0
s_3=ENTROPY(R134a,P=P_3,x=x_3)
"  ********************STATE 4*****************  "
h_4=h_3
P_4=P_1
x=(-h_1f+h_3)/(h_1g-h_1f)
```

```
h_1f=Enthalpy(R134a,x=0,P=P_1)
h_1g=Enthalpy(R134a,x=1,P=P_1)
h_4x=ENTHALPY(R134a,P=P_1,x=x)
" ********************Exergy ***************** "
eta_II=ex_used/ex_in
ex_in=W_dot_comp1
ex_used=Q_dot_evap1/(T_1+273) *  ((300)-(T_1+273)    )

" ********************Model ***************** "

T_super=T_1+10
N=2500
S=1.5
PD_comp=38.1 [cm3/rev]
eta_vol= 1-0.04*(((CR)^(1/1.24))-1)
rho_1=1/v_1_sim
m_dot_sim=PD*N*S*rho_1*eta_vol
m_dot_sim_sec=PD*N*S*rho_1*eta_vol/60
PD=0.000038  [m3/rev]
v_1_sim=volume(R134a,T=T_super,P=P_1)
h_1_sim=Enthalpy(R134a,T=T_super,P=P_1)
h_2_sim=ENTHALPY(R134a,T=T_sat_2,s=s_2s)
h_3_sim=ENTHALPY(R134a,P=P_3,x=x_3)
Q_dot_evap_sim=m_dot_sim_sec*(h_1_sim-h_3_sim)
W_dot_comp_sim=m_dot_sim_sec*(h_2_sim-h_1_sim)
COP_sim=Q_dot_evap_sim/W_dot_comp_sim
```

IV. MODELING CODE R404A REFRIGERANT

```
"EES Code generated by Salah Ali"
"This code solve the ideal case R.U for gas R$"
R$='R404a'
T0=20+273
" ******************Energy ********** "
"evap1"
Q_dot_evap1= m_dot_ref/60* (h_1-h_4x)
"comp1"
W_dot_comp1= m_dot_ref/60*(h_2-h_1)
"cond1"
Q_dot_cond1=m_dot_ref/60*(h_2-h_3)

" ******************Overall System********** "
eta_comp1_mech=1
eta_comp1_mech= (h_2s-h_1)/(h_2-h_1)
COP_act=Q_dot_evap1/W_dot_comp1

" ******************STATE 1********** "
T_1_super=T_1+5
h_1=Enthalpy(R404a,x=1,P=P_1)
s_1=ENTROPY(R$,x=1,P=P_1)
{T_1}
P_sat_1=P_sat(R404a,T=T_1)
P_1=P_sat_1
"  ******************STATE 2**********  "
CR=P_2/P_1
{T_sat_2=T_sat(R404a,P=P_2)}
h_2s=ENTHALPY(R$,T=T_2,s=s_2s)
s_2s=s_1
s_2=s_2s
h_2=ENTHALPY(R$,T=T_sat_2,s=s_2s)
"  ******************STATE 3**********  "
P_3= P_2-50
h_3=ENTHALPY(R$,P=P_3,x=x_3)
x_3=0
s_3=ENTROPY(R$,P=P_3,x=x_3)

"  ******************STATE 4**********  "
h_4=h_3
P_4=P_1
x=(-h_1f+h_3)/(h_1g-h_1f)
h_1f=Enthalpy(R$,x=0,P=P_1)
h_1g=Enthalpy(R$,x=1,P=P_1)
h_4x=ENTHALPY(R$,P=P_1,x=x)
" ******************Exergy ********** "
eta_II=ex_used/ex_in
ex_in=W_dot_comp1
ex_used=Q_dot_evap1/(T_1+273) *  ((300)-(T_1+273)    )
```

Vita

Salah Ali Alshaibani was born on June 6, 1986 in Yemen. He received a comprehensive education in Mohammed Ali Othman National School in Yemen. He completed his GCE A levels before joining the American University of Sharjah in 2005 for his undergraduate studies in Mechanical Engineering. He graduated from AUS in 2010 with a minor in Engineering Management.

Salah then attended the master program at the same university. He worked at the mechanical department as a teaching assistant for two years wherein he was working as graduate teaching assistant in thermofluids laboratory. During his educational career, he attended various energy summits, local conferences and business forums. He then joined Hayel Saeed Anam Group as an Energy Audit Engineer.